This is to certify that the

dissertation entitled

Identification of gibberellin-induced genes in deepwater rice and the role of these genes in plant growth

presented by

Esther Klazina Maria van der Knaap

has been accepted towards fulfillment
of the requirements for

PhD degree in Genetics

Major professor

Date May 13, 1998

IDENTIFICATION OF GIBBERELLIN-INDUCED GENES IN DEEPWATER RICE AND THE ROLE OF THESE GENES IN PLANT GROWTH

By

Esther Klazina Maria van der Knaap

A DISSERTATION

Submitted to
Michigan State University
in partial fulfillment of the requirements
for the degree of

DOCTOR OF PHILOSOPHY

Program in Genetics

1998

ABSTRACT

IDENTIFICATION OF GIBBERELLIN-INDUCED GENES IN DEEPWATER RICE AND THE ROLE OF THESE GENES IN PLANT GROWTH

By

Esther Klazina Maria van der Knaap

Several gibberellin (GA)-regulated genes were identified by differential display in the intercalary meristem of deepwater rice internodes. Some of these genes encoded proteins that played a role in the cell cycle. Other genes encoded proteins whose function in plant growth was not known. A GA-induced increase in the transcript levels of a histone H3 gene correlated with the increased rate of DNA synthesis. This suggests that histone H3 expression is a marker for the S-phase of the cell cycle. Another GA-regulated gene with sequence similarity to replication protein A1 (RPA1) was shown to complement a yeast *rpa1* mutant. The transcript level of *Os-RPA1* increased earlier after GA application than that of histone H3, indicating a role for this gene in the late G1 phase of the cell cycle. Os-RPA1 is likely to play a role in DNA replication during plant growth. However, it may also play a role in coordinating gene expression that accompanies growth. A leucine-rich repeat receptor-like kinase, OsTMK, was identified, and showed 59% amino acid identity to TMK1 from *Arabidopsis thaliana*. The expression of *OsTMK* was very high in rapidly expanding regions, and transcript levels increased during GA treatment. This suggests a role for this gene in plant growth. The kinase domain of OsTMK was found to be an active, serine/threonine kinase. A

putative downstream component in OsTMK signaling was a kinase-associated protein phosphatase (OsKAPP). It was shown *in vitro* that the kinase-interaction domain of OsKAPP was a substrate for phophorylation by OsTMK. The tissue-specific expression of the *OsKAPP* gene correlated well with that of *OsTMK*, suggesting an *in vivo* interaction. GA treatment also resulted in increased transcript levels for *OsDD3* and *OsDD4*. No homologs of these genes were identified in the databases. However, amino acid sequence features predicted that OsDD3 might be a type 1a receptor located at the plasma membrane. OsDD4 was partially localized in the nucleus and could regulate transcription of genes in the GA response pathway. The expression of both genes was found to be higher in tissues containing meristems than in other tissues, and *OsDD4* seemed to be expressed exclusively in meristems. The role of OsDD4 in plant growth was investigated by overexpression of this gene in *Arabidopsis thaliana*. Transgenic plants were delayed in bolting, and several inflorescence stems showed fasciation followed by bifurcation. The severe phenotype showed flowering before bolting, reduced inflorescence stem elongation and reduced apical dominance. The phenotype of the flowers from the severe lines ranged from partially unfused carpels to flowers in which all organs displayed leaf-like carpels.

To my parents and brothers

ACKNOWLEDGEMENTS

I want to thank my advisor, Hans Kende, for his support, guidance and for letting me develop this thesis project. My committee members: Frans de Bruijn, Dave DeWitt and Mike Thomashow for their encouraging and constructive comments along the way. Thanks to past and current Kende lab members, as well as other members of the Plant Research Lab for insightful discussions and help with various experiments. In particular Sandrine Jagoueix, for an amazing job in search of more differentially expressed genes, and Becca Wilford and Nate Krivitzky for your help with experiments. Thanks to Jim Klug for keeping the rice growing even faster than under submerged conditions; Kurt Stepnitz and Marlene Cameron for making beautiful last minute slides and images; "Sparkles" for emptying trash cans, changing light bulbs and keeping me informed about conditions inside and outside the building. My swimming buddies Beth, Antje, Nikki and Sigrun for dragging me out of the lab and making me exercise (running around the lab and biking year-round do not qualify!). Thank you Scott & Antje for being dear friends and helping me start my life in Michigan. Art & Marlene, Kirsten & Søren for camping and stamping parties. Sue, Steve & Dagan for the dinner/hot tub/hurt-stories on Sunday nights. Thanks Merideth for being our favorite neighbor, the Monday night blues and the walks in the woods. Frank, Marc, Anja, Jos & Riki, Isgouhi for keeping the friendships predating graduate school alive. Thanks to my family for their unconditional love and support ("we thought you working on plant nematodes!") and above all thanks to Eric Stockinger for allowing me to be who I am and without whom life would not be as special.

PREFACE

All experiments described in Chapter 2, e.g., RNA isolations, control reactions, Northern blot analysis, differential display I, and library construction, were performed by the author of this thesis. The differential display II experiment and the cDNA library screen to obtain the full length *Os-DD12* cDNA were performed by Dr. Sandrine Jagoueix.

With regard to Chapter 3, the *Os-RPA1* (*Os-DD12*) gene was originally identified by Dr. Sandrine Jagoueix, who also generated the constructs for the yeast complementation experiments. All other experiments, such as RNA isolation, Northern blot analysis, and the yeast complementation were performed by the author of this thesis. This chapter has appeared in the Proceedings of the National Acadamy of Science of the USA 94:9979-9983.

With regard to Chapter 4, the *OsKIN* gene was originally identified by Margret Sauter, and the experiment shown in Figure 4.2 was carried out in collaboration with her. All other experiments, such as RNA and DNA isolations, Northern and Southern blot analysis, library screening, overexpression and phosphorylation studies were performed by the author of this thesis.

With regard to Chapter 5, the DD4::GUS construct for nuclear localization studies was constructed by the author of this thesis. The onion bombardment experiments were performed by Emily Avila in Dr. M. Varagona's laboratory at New Mexico State University in Las Crucas. All other experiments, such as the generation of transgenic *Arabidopsis* plants, were performed by the author of this thesis.

With regard to Chapter 6, all experiments were performed by the author of this thesis.

TABLE OF CONTENTS

LIST OF TABLES

LIST OF FIGURES

CHAPTER 1

Regulation of submergence-induced growth in deepwater rice and role of gibberellin in vegetative growth

1.1. RICE

Rice (*Oryza* spp.) is one of the most important food crops and a primary food source for more than a third of the world's population. More than 90% of the world's rice is grown and consumed in Asia, where rice in the diet can account for over 70% of the daily calorie intake (Hossain, 1996; Khush, 1997). Rice is a major factor in national economies as well, providing up to 30 to 50% of the agricultural value added in the poorer countries in Asia (Hossain, 1996).

The genus *Oryza* comprises about 20 different species and belongs to a group of ancient grasses. Two major cultigens, the Asian *O. sativa* and the African *O. glaberrima*, together with their wild progenitors *O. rufipogon*, *O. nivara* and *O. longistaminata*, *O. bartii*, respectively, belong to the AA genome (2n=24) of the *O. sativa* complex (Oka, 1988). Cultivation of rice for at least 7000 years (Oka, 1988) has resulted in the generation of ~ 120,000 distinct rice varieties (Khush, 1997). These cultivars display several distinctive characteristics and show more genetic and morphological diversity than most other cultivated crops. Rice is cultivated in five different ecosystems in which the flooding pattern (*i.e.*, depth and duration) is a major determinant. The ecosystems are irrigated, rainfed lowland, deepwater, upland, and tidal wetlands (IRRI, 1984). The most productive rice growing system is the irrigated environment, yielding 75% of the world's rice production (IRRI, 1990). This high productivity is mainly achieved by using high-yielding,

short-stemmed modern varieties, which are also highly responsive to fertilizer. The productivity in the other ecosystems is lower, in part, because the high-yielding modern rice varieties do not tolerate less-controlled water regimes.

1.1.1. DEEPWATER RICE

Rice grown in the deepwater ecosystem distinguishes itself from most modern rice varieties by its ability to survive in water depths of 50 cm or more for at least one month during the growing season (Catling *et al.*, 1988). Deepwater rice areas in Asia are found in the floodplains and river deltas of the Ganges-Brahmaputra in North-East India and in Bangladesh, of the Irrawaddy in Myanmar, of the Chao Phraya in Thailand, and of the Mekong in Vietnam and Cambodia. Although the rice production from deepwater environments is only 6% of the worldwide production (IRRI, 1990), it provides the major calorie intake of 100 million people living along the rivers and is the only crop that can be grown by subsistence farmers during the monsoon season (Catling, 1992).

The two strategies for survival of rice under deepwater conditions are tall stature and ability to elongate. Two groups can be distinguished among the deepwater rice varieties: traditional tall and floating rices. The traditional tall rices grow in water depths between 50 to 100 cm and are relatively tall even when not flooded. Because they have limited or no ability to elongate when submerged, traditional tall rices are not suited for sustained water depths of more than 100 cm. Under these circumstances, the elongation ability of the floating rices is essential (Catling, 1992). When well established, floating rices are able to elongate at rates of up to 25 cm per day, resulting in

plants that are up to 7 m tall (Vergara *et al.*, 1977; Catling, 1992). Almost all wild rices show floating ability, often exceeding that of the best elongating rice cultivars. Therefore, the elongation ability was probably retained from wild progenitors (Oka, 1988).

1.2. DEVELOPMENTAL AND GENETIC ANALYSIS OF RICE INTERNODAL ELONGATION

Post-embryonic plant development can be divided in a juvenile and an adult phase. The adult phase is further divided in a vegetative and reproductive phase (Catling, 1992). The juvenile phase starts after germination and lasts until the plant is established (3 to 5 weeks after germination). The vegetative adult phase follows the juvenile phase and lasts until the beginning of the reproductive phase, the length of which varies with each cultivar and is often influenced by day length. The reproductive phase begins at the initiation of panicle formation and lasts until flowering. Elongation growth in both the juvenile phase (Raskin and Kende, 1983) and the reproductive phase (Morishima, 1975; Vergara, 1985; Keith *et al.*, 1986) are similar in deepwater and modern rice varieties. For example, elongation at the onset of the reproductive phase occurs and is further increased by submergence in all rice cultivars (Keith *et al.*, 1986). What distinguishes deepwater rice from most modern rice varieties is the vegetative adult phase. The ability to grow rapidly out of the water when partially submerged is primarily attributed to enhanced internodal elongation. Modern rice varieties and most traditional tall varieties do not respond at this stage to rapidly rising water levels, and partial submergence severely damages the plants.

The genetic basis for enhanced internodal elongation has received little attention. Studies have shown that this trait is controlled by a few major and many minor genes (Catling, 1992). Suge (1988) has indicated that elongation during submergence is based on the ability of an internode to elongate, as well as the degree of elongation. In this study, one dominant gene was identified conferring elongation ability (in addition to a locus controlling gibberellin [GA] biosynthesis; Suge, 1988; see below). In another study, one dominant gene responsible for early nodal differentiation was identified (Tripathi and Balakrishna Rao, 1985). This trait was linked to nodal rooting and tillering, which are typical characteristics of floating rice. Whether the same locus was identified in both studies is not known.

Another locus for elongation ability was identified in a study where a modern non-elongating rice cultivar was used as the recurrent parent for introgression of a locus from a perennial *O. rufipogon* accession. *O. rufipogon* is the progenitor of *O. sativa*, exhibiting great floating abilities. The near-isogenic line thus created indicated the presence of a recessive allele conferring internodal elongation in response to submergence in the vegetative adult phase (Eiguchi *et al.*, 1993). These authors may have identified a heterochronic gene that changes the timing of internodal elongation depending on environmental conditions. This is a major trait distinguishing modern, non-elongating from elongating varieties (Morishima, 1975; Keith *et al.*, 1986). The above results indicate the presence of two or three major genes conferring internodal elongation ability. However, to survive 2- to 4-m-deep floodwaters, the degree of elongation, *i.e.*, rapid increase in growth rate and total elongation, is essential and the degree of elongation is probably controlled by many genes (Suge, 1988).

Yields of modern rice cultivars average 6 tons per hectare, whereas those of deepwater rice are 2 to 3 tons per hectare (Catling, 1992; Setboonsarng, 1996). The efforts to improve the yield and grain quality of deepwater rice varieties have been met with limited success. Breeding for short-stemmed rice varieties with conditional elongation ability (possibly involving the loci described above) has resulted in the generation of varieties that fared well under moderate flooding conditions (up to 150 cm; Catling, 1992). However, increases in yield and retention of the floating ability has never been combined in one single cultivar. Improvement of floating rice cultivars, which represent the most extreme example of adaptation to flooding, may not be feasible according to breeders (Catling, 1992) and economists (Setboonsarng, 1996). Studies on how rapid increases in rates of elongation are achieved in these cultivars will be very useful, however, to improve cultivars grown in other ecosystems.

1.3. PHYSIOLOGY OF THE ELONGATION OF DEEPWATER RICE INTERNODES

Partial submergence of floating rice varieties leads to rapid increases in the growth rates of rice internodes (Métraux and Kende, 1983; Vergara *et al.*, 1977). This increased growth is also observed when plants are exposed to 1 µl/l ethylene, which is the natural concentration found in submerged internodes (Raskin and Kende, 1984a; Stünzi and Kende, 1989). Moreover, plants treated with aminoethoxyvinylglycine, an inhibitor of ethylene biosynthesis, do not show internodal elongation upon submergence (Métraux and Kende, 1983; Raskin and Kende, 1984a). Ethylene levels increase in

submerged internodes, and this rise precedes internodal elongation (Rose-John and Kende, 1985). The initial increase in internodal ethylene levels is due to accumulation from basal production and the subsequent entrapment of the gas under submerged conditions (Zarembinski and Theologis, 1997). Long-term increases in ethylene levels are likely to be due to enhanced ethylene biosynthesis. Enzyme and transcript levels of the gene encoding 1-aminocyclopropane-1-carboxylate (ACC) oxidase increases several fold after 8 h of submergence (Mekhedov and Kende, 1996). ACC synthase 1 transcript levels marginally increases after 12 h of submergence only in the growing region of the internode, while in other regions of the internode the levels decreases (Zarembinski and Theologis, 1997). This indicates that the increase in ethylene biosynthesis is primarily due to increased transcript levels and increased activity of ACC oxidase, the terminal enzyme in ethylene biosynthesis (Mekhedov and Kende, 1996).

The internode that can grow and respond rapidly to rising water levels is the uppermost internode. Rice stem sections containing the uppermost internode respond to submergence and high ethylene concentrations in a manner similar to that observed in whole plants (Raskin and Kende, 1984a). The growth response of rice stem sections induced by submergence or ethylene is blocked when the plants and sections are treated with the GA biosynthesis inhibitor tetcyclacis (Raskin and Kende, 1984b), or with ancymidol (Suge, 1985), prior to ethylene treatment. Addition of GA to the tetcyclacis-treated sections restores the growth response. GA is more effective in inducing growth in an atmosphere containing ethylene than in air, indicating that ethylene increases the sensitivity of the tissue to GA (Raskin and Kende, 1984b). The enhancement of the sensitivity of the tissue to GA is thought to be mediated through a decrease of the abscisic acid (ABA) levels in

the plant. ABA has been shown to antagonize the growth-promoting action of GA in rice stem sections (Hoffmann-Benning and Kende, 1992). Whole plants submerged or treated with ethylene for 3 h show a 75% reduction in ABA levels; therefore, the responsiveness to GA may be a function of ABA content (Hoffmann-Benning and Kende, 1992). The induction of growth by either submergence, ethylene or GA has been measured with an angular transducer attached to the growing internode. Growth induced by submergence of rice stem sections shows a 3 h 20 min lag phase. The lag phase is 60 min for treatment with ethylene and low O_2 (Rose-John and Kende, 1985) and 40 min for GA (Sauter and Kende, 1992b). Furthermore, using a rice GA biosynthetic mutant line, GA has been shown to be a prerequisite for elongation ability during submergence (Suge, 1988). Therefore, the physiological and genetic studies and the short lag phase all indicate that GA is the ultimate hormone eliciting the growth response. Submergence increases the level of ethylene, which enhances the sensitivity of the internode to GA, at least in part through a decrease in ABA content. This effect is not unique to rice. Gibberellins have also been shown to mediate the stimulatory effect of ethylene on stem elongation in other semi-aquatic plants (Musgrave *et al.*, 1972; Rijnders *et al.*, 1997).

1.4. ROLE OF GA IN PLANT GROWTH AND DEVELOPMENT

Gibberellins were first identified and purified from the fungus *Gibberella fujikuroi* which causes infected rice plants to grow excessively tall (Yabuta and Sumiki, 1938). Gibberellins have been implicated in many plant processes, such as germination and mobilization of reserves immediately

after germination of cereal grains, juvenile-to-adult and vegetative-to-reproductive phase changes, apical dominance, flower initiation, in anther, seed and fruit development, sex determination and, above all, shoot and leaf elongation.

1.4.1. GA BIOSYNTHESIS

The role of GA in plant growth and development has been documented in several plant species via the generation of dwarf mutants, whose phenotypes are reversed upon GA treatment. The characterization of these mutants has also allowed the elucidation of the GA biosynthetic pathway. Recently, many of the GA biosynthetic genes have been cloned. GA biosynthesis branches from the general terpene biosynthetic pathway at geranylgeranyl pyrophosphate (GGPP). The first committed step is the formation of *ent*-kaurene from GGPP, which is catalyzed by *ent*-kaurene synthases A and B (KSA and KSB, respectively). The gene encoding KSA has been identified from *Arabidopsis* (Sun *et al.*, 1992) and the gene encoding KSB from pumpkin (Yamaguchi *et al.*, 1996). Transcript levels of the *KSA* and *KSB* genes is detected in immature and growing regions of the plant, and the enzymes are most likely located in proplastids of meristematic cells (Silverstone *et al.*, 1997a; Aach *et al.*, 1997). The next steps in the biosynthetic pathway are the stepwise oxidation of *ent*-kaurene to GA_{12}-aldehyde by membrane-bound P450 monooxygenases. The final step is the conversion of GA_{12}-aldehyde to bioactive GAs (GA_1, GA_3 and GA_4) and is mediated by at least two enzymes which belong to the class of 2-oxoglutarate-dependent dioxygenases located in the cytosol (Kende and Zeevaart, 1997). GA 20-oxidase is responsible for the oxidation and subsequent elimination of C-20, a pivotal

step in the pathway. Several genes encoding GA 20-oxidases have been cloned from pumpkin (Lange, 1997), spinach (Wu *et al.*, 1996) and *Arabidopsis* (Xu *et al.*, 1995; Phillips *et al.*, 1995). These enzymes were shown to have broad substrate specificity. Genes encoding GA 20-oxidases are part of a gene family, and Northern blot analysis has indicated tissue-specific expression patterns for three of the *Arabidopsis* GA 20-oxidase genes (Phillips *et al.*, 1995). Application of GA results in a decrease in transcript levels, indicating negative feedback regulation (Phillips *et al.*, 1995). Feedback regulation of the gene encoding 3β-hydroxylase, the last step in GA biosynthesis, has been observed in *Arabidopsis* (Chiang *et al.*, 1995) and in pea as well (Martin *et al.*, 1997). While 3β-hydroxylation is essential in the formation of bioactive GA, the 2β-hydroxylation irreversibly inactivates GA. The "slender" mutant of pea is the only mutant known to be blocked in catabolism of bioactive GA. However, the gene encoding this 2β-hydroxylase has not yet been identified (Ross *et al.*, 1995).

1.4.2. GA SIGNAL TRANSDUCTION

Plant hormone responses are mediated by both the amount of hormone and by tissue responsiveness. The ability of GA to induce growth in pea internodes, for example, has been correlated with the amount of GA, as well as with tissue responsiveness (Ross and Reid, 1992). The importance of tissue responsiveness to GA is also evident in the internodal elongation of rice, where modern varieties are unresponsive to both submergence and GA during the vegetative adult phase (Inouye, 1985; Keith *et al.*, 1986, Eiguchi *et al.*, 1993). Whereas much is known about GA biosynthesis (see above), less is

known about GA signal transduction. Recently, however, significant progress has been made in this area of research.

There are a few mutants with altered stature whose phenotypes appear to correlate with an increase or a decrease in GA signal transduction (see Table 1.1). In case of these mutants, many or all of the pleiotropic effects of GA or the lack thereof (*i.e.*, effects on germination and male fertility) have been observed. The phenotype of an increase in GA signaling resembles that of a wild-type plant treated with saturating doses of GA. All mutants disturbed in this process are recessive, indicating a loss of function of a repressor-like molecule. The *sln* mutant in barley (*slender;* Chandler, 1988) and the *la cry*^{s} double mutant in pea (Potts *et al.*, 1985) show no change in height regardless of endogenous GA levels. Both loci in pea, *LA* and*CRY*, need to be mutated to confer the *slender* phenotype. The *spy* mutant (*spindly*) in *Arabidopsis* confers a *slender* phenotype as well, but this mutant is somewhat responsive to GA. The *spy* mutant was identified in a screen for GA-independent germination by using an inhibitor of GA biosynthesis, paclobutrazol (Jacobsen and Olszewski, 1993). The *SPY* gene was found to encode a protein containing a tetratricopeptide repeat, which may be involved in protein-protein interactions, and a domain with O-linked N-acetylglucosamine transferase activity (Jacobsen *et al.*, 1996; Olszewski, 1997). Several mutant alleles of *SPY* have been identified and indicate the importance of both the tetratricopeptide repeat as well as the O-linked N-acetylglucosamine transferase activity in GA signaling (Olszewski, 1997). Whether the *SLN* (barley) or *LA* and *CRY* (pea) genes encode *SPY* orthologs is unknown.

The mutants which display a decrease in GA signaling are dwarf in appearance, reminiscent of GA deficiency. All mutants are semi-dominant or dominant and do not respond to applied GA. However, paclobutrazol further

Table 1.1. GA signal transduction mutants. *ga1-3* is a severe, GA responsive dwarf mutant (Koornneef and van der Veen, 1980).

Mutant	Phenotype	Species	Wild-type protein function	Reference
spy	slender, repressor of *ga1-3* and *gai*	*Arabidopsis*	tetratrico repeat and O-linked N-acetylglucosamine transferase	Jacobsen *et al.*, 1996; Olszewski, 1997
sln	slender	barley	?	Chandler, 1988
la cry^s	slender	pea	?	Potts *et al.*, 1985
gai	GA-insensitive	*Arabidopsis*	transcription factor ?	Peng *et al.*, 1997
rht3	GA-insensitive	wheat	?	Gale *et al.*, 1975
d8	GA-insensitive	corn	?	Winkler and Freeling, 1994
rga (grs)	repressor of *ga1-3*	*Arabidopsis*	transcription factor ?	Silverstone *et al.*, 1998
gar2	repressor of *gai*	*Arabidopsis*	?	Wilson and Somerville, 1995

decreases the height in the plants, which is reversible upon GA treatment. This indicates that the ability to respond to GA exists, but also that the response is saturated under physiological conditions. Genetic analysis has shown that the *d8* locus in maize (*dwarf 8*; Winkler and Freeling, 1994), *rht3* in wheat (*reduced height 3*; Gale *et al.*, 1975) and *gai* in *Arabidopsis* (*GA-insensitive*; Wilson and Somerville, 1995) are "gain-of-function" mutants. Recently, the *GAI* gene has been identified (Peng *et al.*, 1997), and found to have high amino acid similarity to the protein encoded by the *SCR* (*SCARECROW*) gene. SCR is required for asymmetric cell division during root development in *Arabidopsis* (Di Laurenzio *et al.*, 1996). The proteins encoded by the *GAI* and *SCR* genes may belong to a new class of plant transcription factors (Peng *et al.*, 1997). A gene related to *GAI* is *GRS* and the proteins encoded by these genes are 83% identical. Interestingly, both the *GAI* and *RGS* genes were identified previously in a screen for *Arabidopsis* genes able to rescue a yeast strain deficient in the production of a transcription factor regulating nitrogen metabolism (Truong *et al.*, 1997). It is unknown whether there is a link between nitrogen metabolism and GA signaling.

A screen for suppressor mutations of *gai* have resulted, in many cases, in the generation of intragenic suppressor mutants, indicating that the wild-type function of the GAI protein is dispensible (Peng and Harberd, 1993; Wilson and Somerville, 1995). However, two extragenic loci have been identified, that partially suppress the *gai* phenotype. The *gas1* mutant gene (*gai* suppressor) is an allele of *SPY*, while *gar2* (*gai* revertant) appears to be a mutated allele at a new locus involved in GA signaling (Wilson and Somerville, 1995; Carol *et al.*, 1995; Peng *et al.*, 1997). Interestingly, the *spy* mutant has not only been identified as a suppressor of *gai*, but also as suppressor of *ga1-3*, a severe GA biosynthesis mutant in *Arabidopsis*

(Silverstone *et al.*, 1997b). In the latter study, a mutant allele at another locus was identified, *rga* (*repressor of ga1-3*; Silverstone *et al.*, 1997b). The gene affected in the *rga* mutant appears to be *GRS*, previously identified because of its high amino acid sequence similarity to GAI (see above; Silverstone *et al.*, 1998). In the *ga1-3* mutant, the recessive mutant alleles at the *RGA* (*GRS*) locus partially restores stem growth and apical dominance to wild-type levels, while germination and male fertility are not restored (Silverstone *et al.*, 1997b). This indicates that RGA (GRS) affects only part of the GA response pathway. The *spy* mutation on the other hand, partially restores all defects caused by GA deficiency (Silverstone *et al.*, 1997b).

The studies described above have shown that GA most likely controls stem elongation not through activation of the signal transduction pathway but by derepression. The repressor function of GAI may be relieved by GA, while the mutant protein has lost the ability to be derepressed. The SPY protein appears to be a negative regulator of GA signaling and the *spy* mutation is epistatic to the *gai* mutation (Wilson and Somerville, 1995; Jacobsen *et al.*, 1996). At the molecular level, it is possible that SPY post-translationally modifies GAI and RGA (GRS), thereby altering the activity of these putative transcription factors (Olszewski, 1997; Peng *et al.*, 1997; Silverstone *et al.*, 1998). While the *spy* mutant partially reverts *gai* to wild-type, the triple homozygous mutant, *gai spy gar2*, completely suppresses the phenotype displaying a decrease in GA signaling (Peng *et al.*, 1997). The phenotype displayed by the GA biosynthesis mutant *ga1-3* is also completely suppressed by additional mutations at the *SPY* and *RGA* (*GRS*) loci (Silverstone *et al.*, 1997b). These studies indicate that stem elongation in both homozygous triple mutants appears to be mediated independently of GA.

1.4.3. GA-REGULATED GENE EXPRESSION DURING ELONGATION

Complementary to genetic analyses of GA-regulated processes is the identification of genes whose expression is specifically regulated by GA. Previously, two-dimensional gel electrophoresis studies have revealed changes in protein profiles of GA-deficient maize and pea shoots after treatment with GA (Chory *et al.*, 1987). While these latter studies have led to the identification of several proteins whose level increase or decrease, a later study, using the stems of a GA-deficient tomato mutant line have displayed only proteins whose level decrease upon GA treatment (Jacobsen *et al.*, 1994). Using leaves of a GA-deficient barley plant, two (Speulman and Salamini, 1995) or no (Zwar and Chandler, 1995) proteins have been identified, which change in abundance after GA application.

Differential screening methods have been used to identify genes regulated by GA (see Table 1.2). The first gene identified in stems of a GA-deficient tomato line is *GAST1* (*GA stimulated transcript 1*). *GAST1* transcript levels accumulate after GA treatment, while ABA, auxin and cytokinin have no effect (Shi *et al.*, 1992). The *GAST1* gene encodes a putative 112-amino acid protein containing a signal sequence, which indicate that it may be secreted (Shi *et al.*, 1992). A *Petunia* homolog, *GIP* (*GA-induced gene*), has been identified and the protein it encodes shows 82% amino acid identity with GAST1 including the signal sequence. High levels of *GIP* transcript are present in elongating corollas and young stem internodes, and their level increases further by GA treatment (Ben-Nissan and Weiss, 1996). Another homolog of GAST1 is RSI-1 (root system inducible-1; 79% amino acid identity without signal sequence) from tomato (Taylor and Scheuring, 1994). The gene

Table 1.2. GA-regulated genes in vegetative growth.

Gene	Transcript levels	Plant line	Protein function	Reference
GAST1	transient increase	GA-deficient tomato	secreted protein	Shi *et al.*, 1992
GIP	increase	*Petunia*	similarity to GAST1	Ben-Nissan and Weiss, 1996
GASA1	transient increase	GA-deficient *Arabidopsis*	similarity to GAST1	Herzog *et al.*, 1995
GASA4	transient increase	GA-deficient *Arabidopsis*	similarity to GAST1	Herzog *et al.*, 1995
γ-TIP	increase	GA-deficient *Arabidopsis*	tonoplast water channel protein	Phillips and Huttly, 1994
invertase	transient increase	GA-deficient pea	invertase	Wu *et al.*, 1993
PsG-A	transient increase	GA-deficient pea	?	Cohn *et al.*, 1994
PsG-F	transient increase	GA-deficient pea	?	Cohn *et al.*, 1994
EXT11	increase	GA-deficient barley	XET	Smith *et al.*, 1996
PM2	increase	GA-deficient barley	similarity to XET	Smith *et al.*, 1996
ESA1	transient increase	GA-deficient barley	similarity to EGF	Speulman and Salamini, 1995

ESA2	transient increase	GA-deficient barley	similarity to LEA	Speulman and Salamini, 1995
CRG16	increase	cucumber	?	Chono *et al.,* 1996
cycOs1	increase	deepwater rice	mitotic cyclin	Sauter, 1997
cycOs2	increase	deepwater rice	mitotic cyclin	Sauter, 1997
cdc2Os-2	increase	deepwater rice	similarity to cdc2	Sauter *et al.*, 1995
PCR clone 9B	increase	deepwater rice	histone H3	Van der Knaap and Kende, 1995
Os-EXP2	increase	deepwater rice	expansin	Cho and Kende, 1997b
Os-EXP4	increase	deepwater rice	expansin	Cho and Kende, 1997b
GAD1	decrease	GA-deficient tomato	similarity to proteinase inhibitors	Jacobsen and Olszewski, 1996
GAD2	decrease	GA-deficient tomato	similarity to 2-oxoglutarate-dependent dioxygenases	Jacobsen and Olszewski, 1996
GAD3	decrease	GA-deficient tomato	similarity to alcohol dehydrogenases	Jacobsen and Olszewski, 1996
At2301	decrease	GA-deficient *Arabidopsis*	GA 20-oxidase	Phillips *et al.,* 1995
At2353	decrease	GA-deficient *Arabidopsis*	GA 20-oxidase	Phillips *et al.*, 1995
YAP169	decrease	GA-deficient *Arabidopsis*	GA 20-oxidase	Phillips *et al.*, 1995

encoded by RSI-1 is identified because of increase in transcript levels in lateral root primordia, especially after auxin treatment. While *GAST1* is predominantly expressed in the shoot, *RSI-1* is predominantly expressed in the root. Whether GA plays a role in *RSI-1* transcript accumulation is unknown. Four less related genes have been identified in *Arabidopsis*, *GASA1* to *GASA4* (Herzog *et al.*, 1995). These genes display a tissue-specific expression pattern, and transcript levels of *GASA1* and *GASA4* are transiently increased by GA. The sequence similarity between GASA1, -2, -3, and -4 on the one hand, and GAST1, RSI-1 and GIP on the other hand, is restricted to the C-terminal half of the protein. However, all putative proteins are predicted to contain a signal sequence, and hydrophobic cluster analysis indicates the presence of similar domains in all of them (Herzog *et al.*, 1995).

In seedlings of a GA-deficient pea line, increased transcript and enzyme activity levels of an invertase have been observed after GA treatment (Wu *et al.*, 1993), as well as a marginal, transient increase in the transcript levels of two genes, *PsG-A* and *PsG-F*, whose sequences are not yet known (Cohn *et al.*, 1994). GA treatment of GA-deficient *Arabidopsis* plants have been found to result in the increase in transcript levels of a gene encoding a tonoplast water channel protein, γ-TIP (Phillips and Huttly, 1994). In the leaf blades of a GA-deficient barley line, an increase in transcript levels of two genes whose encoded proteins share sequence similarity to xyloglucan endotransglycosylase enzymes (XET; Smith *et al.*, 1996), EXT11 and PM2, have been observed after GA treatment. During rapid growth, cells expand and have to maintain turgor pressure. Invertases and water channel proteins are implicated in this process. As will be described below, XET may be involved in cell wall expansion. In another study, transcript levels of two genes, *ESA1* and *ESA2*, accumulate in response to GA in the leaf blades of GA-deficient

barley plants (Speulman and Salamini, 1995). Interestingly, *ESA1* has potentially two ORFs, one of which has similarity to epidermal growth factor. ESA2 has similarity to LEA (late embryogenesis abundant) proteins induced during dehydration and by ABA. The *ESA1* and *ESA2* genes are, however, neither auxin nor ABA regulated (Speulman and Salamini, 1995). In cucumber seedlings, a gene has been identified, *CRG16*, whose transcript levels increase marginally after GA application. No amino acid sequence similarity to known proteins was found. However, the promoter of this gene contains a putative GA responsive element (GARE) found in promoters of α-amylase genes whose transcription is induced by GA in the aleurone of cereal grains (Chono *et al.*, 1996).

The genes decribed above show an increase in transcript levels after GA treatment. Jacobsen and Olszewski (1996) have identified three genes (*GA down*: *GAD1* to *GAD3*) whose transcript levels decrease upon GA treatment. The protein encoded by the *GAD1* gene shows similarity to proteinase inhibitors, and transcript levels of this same gene are found to be increased during auxin-induced lateral root initiation as well (Taylor *et al.*, 1993). GAD2 has similarity to 2-oxoglutarate-dependent dioxygenases but is not related to GA 20-oxidases or 3β-hydroxylases involved in GA biosynthesis. GAD3 has similarity to alcohol dehydrogenases. The decrease in transcript levels of these three *GAD* genes is not specific to GA; auxin and ethylene also decrease the transcript levels of the *GAD* genes (Jacobsen and Olszewski, 1996). As was described above, a decrease in transcript levels is also observed for three genes encoding GA 20-oxidases involved in GA biosynthesis (Phillips *et al.*, 1995).

Plant elongation is not only regulated by GA but also by other plant hormones and environmental factors. This is particularly well illustrated by

mutants in pea (*lkb* and *lk*) and tomato (*d*), which were thought to belong to the reduced GA signaling class but have recently been shown to have defects in brassinolide biosynthesis (Bishop *et al.*, 1996; Nomura *et al.*, 1997). Light has a profound effect on elongation via the action of phytochrome and some phytochrome mutants look like GA-treated wild-type plants. Dose-response curves with *Arabidopsis* hypocotyls show that the double mutant *phyB ga1-3* is more responsive to applied GA than the single mutant *ga1-3*, indicating that the *phyB* mutant magnifies the response to GA (Reed *et al.*, 1996).

It is important to carefully select the system in which to study GA-regulated processes. Most of the gene expression studies described above were done with GA-deficient seedlings. In seedlings, many developmental processes are taking place concurrently, and several plant hormones, as well as environmental factors, play an intricate role in the outcome. Also, treatment of "severe" GA-deficient mutants with GA may have a similar effect as removal of hydroxyurea or colchicine from cell cultures to release the block of progression through the cell cycle. Suddenly, several genes transiently change their expression pattern of which many may have nothing to do with the GA-regulated process *per se*.

Knowledge gained from one system cannot automatically be applied to another system. For example, both barley leaf blades and leaf sheaths show increased elongation upon GA treatment. However, the transcript levels of the *ESA1* and *ESA2* genes increase only in leaf blades (Speulman and Salamini, 1995). Promotion of growth in cucumber leaves is clearly promoted by GA, but transcript levels of the *CRG16* gene do not increase in leaves as they do in hypocotyls (Chono *et al.*, 1996). Lastly, transcript levels of the same gene can increase in young roots and hypocotyls (Taylor *et al.*, 1993), while

decreasing in more mature tissue in response to the same stimulus (Jacobsen and Olszewski, 1996).

Deepwater rice internodes in the vegetative adult phase are induced to elongate rapidly during partial submergence. The increase in elongation rate is, ultimately, mediated by GA, while auxin, another growth-promoting hormone, has no effect in these internodes. The following paragraphs describe in detail the analyses of submergence- and GA-mediated rapid growth response in deepwater rice internodes.

1.5. THE ANATOMY OF THE RICE INTERNODE AND CELL WALL CHANGES DURING RAPID GROWTH

Based on cell size measurements and [^{3}H]thymidine incorporation studies (Métraux and Kende, 1984; Bleecker *et al.*, 1986), the internode can be divided into three regions, as shown in Figure 1.1. At the base of the internode is the intercalary meristem (IM), 2-3 mm in length where cells divide; the elongation zone (EZ) where cells reach their final length; and the differentiation zone (DZ) where secondary wall and xylem formation takes place. The high growth rates attained upon submergence, ethylene or GA treatment are achieved by a 3-fold increase in the rate at which cells are produced in the IM and a 3- to 4-fold increase in the final length of cells in the EZ (Raskin and Kende, 1984b; Métraux and Kende, 1984; Bleecker *et al.*, 1986).

Upon submergence, differences in cell wall composition are observed between newly elongated parts of the internode and pre-existing parts or air-grown internodes (Rose-John and Kende, 1984; Azuma *et al.*, 1996). Primary cell walls consist of cellulose microfibrils interconnected by matrix

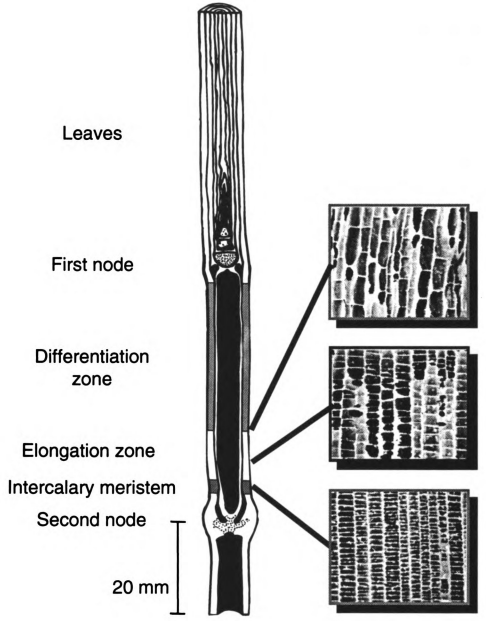

Figure 1.1. Longitudinal median section through a 20-cm-long rice stem section. The second node is separated from the first node by the youngest internode. The locations of the intercalary meristem, the elongation zone, and the differentiation zone are indicated along the internode. The stem section above the first node consists of leaf sheaths and developing leaves. On the right are scanning electron micrographs of parenchyma cells from a stem section treated with 50 μM GA_3 for 24 h. The top micrograph are cells from the differentiation zone, the middle micrograph are cells from the elongation zone and the bottom micrograph are cells from the intercalary meristem. From Sauter and Kende, 1992b.

polysaccharides. The direction of cell growth is determined by the arrangement of the cellulose microfibrils which, in turn, is determined by the orientation of cortical microtubules. Elongation is favored when the the cellulose microfibrils are oriented transversly to the direction of growth. In rice internodes, the orientation of the cellulose microfibrils is transverse in the growing zone, and this orientation does not change in the parenchyma cell walls even outside the growing region. In the outer epidermal cell walls, however, the orientation is oblique in the non-growing zones, indicating that the epidermis is a growth-limiting structure (Kutschera and Kende, 1988; Sauter *et al.*, 1993). In GA-treated rapidly growing internodes, the change from transverse to oblique is more gradual and extends over the length of the elongation zone (Sauter *et al.*, 1993). One of the major matrix polysaccharide in monocots is (1->3, 1->4)-β-glucan, which is thought to be involved in cell growth (Carpita and Gibeaut, 1993). Higher levels of β-glucan are found in cell walls of elongating cells than in walls of non-growing cells. Submergence greatly extends the EZ as well as the zone of high β-glucan levels (Sauter and Kende, 1992a). In contrast, lignin content and activity of coniferyl alcohol dehydrogenase and phenylalanine ammonia-lyase, two enzymes in the lignin biosynthesis pathway, are up to six-fold lower in rapidly growing rice internodes than in air-grown rice internodes. It seems that the process of lignification is suppressed to permit rapid growth (Sauter and Kende, 1992a). The above results indicate that GA extends the EZ in rice internodes by delaying cell wall processes involved in cessation of growth and permitting cell wall processes that favor growth to continue over a longer distance. This effect of GA has also been observed during wheat leaf blade elongation, where the initial relative elemental growth rate (REGR) and maximal REGR remain unchanged whether GA is applied or not (Tonkinson *et al.*, 1995). However,

the extension zone beyond the point of maximum REGR is extended in the presence of GA as compared to control. The addition of paclobutrazol, an inhibitor of GA biosynthesis, decreases the extension zone further; this effect is reversed by the addition of GA, indicating an important role for GA in extending the EZ (Tonkinson *et al.*, 1997). Although GA increases the length of the EZ and the length of the cells in the EZ, it cannot change the fate of cells already in the EZ at the start of GA treatment. For example, GA does not reorient cellulose microfibrils from oblique to transverse in rice internodes. Furthermore, stem sections in which the IM has been removed do not respond to GA treatment (Sauter *et al.*, 1993). Thus, the tissue that responds to GA is the IM, and only cells that move out of the IM into the EZ during GA treatment will increase further in size.

1.6. EVENTS INITIATED BY GA IN THE IM OF ELONGATING RICE INTERNODES

Research in deepwater rice has shown several early effects of GA-induced growth. After 2 h of GA application, the cells in the IM have increased their average length (Sauter and Kende, 1992b). Cell elongation is driven by water uptake into the central vacuole. In rice, increased internodal elongation after submergence is not due to increased hydrolic conductance or decrease in osmotic potential, but to changes in yielding properties of the cell wall (Kutschera and Kende, 1988). The stress relaxation of the cell wall is manifested by an increase in extensibility after submergence (Kutschera and Kende, 1988; Cho and Kende, 1997a). GA also increases cell wall extensibility as has been shown in oat internodal segments (Adams *et al.*, 1975) and in

immature wheat leaves (Keyes *et al.*, 1990). Relaxation of cell wall stress is thought to result from the action of cell wall-loosening factors. Amongst them are cell wall enzymes that break covalent bonds, such as hydrolases and endotransglycosylases. In particular, the xyloglucan endotransglycosylase enzyme (XET) has been implicated in the cell wall loosening process (Fry *et al.*, 1992) because of a correlation between XET activity and tissue growth rate. XET activity also provides a mechanism to cause wall loosening without weakening of the wall. GA has been shown to increase XET activity in internodes of a GA biosynthesis mutant pea line (Potter and Fry, 1993) and in leaf blades of a GA biosynthetic barley mutant plant (Smith *et al.*, 1996). The mRNA transcript levels for *EXT11*, encoding XET, is also increased after GA treatment (Smith *et al.*, 1996). However, the role of XET in cell growth is unclear since the enzyme has no effect on extension of isolated cucumber cell walls (McQueen-Mason *et al.*, 1993).

Another group of cell wall loosening factors are the expansins, which act by breaking hydrogen bonds between the cellulose microfibrils and the matrix polysaccharides (McQueen-Mason and Cosgrove, 1994). In rice, expansin protein is detected mainly in the growing region of the internode. During submergence, the amount of expansin increases as does the sensitivity of the tissue to expansin action (Cho and Kende, 1997a). Furthermore, the mRNA level of most expansin genes was highest in growing regions of the plant. One expansin gene, *Os-EXP4*, shows an increase in transcript levels within one hour after GA-treatment and submergence, while that of *Os-EXP2* has increased after 6 h of submergence (Cho and Kende, 1997b). Whether the onset of increased transcript levels for *Os-EXP4* correlate with the onset of increased extensibility remains to be determined. However, the onset of increased mRNA accumulation of *Os-EXP4* correlates very well with the 40-

min lag phase of GA-induced growth (Sauter and Kende, 1992b; Cho and Kende, 1997b).

Besides cell enlargement, GA application also leads to changes in cell cycle activity. The transcript levels of *cdc2Os-2* are increased 1 h after addition of GA (Sauter *et al.*, 1995). After 4 h, the number of cells in the G2 phase of the cell cycle decreases, indicating an accelerated rate of mitosis (Sauter and Kende, 1992b). This change coincides with an increase in the *in vitro* phosphorylation of histone H1 and an increase in the expression of two mitotic cyclin genes (Sauter *et al.*, 1995). After 7 h of GA treatment, the rate of DNA synthesis increases. This increase coincides with an increase in expression of another gene encoding a histone H3, which is correlated with the S-phase of the cell cycle (Van der Knaap and Kende, 1995). These results lead us to conclude that GA promotes cell elongation and subsequently cell division in the IM. In addition, the cell cycle appears to be first induced at the G2/M phase transition followed by an increase in DNA synthesis (Sauter and Kende, 1992b).

Internodal elongation of deepwater rice during the vegetative adult phase is a very good system to study growth and GA-regulated gene expression. The response is physiologically very important for survival of the plant, it is fast, and specific for GA. The internode of deepwater rice has been studied extensively to identify early GA-regulated events in the IM, which is the primary site of action for GA. The identification of early GA-regulated genes from the IM of deepwater rice internodes may help us understand how this remarkable growth response is achieved. The following Chapters describe the experiments designed to identify and characterize early GA-regulated genes. The identification of these genes will allow an assessment of their role

in GA-regulated processes in the IM of rice internodes in terms of how they regulate cell elongation and/or the cell cycle. After identification of early-regulated genes we can also address how GA regulates changes in transcript levels.

1.7. LITERATURE

Aach, H., Bode, H., Robinson, D.G. and Graebe, J.E. (1997) *ent*-Kaurene synthase is located in proplastids of meristematic shoot tissues. Planta **202**:211-219.

Adams, P.A., Montague M.J., Tepfer, M., Rayle, D.L., Ikuma, H. and Kaufman, P.B. (1975) Effect of gibberellic acid on the plasticity and elasticity of *Avena* stem segments. Plant Physiol **56**:757-760.

Azuma, T., Sumida, Y., Kaneda, Y., Uchida, N. and Yasuda, T. (1996) Changes in cell wall polysaccharides in the internodes of submerged floating rice. Plant Growth Reg **19**:183-187.

Ben-Nissan, G. and Weiss, D. (1996) The petunia homologue of tomato *gast1*: transcript accumulation coincides with gibberellin-induced corolla cell elongation. Plant Mol Biol **32**:1067-1074.

Bishop, G.J., Harrison, K. and Jones, J.D.G. (1996) The tomato *dwarf* gene isolated by heterologous transposon tagging encodes the first member of a new cytochrome P450 family. Plant Cell **8**:959-969.

Bleecker, A.B., Schuette, J.L. and Kende, H. (1986) Anatomical analyisis of growth and developmental patterns in the internode of deepwater rice. Planta **169**:490-497.

Carol, P., Peng, J. and Harberd, N.P. (1995) Isolation and preliminary characterization of *gas1-1*, a mutation causing partial suppression of the phenotype conferred by the gibberellin-insensitive (*gai*) mutation in *Arabidopsis thaliana* (L.) Heyhn. Planta **197**:414-417.

Carpita, N.C. and Gibeaut, D.M. (1993) Structural models of primary cell walls in flowering plants: consistency of molecular structure with the physical properties of the walls during growth. Plant J **3**:1-30.

Catling, H.D., Puckridge, D.W. and HilleRisLambers, D. (1988) The environment of Asian deepwater rice. *In* Proceedings of the 1987 International Deepwater Rice Workshop, Bangkok, Thailand. International Rice Research Institute, Manila, Philippines, pp 11-34

Catling, H.D. (1992) Rice in Deep Water. The Macmillan Press Ltd, London and Basingstoke, UK.

Chandler, P.M. (1988) Hormonal regulation of gene expression in the "slender" mutant of barley (*Hordeum vulgare* L.). Planta **175**:115-120.

Chiang, H.-H., Hwang, I. and Goodman, H.M. (1995) Isolation of the *Arabidopsis GA4* locus. Plant Cell **7**:195-201.

Cho, H.-T. and Kende, H. (1997a) Expansins and internodal growth of deepwater rice. Plant Physiol **113**:1145-1151.

Cho, H.-T. and Kende, H. (1997b) Expression of expansin genes is correlated with growth in deepwater rice. Plant Cell **9**:1661-1671.

Chono, M., Yamauchi, T., Yamaguchi, S., Yamane, H. and Murofushi, N. (1996) cDNA cloning and characterization of a gibberellin-responsive gene in hypocotyls of *Cucumis sativus* L. Plant Cell Physiol **37**:686-691.

Chory, J., Voytas, D.F., Olszewski, N.E. and Ausubel, F.M. (1987) Gibberellin-induced changes in the populations of translatable mRNAs and accumulated polypeptides in dwarfs of maize and pea. Plant Physiol **83**:15-23.

Cohn, N.S., Zhang, L., Mitchell, J.P. and Vierheller, C.-Z.J. (1994) Gibberellin-stimulated changes in abundance of two mRNAs in the developing shoot of dwarf peas (*Pisum sativum* L.). Int J Plant Sci **155**:498-505.

Di Laurenzio, L., Wysocka-Diller, J., Malamy, J.E., Pysh, L., Helariutta, Y., Freshour, G., Hahn, M.G., Feldmann, K.A. and Benfey, P.N. (1996) The *SCARECROW* gene regulates an asymmetric cell division that is essential for generating the radial organization of the *Arabidopsis* root. Cell **86**:423-433.

Eiguchi, M., Sano, R., Hirano, H.-Y. and Sano, Y. (1993) Genetic and developmental bases for phenotypic plasticity in deepwater rice. J Heredity **84**:201-205.

Fry, S.C., Smith, R.C., Renwick, K.F., Martin, D.J., Hodge, S.K. and Matthews, K.J. (1992) Xyloglucan endotransglycosylase, a new wall-loosening enzyme activity from plants. Biochem J **282**:821-828.

Gale, M.D., Law, C.N., Marshall, G.A. and Worland, A.J. (1975) The genetic control of gibberellic acid insensitivity and coleoptile length in a "dwarf" wheat. Heredity **34**:393-399.

Herzog, M., Dorne, A.-M. and Grellet, F. (1995) *GASA*, a gibberellin-regulated gene family from *Arabidopsis thaliana* reated to the tomato *GAST1* gene. Plant Mol Biol **27**:743-752.

Hoffmann-Benning, S. and Kende, H. (1992) On the role of abscisic acid and gibberellin in the regulation of growth in rice. Plant Physiol **99**:1156-1161.

Hossain, M. (1996) Recent developments in the Asian rice economy: challenges for rice research. *In* Rice Research in Asia: Progress and Priorities. Eds: Evenson, R.E., Herdt, R.W. and Hossain, M. CAB INTERNATIONAL and International Rice Research Institute, University Press Cambridge, UK pp 17-33.

Inouye, J. (1985) Varietion of elongation ability in the Asian floating rice (L.) Jap Agri Res Quart **19**:86-91.

International Rice Research Institute. (1984) Terminology for rice growing environments. IRRI, Los Banos, Philippines.

International Rice Research Institute. (1990) World rice database (RICESTAT). IRRI, Los Banos, Philippines.

Jacobsen, S.E. and Olszewski, N.E. (1993) Mutations at the *SPINDLY* locus of *Arabidopsis* alter gibberellin signal transduction. Plant Cell **5**:887-896.

Jacobsen, S.E., Shi, L., Xin, Z. and Olszewski, N.E. (1994) Gibberellin-induced changes in the translatable mRNA populations of stamens and shoots of gibberellin-deficient tomato. Planta **192**:372-378.

Jacobsen, S.E. and Olszewski, N.E. (1996) Gibberellins regulate the abundance of RNAs with sequence similarity to proteinase inhibitors, dioxygenases and dehydrogenases. Planta **198**:78-86.

Jacobsen, S.E., Binkowski, K.A. and Olszewski, N.E. (1996) SPINDLY, a tetratricopeptide repeat protein involved in gibberellin signal transduction in *Arabidopsis*. Proc Natl Acad Sci USA **93**:9292-9296.

Keith, K.A., Raskin, I. and Kende, H. (1986) A comparison of the submergence response of deepwater and non-deepwater rice. Plant Physiol **80**:479-482.

Kende, H. and Zeevaart, J.A.D. (1997) The five "classical" plant hormones. Plant Cell **9**:1197-1210.

Keyes, G., Sorrells, M.E. and Setter, T.L. (1990) Gibberellic acid regulates cell wall extensibility in wheat (*Triticum aestivum* L.). Plant Physiol **92**:242-245.

Khush, G.S. (1997) Origin, dispersal, cultivation and variation of rice. Plant Mol Biol **35**:25-34.

Koornneef, M. and van der Veen, J.H. (1980) Induction and analysis of gibberellin-sensitive mutants in *Arabidopsis thaliana* (L.) Heynh. Theor Appl Genet **58**:257-263.

Kutschera, U. and Kende, H. (1988) The biophysical basis of elongation growth in internodes of deepwater rice. Plant Physiol **88**:361-366.

Lange, T. (1997) Cloning gibberellin dioxygenase genes from pumpkin endosperm by hetrologous expression of enzyme activities in *Escherichia coli*. Proc Natl Acad Sci USA **94**:6553-6558.

Martin, D.N., Proebsting, W.M. and Hedden, P. (1997) Mendel's dwarfing gene: cDNAs from the *Le* alleles and function of the expressed proteins. Proc Natl Acad Sci USA **94**:8907-8911.

McQueen-Mason, S.J., Fry, S.C., Durachko D.M. and Cosgrove, D.J. (1993) The relationship between xyloglucan endotranglycosylase and in-vitro cell wall extension in cucumber hypocotyls. Planta **190**:327-331.

McQueen-Mason, S.J. and Cosgrove, D.J. (1994) Disruption of hydrogen-bonding between plant-cell wall polymers by proteins that induce wall extension. Proc Natl Acad Sci USA **91**:6574-6578.

Mekhedov, S.L. and Kende, H. (1996) Submergence enhances expression of a gene encoding 1-aminocyclopropane-1-carboxylate oxidase in deepwater rice. Plant Cell Physiol **37**:531-537.

Métraux, J.-P. and Kende, H. (1983) The role of ethylene in the growth response of submerged deepwater rice. Plant Physiol **72**:441-446.

Métraux, J.-P. and Kende, H. (1984) The cellular basis of the elongation response in submerged deepwater rice. Planta **160**:73-77.

Morishima, H. (1975) Floating ability as an adaptive character of rice and its measuring method. *In* Proceedings of the 1974 International Seminar on

Deepwater Rice. Bangladesh Rice Research Institute, Dacca, Bangladesh, pp 109-114.

Musgrave, A., Jackson, M.B. and Ling, E. (1972) *Callitriche* stem elongation is controlled by ethylene and gibberellin. Nature New Biol **238**:93-96.

Nomura, T., Nakayama, M., Reid, J.B., Takeuchi, Y. and Yokota, T. (1997) Blockage of brassinosteroid biosynthesis and sensitivity causes dwarfism in garden pea. Plant Physiol **113**:31-37.

Oka, H.I. (1988) Origin of cultivated rice. *In*: Developments in crop science 14. Japan Scientific Societies Press, Tokyo and Elsevier, Amsterdam, 254 pp.

Olszewski, N. (1997) Evidence that dynamic O-linked N-acetylglucosamine modification of proteins plays a role in gibberellin signal transduction. 8th International conference on Arabidopsis research. Madison, Wisconsin.

Peng, J. and Harberd, N.P. (1993) Derivative alleles of the Arabidopsis gibberellin-insensitive (gai) mutation confer a wildtype phenotype. Plant Cell **5**:351-360.

Peng, J., Carol, P., Richards, D.E., King, K.E., Cowling, R.J., Murphy, G.P. and Harberd N.P. (1997) The *Arabidopsis GAI* gene defines a signaling pathway that negatively regulates gibberellin responses. Genes Dev **11**:3194-3205.

Phillips, A.L. and Huttly, A.K. (1994) Cloning of two gibberellin-regulated cDNAs from *Arabidopsis thaliana* by subtractive hybridization: expression of the tonoplast water channel, γ-TIP, is increased by GA_3. Plant Mol Biol **24**:603-615.

Phillips, A.L., Ward, D.A., Uknes, S., Appleford, N.E.J., Lange, T., Huttly, A.K., Gaskin, P., Graebe, J.E. and Hedden, P. (1995) Isolation and expression of three gibberellin 20-oxidase cDNA clones from *Arabidopsis*. Plant Physiol **108**:1049-1057.

Potter, I. and Fry, S.C. (1993) Xyloglucan endotranglycosylase activity in pea internodes. Effects of applied gibberellic acid. Plant Physiol **103**:235-241.

Potts, W.C., Reid, J.B. and Murfet, I.C. (1985) Internode length in *Pisum*. Gibberellins and the slender phenotype, Physiol Plant **63**:357-364.

Raskin, I. and Kende, H. (1983) Regulation of growth in rice seedlings. J Plant Growth Regul **2**:193-203.

Raskin, I. and Kende, H. (1984a) Regulation of growth in stem sections of deepwater rice. Planta **160**:66-72.

Raskin, I. and Kende, H. (1984b) Role of gibberellin in the growth response of submerged deepwater rice. Plant Physiol **76**:947-950.

Reed, J.W., Foster, K.R., Morgan, P.W. and Chory, J. (1996) Phytochrome B affects responsiveness to gibberellins in *Arabidopsis*. Plant Physiol. **112**:337-342.

Rijnders, J.G.H.M., Yang, Y.-Y., Kayima, Y., Takahashi, N., Barendse, G.W.M., Blom, C.W.P.M. and Voesenek, L.A.C.J. (1997) Ethylene enhances gibberellin levels and petiole sensitivity in flooding-tolereant *Rumex palustris* but not in flooding-intolerant *R. acetosa*. Planta **203**:20-25.

Rose-John, S. and Kende, H. (1984) Effect of submergence on the cell wall composition of deepwater rice internodes. Plant Physiol **76**:106-111.

Rose-John, S. and Kende, H. (1985) Short-term growth response of deepwater rice to submergence and ethylene. Plant Science **38**:129-134.

Ross, J.J. and Reid, J.B. (1992) Ontogenetic and environmental effects on GA1 levels and the implications for the control of internode length. *In*: Progress in plant growth regulation. Eds. Karssen, van Loon and Vreugdenhil, Kluwer Academic Publishers, Dordrecht, the Netherlands pp 180-187.

Ross, J.J., Reid, J.B., Swain, S.M., Hasan, O., Poole, A.T., Hedden, P. and Willis, C.L. (1995) Genetic regulation of gibberellin deactivation in *Pisum*. Plant J **7**:513-523.

Sauter, M. and Kende, H. (1992a) Levels of b-glucan and lignin in elongating internodes of deepwater rice. Plant Cell Physiol **33**:1089-1097.

Sauter, M. and Kende, H. (1992b) Gibberellin-induced growth and regulation of the cell division cycle in deepwater rice. Planta **188**:362-368.

Sauter, M., Seagull, R.W. and Kende, H. (1993) Internodal elongation and orientation of cellulose microfibrils and microtubules in deepwater rice. Planta **190**:354-362.

Sauter, M., Mekhedov, S.L. and Kende, H. (1995) Gibberellin promotes histone H1 kinase activity and the expression of cdc2 and cyclin genes during the induction of rapid growth in deepwater rice internodes. Plant J **7**:623-632.

Sauter, M. (1997) Differential expression of a CAK (cdc2-activating kinase)-like protein kinase, cyclins and *cdc2* genes from rice during the cell cycle and in response to gibberellin. Plant J **11**:181-190.

Setboonsarng, S. (1996) Rice research priorities in Thailand. *In* Rice Research in Asia: Progress and Priorities. Eds: Evenson, R.E., Herdt, R.W. and Hossain, M. CAB INTERNATIONAL and International Rice Research Institute, University Press Cambridge, UK pp 217-238.

Shi, L., Gast, R.T., Gopalraj, M. and Olszewski, N.E. (1992) Characterization of a shoot-specific, GA_3- and ABA-regulated gene from tomato. Plant J **2**:153-159.

Silverstone, A.L., Chang, C.-w., Krol, E. and Sun, T.-p. (1997a) Developmental regulation of the gibberellin biosynthetic gene *GA1* in *Arabidopsis thaliana*. Plant J **12**:9-19.

Silverstone, A.L., Mak, P.Y.A., Martinez, E.C. and Sun, T.-p. (1997b) The new *RGA* locus encodes a negative regulator of gibberellin response in *Arabidopsis thaliana*. Genetics **146**:1087-1099.

Silverstone, A.L., Ciampaglio, C.N. and Sun, T.-p. (1998) The Arabidopsis *RGA* gene encodes a transcriptional regulator repressing the gibberellin signal transduction pathway. Plant Cell **10**:155-169.

Smith, R.C, Matthews, P.R., Schunmann P.H.D. and Chandler, P.M. (1996) The regulation of leaf elongation and xyloglucan endotransglycosylase by gibberellin in 'Himalaya' barley (*Hordeum vulgare* L.). J Exp Bot **47**:1395-1404.

Speulman, E. and Salamini, F. (1995) GA_3-regulated cDNAs from *Hordeum vulgare* leaves. Plant Mol Biol **28**:915-926.

Stünzi, J.T. and Kende, H. (1989) Gas composition in the internal air spaces of deepwater rice in relation to growth induced by submergence. Plant Cell Physiol **30**:49-56.

Suge, H. (1985) Ethylene and gibberellin: regulation of internodal elongation and nodal root development in floating rice. Plant Cell Physiol **26**:607-614.

Suge, H. (1988) Physiological genetics of internode elongation in submerged deepwater rice. *In* Proceedings of the 1987 International Deepwater Rice Workshop, Bangkok, Thailand. International Rice Research Institute, Manila, Philippines pp 275-285.

Sun, T.-p., Goodman, H.M. and Ausubel, F.M. (1992) Cloning the *Arabidopsis ga1-2* locus by genomic subtraction. Plant Cell **4**:119-128.

Swain, S.M. and Olszewski, N.E. (1996) Genetic analysis of gibberellin signal transduction. Plant Physiol **112**:11-17.

Taylor, B.H., Young, R.J. and Scheuring, C.F. (1993) Induction of a proteinase inhibitor II-class gene by auxin in tomato roots. Plant Mol Biol **23**:1005-1014.

Taylor, B.H. and Scheuring, C.F. (1994) A molecular marker for lateral root initiation: the *RSI-1* gene of tomato (*Lycopersicon esculentum* Mill) is activated in early lateral root primordia. Mol Gen Genet **243**:148-157.

Tonkinson, C.L., Lyndon, R.F., Arnold, G.M. and Lenton, J.R. (1995) Effect of the *Rht3* dwarfing gene on dynamics of cell extension in wheat leaves, and its modification by gibberellic acid and paclobutrazol. J Exp Bot **46**:1085-1092.

Tonkinson, C.L., Lyndon, R.F., Arnold, G.M. and Lenton, J.R. (1997) The effects of temperature and the *Rht3* dwarfing gene on growth, cell extension, and gibberellin content and responsiveness in the wheat leaf. J Exp Bot **48**:963-970.

Tripathi, R.S. and Balakrishna Rao, M.J. (1985) Inheritance studies of characters associated with floating habit and their linkage relationhip in rice. Euphytica **34**:875-881.

Truong, H.-N., Caboche, M. and Daniel-Vedele, F. (1997) Sequence and characterization of two *Arabidopsis thaliana* cDNAs isolated by functional complementation of a yeast *gln3 gdh1* mutant. FEBS letters **410**:213-218.

Van der Knaap, E. and Kende, H. (1995) Identification of a gibberellin-induced gene in deepwater rice using differential display of mRNA. Pl Mol Biol **28**:589-592.

Vergara, B.S., Jackson, B. and De Datta, S.K. (1977) Deep water rice and its response to deep water stress. *In* Climate and Rice: proceedings of the 1976 symposium. International Rice Research Institute, Los Banos, Philippines, pp 301-319.

Vergara, B.S. (1985) Growth and development of the deepwater rice plant. IRRI res paper ser no 103. International Rice Research Institute, Manila, Philippines 38 pp.

Wilson, R.N. and Somerville, C.R. (1995) Phenotypic suppression of the gibberellin-insensitive mutant (*gai*) of *Arabidopsis*. Plant Physiol **108**:495-502.

Winkler, R.G. and Freeling, M. (1994) Physiological genetics of the dominant gibberellin-nonresponsive maize dwarfs, *Dwarf8* and *Dwarf9*. Planta **193**:341-348.

Wu, K., Li, L., Gage, D.A. and Zeevaart, J.A.D. (1996) Molecular cloning and photoperiod-regulated expression of gibberellin 20-oxidase form the long-day plant spinach. Plant Physiol **110**:547-554.

Wu, L.-L., Mitchell, J.P., Cohn, N.S. and Kaufman, P.B. (1993) Gibberellin (GA3) enhances cell wall invertase activity and mRNA levels in elongating dwarf pea (*Pisum sativum*) shoots. Int J Plant Sci **154**:280-289.

Xu, Y.-L., Li, L., Wu, K., Peeters, A.J.M., Gage, D.A. and Zeevaart, J.A.D. (1995) The *GA5* locus of *Arabidopsis thaliana* encodes a multifunctional gibberellin 20-oxidase: Molecular cloning and functional expression. Proc Natl Acad Sci USA **92**:6640-6644.

Yabuta, T. and Sumiki, Y. (1938) On the crystal of gibberellin, a substance to promote plant growth. J Agr Chem Soc Jpn **14**:1526.

Yamaguchi, S., Saito, T., Abe, H., Yamane, H., Murofushi, N. and Kamiya, Y. (1996) Molecular cloning and characterization of a cDNA encoding the gibberellin biosynthetic enzyme *ent*-kaurene synthase B from pumpkin (*Cucurbita maxima* L.). Plant J **10**:203-213.

Zarembinski, T.I. and Theologis, A. (1997) Expression characteristics of *OS-ACS1* and *OS-ACS2*, two members of the 1-aminocyclopropane-1-carboxylate synthase family in rice (*Oryza sativa* L. cv. Habiganj Aman II) during partial submergence. Plant Mol Biol **33**:71-77.

Zwar, J.A. and Chandler, P.M. (1995) α-Amylase production and leaf protein synthesis in a gibberellin-responsive dwarf mutant of "Himalaya" barley (*Hordeum vulgare* L.). Planta **197**:39-48.

CHAPTER 2

Modification of the differential display method and identification of differentially expressed genes in gibberellin-treated deepwater rice internodes

2.1. ABSTRACT

Differential display was performed to identify genes differentially expressed following gibberellin (GA) treatment of rice stem sections. The technique was optimized and resulted in the identification of four differentially expressed genes. The transcript levels of *dd3*, *dd4*, *dd12* and histone H3 increased after GA treatment, while transcript levels remained constant in control stem sections. Another differentially expressed gene, *OsTMK* was identified serendipitously. A cDNA library was constructed from RNA isolated from intercalary meristems of rice internodes, and full-length cDNA clones of *dd3*, *dd4*, *dd12* and *OsTMK* were isolated.

2.2. INTRODUCTION

Survival of deepwater rice during flooding is based on its capacity for rapid internodal elongation when it becomes submerged. The signal for accelerated growth is an increase in ethylene levels, which enhances the responsiveness of the internode to GA (Raskin and Kende, 1984a). Enhanced growth is initiated in the intercalary meristem (IM) at the base of the growing internode and is based on increased production of cells and increased elongation of these cells after they emerge from the meristem into the elongation zone (EZ) (Bleecker *et al.*, 1986; Sauter and Kende, 1992). Rice stem sections containing the growing internode can be isolated and respond to submergence, ethylene and GA in the same fashion as whole plants (Raskin and Kende, 1984b). The lag phase of GA-induced growth in stem sections is 40 min (Sauter and Kende, 1992). After 2 h of GA application, the cells in the IM have increased their average length. After 4 h, the number of cells in the G2 phase of the cell cycle has decreased indicating an accelerated rate of mitosis (Sauter and Kende, 1992). After 7 h of GA treatment, the rate of DNA synthesis increases. These results have led to the conclusion that GA promotes cell elongation and then cell division in the IM (Sauter and Kende, 1992).

We were interested in identifying genes whose transcript levels are altered in response to GA. There are three principal methods to identify differentially expressed genes. (i) In differential screening, duplicate filters containing a cDNA library are screened with a probe derived either from RNA isolated from induced or uninduced tissues. By comparing hybridization signal intensity of the duplicate filters, cDNA clones can be identified whose transcript levels are differentially expressed (St. John and

Davis, 1979). Many differentially expressed genes have been identified with this method. However, this method can only be used for the analysis of relatively abundant genes with large differences in transcript levels. (ii) A more widely used technique is subtractive hybridization. Genes with similar transcript levels in both induced and uninduced tissues are removed by hybridization to each other, leaving behind single stranded transcripts specifically present in induced tissue (Sargent and Dawid, 1983). Although this technique is more sensitive than differential screening, it is technically challenging and suffers from a lack of reproducibility in that different genes may be identified at different times. Also, genes whose transcript levels increase or decrease cannot be identified at the same time. (iii) Recently, a new technique has been developed: differential display of mRNA. RNA isolated from induced and uninduced tissue is reverse transcribed and amplified with an oligo dT containing and a random decamer primer in the presence of a radioactive nucleotide. The amplified products are separated on a DNA sequencing gel, and the amplified cDNA bands derived from induced and uninduced RNA can be compared. Bands disappearing or appearing as a result of a particular induction can be isolated and further analyzed (Liang and Pardee, 1992). The advantage of this technique is that initial screening is fast, the technique requires only small amounts of RNA, detects transcripts of low abundance and may allow the identification of all differentially expressed genes in the cell. Moreover, genes whose transcripts levels increase or decrease can be detected simultanously, and RNA samples from different time points and/or treatments can be analyzed in the same experiment.

The role of GA-regulated genes in vegetative growth has received relatively little attention. The identification of genes whose transcript levels are increased or decreased early after GA treatment are likely candidates for

key regulatory steps leading to accelerated growth. Therefore, the identification of these genes would allow an assessment of their role in GA-regulated processes in the IM of rice internodes in terms of how they regulate cell elongation and/or the cell cycle. After identification of early-regulated genes we would also be able to address how GA regulates changes in transcript levels. These analyses, in turn, would be complementary to a genetic dissection of the signal transduction pathway leading from GA application to changed gene expression. As described above, GA promotes growth of rice internodes within 40 min. Therefore, we chose to perform a differential display analysis at early timepoints after GA application, namely 0.5, 2.5 and 6.5 h after start of treatment for the pilot study (DD I), and 2 h after start of treatment in case of the larger screen (DD II).

2.3. MATERIALS AND METHODS

PLANT MATERIAL AND GROWTH CONDITIONS

Seeds of deepwater rice (*Oryza sativa* L., cv. Pin Gaew 56) were obtained from the International Rice Research Institute (Los Baños, Philippines). Seeds were germinated in darkness in Petri dishes on moist filter paper at 30°C for three days. Two seedlings were sown in one-quart plastic pots containing Baccto. Ten pots were placed in 6-cm-deep trays, and seedlings were carefully and sparingly watered from the top. After 3 weeks, trays were filled on alternating days with water or half-strength Hoagland solution. Gravel was placed on top of the soil to prevent algal growth, and the plants were staked. After 6 weeks, trays were filled with half-strength Hoagland solution every morning and

with water every afternoon. The plants were grown in an environmental chamber under the following conditions: 13 h light, 27°C; 11 h dark 20°C; relative humidity 80%; 400 μmol m^{-2} s^{-1}. Twenty-cm-long stem sections containing the highest internode were excised from the main stems and tillers of 11- to 13-week-old plants. The sections were cut in such a fashion that that lower node was 2 cm above the basal cut. Only sections in which the growing internode was 3 to 9 cm long were used. All leaf sheaths originating from the nodes not included in the sections were peeled off. The sections were placed in 250-ml beakers containing 30 ml of distilled water and placed in a 2.5-L plastic cylinder through which water-saturated, ethylene-free air at 80 ml min^{-1} was passed. After preincubation for 3 h, GA_3 was added to half of the sections to a final concentration of 50 μM, while the other half was kept in H_2O. Incubation was allowed to proceed for the times indicated under continuous light after which the IM (a 3- to 4-mm-long region above the second highest node) was excised, frozen immediately in liquid nitrogen, and stored at -80°C until use.

RNA ISOLATION

In all cases, except when specified otherwise, RNA was isolated by the guanidine/acid-phenol method (Chomczynski and Sacchi, 1987). The tissue (< 1 g FW) was ground in liquid nitrogen and thawed in 5 ml 4 M guanidine thiocyanate, 25 mM Na-citrate, 0.5% sarkosyl, and 0.1 M β-mercaptoethanol. After addition of 0.5 ml 2 M Na-acetate, pH 4.0, RNA was purified by organic extraction with 5 ml of water-saturated phenol and 1 ml of chloroform. The phases were separated by centrifugation at 12,000*g* for 10 min at 4°C. The RNA in the aquaous phase was precipitated by addition of 5 ml of

isopropanol. After centrifugation at 12.000*g* for 10 min, the RNA pellet was transferred to a 2-ml Eppendorf tube. The RNA was dissolved in 1.5 ml of 4 M LiCl by vortexing for 15 min. It was precipitated by centrifugation at 12,000*g* for 15 min, and the RNA pellet was resuspended again in 1 ml of 4 M LiCl. After vortexing for 15 min, the RNA was precipitated by centrifugation. To remove residual proteins, the RNA pellet was dissolved in 0.6 ml buffer consisting of 10 mM Tris-HCl, pH 7.5, 0.5% SDS, and 1 mM EDTA by vortexing for 10 min and placing the sample at 50°C for 10 min. RNA was extracted with 0.6 ml of 10 mM Tris-HCl, pH 8.0, 1 mM EDTA-equilibrated-phenol (TE-phenol). After centrifugation, the phenol-phase was extracted once again with 0.2 ml 10 mM Tris-HCl, pH 7.5, 0.5% SDS, and 1 mM EDTA. The aqueous phases were pooled and extracted twice with 0.8 ml chloroform, after which the RNA was precipitated with 80 µl 3 M Na-acetate, pH 5.2 and 0.8 ml isopropanol. The pellet was washed with 70% ethanol, dried, and RNA was dissolved in the appropriate amount of water.

The second method for RNA isolation was the phenol method. Tissue (FW < 1 g) was ground in liquid nitrogen and thawed in 5 ml extraction buffer consisting of 50 mM Tris-HCl, pH 7.5, 5 mM EDTA, 100 mM LiCl, 1% SDS, 1% β-mercaptoethanol, and 2.5 ml TE-phenol. The tissue was further homogenized in a Polytron for 3 min. After addition of 7.5 ml chloroform, the organic phase was separated from the aqueous phase by centrifugation at 10,000*g* for 10 min at 4°C. The aqueous phase was extracted once more with chloroform, the RNA was precipitated by addition of 2.5 ml 8 M LiCl, and collected by centrifugation at 12,000*g* for 10 min at 4°C. The RNA pellet was dissolved in 900 µl TE. To remove traces of DNA, the RNA was precipitated by addition of 300 µL 8 M LiCl and collected by centrifugation at 12,000*g* for 10 min at 4°C. To remove the LiCl, which can inhibit reverse transcription, the

RNA was dissolved in 200 µl TE and precipitated again in the presence of 0.3 M Na-acetate, pH 5.2 and 2.5 times the volume of ethanol.

The third RNA isolation method was the TriReagent™ method (Molecular Research Center, Cincinnati, OH). Tissue (FW < 1 g) was ground in liquid nitrogen and thawed in 10 ml of TriReagent solution. The tissue was homogenized in Polytron for 3 min. After addition of 2 ml chloroform, the organic phase was separated from the aqueous phase by centrifugation at 10,000*g* for 10 min at 4°C. The aqueous phase was extracted once more with chloroform, and the RNA was precipitated by addition of an equal volume of isopropanol. Although this RNA should be ready for Northern blot analysis and reverse transcriptase reactions, the pellet dissolved poorly in 600 µl TE and contained many particulates. RNA was, therefore, precipitated again by addition of 600 µl 4 M LiCl and collected by centrifugation for 10 min at 12,000*g* at 4°C. To remove residual proteins, the RNA pellet was dissolved in 0.6 ml 10 mM Tris-HCl, pH 7.5, 0.5% SDS, and 1 mM EDTA by vortexing for 10 min and placing the sample at 50°C for 10 min, after which the sample was extracted with 0.6 ml of TE-phenol. After centrifugation the phenol-phase was extracted once again with 0.2 ml 10 mM Tris-HCl, pH 7.5, 0.5% SDS, and 1 mM EDTA. The pooled aqueous phases were extracted twice with 0.8 ml of chloroform, and the RNA was precipitated with 80 µl 3 M Na-acetate, pH 5.2, and 0.8 ml isopropanol. The pellet was washed in 70% ethanol, dried, and the RNA was dissolved in the appropriate amount of water.

DIFFERENTIAL DISPLAY

To remove traces of DNA, 100 µg of RNA was treated with 100 U DNase I (Boehringer Mannheim Biochemicals [BMB]) in 100 mM Na-acetate, pH 6.2

and 5 mM $MgCl_2$ prior to reverse transcription. The RNA was purified by organic extraction with TE-phenol/chloroform and precipitated with ethanol. The RNA was dissolved in the appropriate amount H_2O, and its integrity was checked by formaldehyde-agarose gel electrophoresis (see below).

Differential display I

Differential display analysis was performed using two different variations of the method (see Figure 2.1). A pilot experiment was set up to study the feasiblity of the technique and to perform control reactions. The primers used in differential display I (DD I) were as follows: one degenerate anchored oligo dT primer $T_{12}MG$ (M stands for A, C and G) synthesized at the Macromolecular Facility at Michigan State University, East Lansing, and 20 random decamer primers OPA 01 to OPA 20 purchased from Operon Technologies (Alameida, CA). Total RNA, 0.4 or 0.8 µg, was annealed to 1 µM of one anchored oligo dT primer and reverse transcribed in a final volume of 20 µl with 100 U of M-MLV reverse transcriptase (Promega) in the presence of 20 µM dNTP, 50 mM Tris-HCl, pH 8.3, 75 mM KCl, 3 mM $MgCl_2$, and 10 mM DTT for 1 h at 37°C. Alternatively, when SUPERSCRIPT II RT (Gibco-BRL) was used, the reaction mixture was incubated for 10 min at 37°C, followed by 50 min at 42°C, under otherwise identical conditions. One-tenth of the reaction mixture was amplified by PCR with 1 µM of the same anchored oligo dT primer, end-labeled with 1.7 µCi of γ-[^{32}P]ATP (6000 Ci/mmol, New England Nuclear [NEN]) per reaction using polynucleotide kinase, and 0.2 µM of one random 10-mer in a final volume of 20 µl containing 10 mM Tris-HCl, pH 8.3, 50 mM KCl, 1 mM $MgCl_2$, 4 µM dNTP, and 2 U Taq polymerase. After 40 cycles, each consisting of 94°C for 30 sec, 40°C for 2 min, and 72°C for 30 sec,

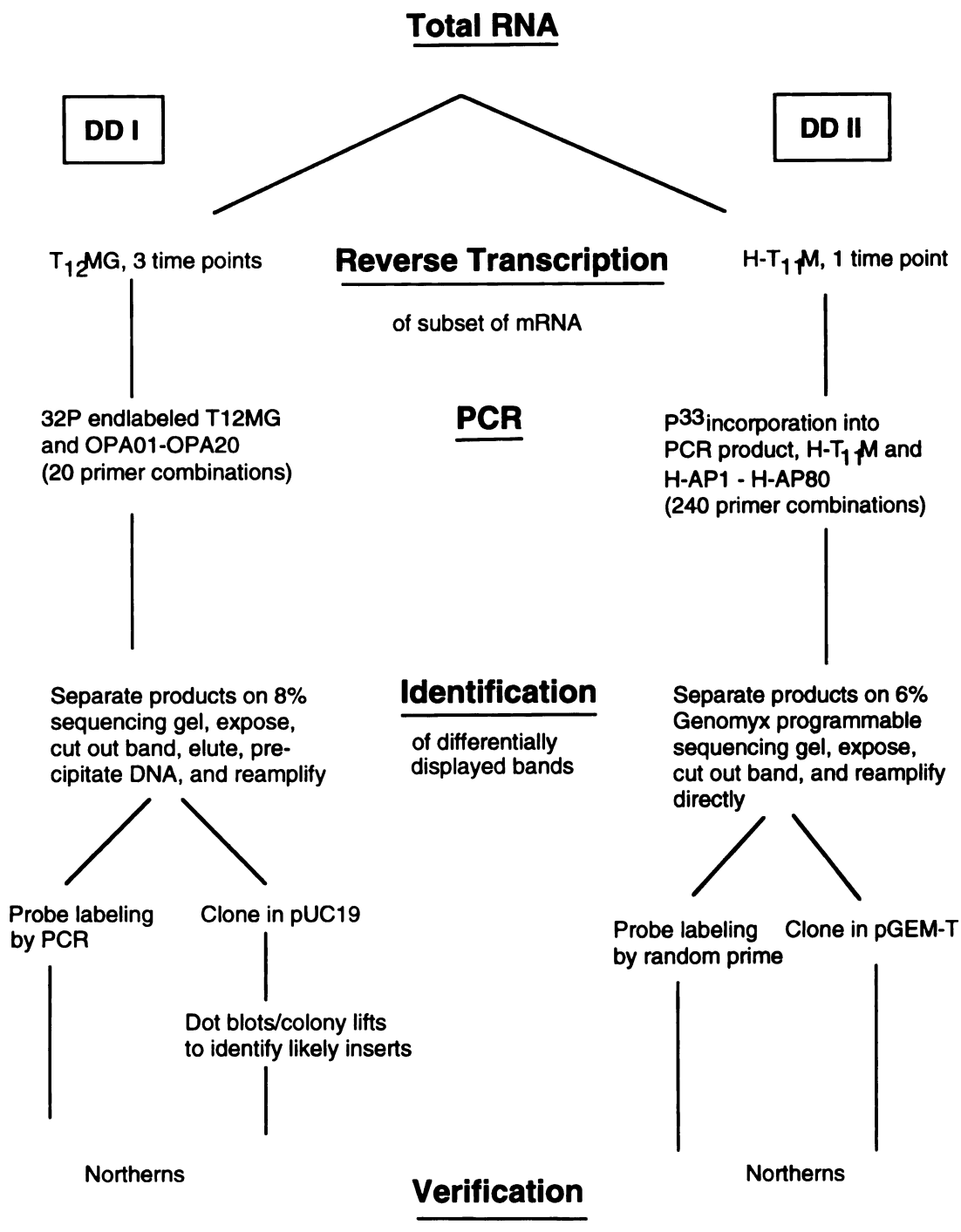

Figure 2.1. Flow chart for the two differential display protocols used in this study.

the PCR products were electrophoretically separated on a 8% denaturing polyacrylamide gel, after which the gel was dried without fixing. X-ray film was exposed to the gel overnight at room temperature.

Reamplification and cloning of DD I products

Differentially displayed products were excised from the gel and eluted by boiling in 100 µl H_2O for 15 min. The DNA was precipitated with ethanol in the presence of 40 µg glycogen as a carrier. The DNA was reamplified without addition of radioactive label under the same reaction conditions as described above, except that the final concentration of dNTP was 20 µM in a volume of 40 µl. After PCR-mediated amplification, the DNA products were incubated in the presence of 20 µg of proteinase K for 1 h at 65°C, purified by TE-phenol/chloroform extraction, and precipitated with ethanol. The generation of blunt-end DNA fragments was mediated by incubation with Klenow enzyme (BMB) for 30 min at room temperature in the presence of 20 µM dNTP. The DNA fragments were phosphorylated with 300 µM ATP and polynucleotide kinase (BMB) for 30 min at 37°C. The products were electrophoretically separated on a non-denaturing polyacrylamide gel. DNA fragments of expected size were isolated by shaking the corresponding gel-slice overnight in 7.5 M NH_4-acetate, 10 mM Mg-acetate, 1 mM EDTA, and 0.1% SDS. DNA was precipitated with ethanol and either labeled for use as a probe or inserted into the dephosphorylated *Sma*I site of pUC 19.

Labeling of DD I products for use as probes

A one-hundredth dilution of differentially displayed products was reamplified under the same reaction conditions as described above, except that 5 µl of α-[^{32}P]dCTP (3000 Ci/mmol, NEN) was added to the PCR, and the final concentration of non-radioactive dCTP was 2.5 µM.

Differential display II

The second differential display method (DD II, see Figure 2.1) was performed by Sandrine Jagoueix, who carried out a screen with 240 primer combinations using 10 RNAimage™ kits (GenHunter Corp, Nashville, TN). The experiments were performed with slight modifications of the manufacturer's specifications. Briefly, 0.2 µg of RNA was reverse transcribed in a total volume of 20 µl in the presence of 20 µM dNTP and 0.2 µM H-T_{11}M (16-mer) in which the H stands for a *Hind*III recognition sequence and M stands for either A, C or G. Two µl of cDNA was amplified with the same H-T_{11}M (0.2 µM) and 0.2 µM H-AP primer (12-mer), which is an arbitrary primer containing a *Hind*III recognition site, in the presence of 4 µM dNTP and 0.25 µl α-[^{33}P]dATP (2000 Ci/mmol, 10 mCi/ml, NEN) in a total volume of 20 µl. PCR conditions were: 95°C for 30 sec, 40°C for 2 min, 72°C for 1 min over 40 cycles. PCR products were separated on a 6% DNA sequencing gel in a Genomyx$_{LR}$ programmable DNA sequencer (Genomyx, Foster City, CA). The gel was dried on the glassplate, and PCR products were visualized by autoradiography.

Reamplification and cloning of DD II products.

Differentially displayed products were excised from the gel and reamplified directly in PCR buffer containing 20 μM dNTP in a total volume of 40 μl under otherwise conditions as described above. DNA fragments were separated on 1.5% agarose gel and isolated from the gel using a Wizard™ PCR prep DNA purification system (Promega). Part of the reamplified cDNA was used for random prime probe labeling, and the remaining cDNA was ligated directly into the pGEM®-T vector (Promega).

NORTHERN BLOT ANALYSIS

Twenty μg of total RNA was electrophoretically separated in a 1.2% agarose gel containing 1.3% formaldehyde, 20 mM MOPS [3-(N-morpholino)-propanesulfonic acid], 5 mM Na-acetate, 1 mM EDTA, pH 7, and 0.2 μg/ml ethidium bromide. After visualization of ribosomal RNA by illumination with UV light, the gel was washed three times for 10 min each in H_2O and equilibrated in 10x SSC for 45 min. RNA was transferred to Hybond-N membrane (Amersham) in 20x SSC transfer buffer. DNA fragments to be labeled as probe were isolated from agarose gels by β-agarase digestion (New England Biolabs [NEB]), after which the DNA was precipitated with ethanol. Fifty ng of template DNA was labeled with α-[^{32}P]dCTP (3000 Ci/mmol, NEN) using a random primer DNA labeling kit (BMB). Northern blots were prehybridized for 4 h at 42°C in 5x SSC, 10x Denhardt's solution, 0.1% SDS, 0.1 M K-PO_4 pH 6.8, and 100 μg/ml denatured salmon sperm DNA and hybridized overnight at 42°C in 5x SSC, 10x Denhardt's solution, 0.1 M K-PO_4, pH 6.8, 100 μg/ml denatured salmon sperm DNA, 10% dextrane sulfate, and

30% formamide. The blots were washed twice in 2x SSC and 0.5% SDS and twice in 0.1x SSC and 0.1% SDS at 65°C for 30 min each. The radioactivity was quantified with a PhosphorImager (Molecular Dynamics, Sunnyvale, CA).

DOT BLOT AND COLONY LIFT HYBRIDIZATION

Plasmids (50 ng) were denatured in 0.5 M NaOH, 1.5 M NaCl and spotted onto Hybond N+ membrane (Amersham) in a BioRad dot blot apparatus. After neutralization in 1.5 M NaCl, 0.5 M Tris-HCl, pH 7.2, and 1 mM EDTA, the DNA was crosslinked to the membrane by baking for 2 h at 80°C. Recombinant *E. coli* cultures were streaked out on selective medium and grown overnight. The next day, a nitrocellulose filter was placed on top of the colonies after which the filter was peeled off. DNA was denatured by placing the filters on Whatman paper soaked in 0.5 M NaOH, neutralized in 1 M Tris-HCl, pH 8, washed in 1 M Tris-HCl, pH 8, 1.5 M NaCl, and washed once more in 2x SSC for 2 min each. The filters were air-dried and baked for 2 h at 80°C. Dot blot and colony lifts were prehybridized for 4 h and hybridized with random prime labeled probe overnight in 6x SSC, 0.5% SDS, 5x Denhardt's solution, and 100 µg/ml denatured salmon sperm DNA at 65°C. Excess probe was washed off twice with 2x SSC and 0.5% SDS and twice with 0.2x SSC and 0.1% SDS at 65°C for 30 min each.

cDNA LIBRARY CONSTRUCTION

Total RNA isolated from the IM of stem sections treated with GA for 0.5, 2.5 and 6.5 h was used for polyadenylated RNA isolation. RNA, 150 µg of each timepoint, was pooled, and NaCl was added to a final concentration of 0.5 M.

Polyadenylated RNA was allowed to bind to BioMag Oligo $(dT)_{20}$ beads (Advanced Magnetics, Cambridge, MA), after which the bound polyadenylated RNA was magnetically separated from the non-polyadenylated RNA. Magnetic particles were washed in 7 mM Tris-HCl, pH 8, 170 mM NaCl, and polyadenylated RNA was eluted with H_2O at 55°C for 2 min. The recovery of RNA was spectrophotometrically determined to be 4 µg. The integrety of the RNA was checked by Northern blot analysis prior to library construction. A SUPERSCRIPT™ Choice System for cDNA synthesis was obtained (Gibco-BRL), and the manufacturer's specifications were followed. Briefly, 3 µg of polyadenylated RNA was reverse transcribed with 400 U SUPERSCRIPT II RT (RNase H-) in the presence of 1 µg oligo $(dT)_{12-18}$ and 50 ng random hexamers in a total volume of 20 µl at 37°C for 20 min followed by 45°C for 30 min. Second-strand synthesis was performed in a total volume of 150 µl in the presence of 10 U *E. coli* DNA ligase, 40 U *E. coli* DNA polymerase I, 2 U *E. coli* RNase H, 1 µl α-[^{32}P]dCTP (3000 Ci/mmol, NEN) for 2 h at 16°C. To blunt-end cDNA, 10 U of T4 DNA polymerase was added to second-strand synthesis reaction, and the incubation was continued for an additional 5 min at 16°C. The cDNA was purified by organic extraction with an equal volume of TE-phenol/chloroform, and the cDNA was precipitated with ethanol. The percent conversion from mRNA to second-strand cDNA was 35% as determined by trichloroacetic acid precipitation, resulting in 0.998 µg of cDNA. After ligation of *Eco*RI (*Not*I, *Sal*I) adapters to both ends of the cDNA, the products were size-fractionated on SEPHACRYL® S-500 HR prepacked columns. Fractions were pooled to two final sizes: one containing 0.6 to 6.6 kb inserts (3.6 kb average) and one containing 0.4 to 4.4 kb inserts (2.4 kb average). Two hundred ng of each size was ligated into 5 µg of *Eco*RI-digested λgt11 arms (Promega) for 3 h at 22°C and packaged for 2 h at 21°C in

Gigapack® III Gold Packaging Extract (Stratagene). The extract was diluted 10 times in SM buffer (50 mM Tris-HCl, pH 7.5, 10 mM NaCl, 8 mM $MgSO_4$, and 0.01% gelatin). The total number of plaque forming units (pfu) of the 3.6-kb average-size library was 6.5×10^6 and the pfu of the 2.4-kb average-size library was 1.65×10^7. One million pfu of both libraries were amplified once and stored at 4°C and, after addition of 7% DMSO, at -80°C.

Screening of cDNA libraries

Host *E. coli* strain LE392 was subcultured from an overnight culture in LB medium supplemented with 0.2% maltose and 10 mM $MgSO_4$ until $A_{600} \sim 0.6$ to 0.8. For the primary screen, 5×10^4 pfu in 200 µl SM buffer per plate were incubated with 200 µl LE392 at 37°C for 20 min. Subsequently, 7 ml of top agar (1 g bacto-tryptone, 0.5 g NaCl, 0.8 g agar, 10 mM $MgSO_4$ per 100 ml) at 48°C was added to the phage-*E. coli* mix, which was immediately plated out on prewarmed LB-plates (150 mm). The phages were grown overnight at 37°C. Plates were cooled to 4°C, after which nitrocellulose filters were placed on top of the agar. Filters were marked with India ink and peeled off. After air drying for 10 min, DNA on filters was denatured for 1 to 2 min in 0.2 M NaOH, 1.5 M NaCl, neutralized for 1 to 2 min in 0.4 M Tris-HCl, pH 7.6, 2x SSC, and washed for 1 to 2 min in 2x SSC. DNA was crosslinked to nitrocellulose by baking for 2 h at 80°C. The filters were prehybridized for 4 h and hybridized with random prime labeled probe overnight in 6x SSC, 0.5% SDS, 5x Denhardt's solution, and 100 µg/ml denatured salmon sperm DNA at 62°C. Excess probe was washed off twice with 2x SSC and 0.5% SDS and twice with 0.2x SSC and 0.1% SDS for 30 min each at 62°C. X-ray film was exposed to the filters for 1 to 3 days at -80°C. Plaques were picked with the wide end of a Pasteur pipet and

eluted in 1 ml SM buffer. The secondary screen was performed using the above described conditions, except that 90-mm Petri plates and 3 ml of top agar were used. Purification was continued until the probe hybridized to 100% of phages on one plate.

Phage purification

Phages were eluted from a single plaque overnight at 4°C in 100 µl SM buffer. Two hundred and fifty µl of an overnight culture of LE392 grown in the presence of 0.2% maltose and 10 mM $MgSO_4$ was incubated with 4 µl phage suspension for 20 min at 37°C. This was added to 50 ml of LB supplemented with 10 mM $MgSO_4$ and shaken until lysis occurred (5 to 7 h). Ten µg/ml RNase A and 1 U/ml DNase I were added, and the lysed culture was incubated at room temperature for 20 min. To remove cellular RNA and DNA, an equal volume of DE52 resin equilibrated in LB was mixed with the phage lysate. After centrifugation, the phage supernatant was treated with 20 mM EDTA, 50 µg/ml proteinase K, and 0.1% SDS at 45°C for 20 min. DNA was purified from the phage heads by repeated organic extraction with an equal volume of TE-phenol until the interphase was clean. The aqueous phase was once extracted with chloroform, and the DNA was precipitated by addition of 1/10 of volume 3 M Na-acetate, pH 6, and 1 volume of isopropanol. The DNA pellet was dissolved in 100 µL TE at 4°C.

PCR analysis of phage insert size

The insert sizes of phages were checked after the primary screen using a gene-specific primer and either primer of the λgt11 arms. The sequence of the

vector primer were HK115: 5'-CATATGGGGATTGGTGGCGACGACTCC-3' and HK116: 5'-CCAGACCAACTGGTAATGGTAGCGACC-3'. Gene-specific primers were: for *dd3*, HK130: 5'-AGGTGGTGAAAGTAGCCGAGCCGATCCAG-3'; for *dd4*, HK131: 5'-GTCCACAAGCTGCTGCAGATATTACAAGG-3'; for *dd12*, HK159: 5'-AAGGCTAATACTAGCTAGCATCTATTGCAG-3'; for *OsTMK*, 5'-AACATCCGAAAGAGTAGAGAGCACATTGACAG-3'. Two µl of eluted phage was amplified in the presence of 10 mM Tris-HCl pH 8.3, 50 mM KCl, 1.5 mM $MgCl_2$, 50 µM dNTP, and 0.2 µM of each of the primers. After 35 cycles, each consisting of 94°C for 40 sec, 60°C for 1 min, and 72°C for 2 min, the PCR products were electrophoretically separated and visualized on a 1% agarose gel.

2.4. RESULTS

OPTIMIZATION OF DD I

At the start of the pilot study, the reaction conditions used in the original protocol were applied (Liang and Pardee, 1992). However, several control experiments proved to be necessary to optimize the technique. Therefore, first, the concentration of RNA and the number of PCR cycles were varied. As can be seen in Figure 2.2, the banding pattern did not change qualitatively whether 0.1 µg of polyadenylated RNA, 2 µg of total RNA or 0.2 µg of total RNA was used for the reverse transcription reaction. For selected primer combinations, only 30 cycles were necessary to obtain sufficient amplification using 0.1 µg of polyadenylated RNA or 2 µg total RNA (Fig.

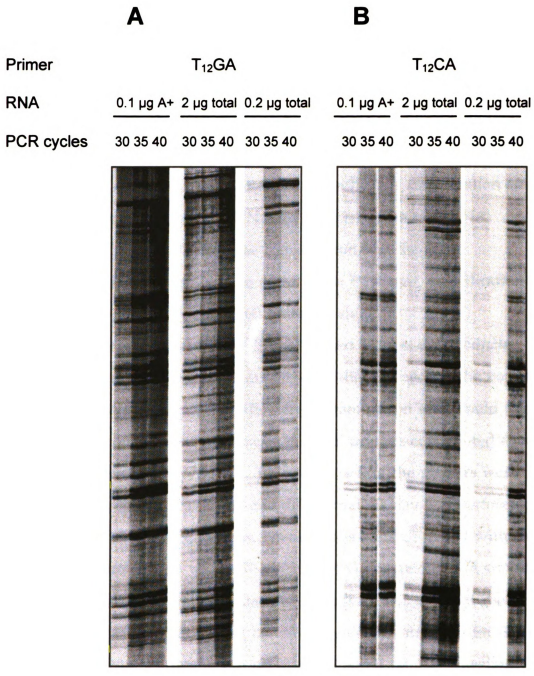

Figure 2.2. Differential display using different RNA concentrations or PCR cycles. Differential display was performed using RNA isolated from GA-treated stem sections at the concentrations indicated above the lanes. The cDNA was amplified in the presence of α-[^{35}S]dATP and 2 µM dNTP at an annealing temperature of 42°C and number of PCR cycles as indicated above the lanes. Otherwise, conditions were as described in Materials and Methods.
(**A**) Differential display using $T_{12}GA$ and 5'-GCGGAGGTA-3' as primer pair.
(**B**) Differential display using $T_{12}CA$ and 5'-GCGGAGGTA-3' as primer pair.

2.2A). For other primer combinations, at least 35 cycles were necessary (Fig. 2.2B). An additional number of amplification cycles did not change the banding pattern. Therefore, the number of PCR cycles was maintained at 40. Using 0.2 μg of total RNA did not always give consistent banding patterns. This was shown in Figure 2.2A, where 0.2 μg of total RNA yielded more bands after 35 cycles than after 40 cycles. In Figure 2.2B, some amplification after 30 cycles was observed, none after 35, and sufficient amplification after 40 cycles starting with 0.2 μg of total RNA. By increasing the total RNA concentration to 0.4 μg in the reverse transcription and the final concentration of dNTP from 2 μM to 4 μM in the PCR step, amplification and reproducibility were greatly enhanced (data not shown).

We also observed that the α-[^{35}S]dATP used to label the products during amplification severely contaminated the thermal cycler. The use of ^{32}P end-labeled primers was found to alleviate contamination and would allow us to address the question whether both 3′ and 5′ primers contributed equally to the amplification of the products. Therefore, each of the primers were end-labeled separately with γ-[^{32}P]rATP, and differential display was performed under otherwise identical conditions. Fewer bands were observed with end-labeled T_{12}AG primer than with end-labeled OPA16 primer at PCR conditions described in the original protocol (Liang and Pardee, 1992; data not shown). This suggested that the PCR cycling conditions were too stringent for the T_{12}AG primer. The experiment was repeated by lowering the annealing temperature by 2°C to 40°C. As can be seen in Figure 2.3A, in this case a similar banding pattern was obtained when either end-labeled T_{12}AG primer or end-labeled OPA16 primer was used. We repeated this experiment with other primer combinations (T_{12}MG-OPA03, T_{12}MG-OPA16, and T_{12}AG-OPA04) and found that the banding patterns were similar. We concluded that,

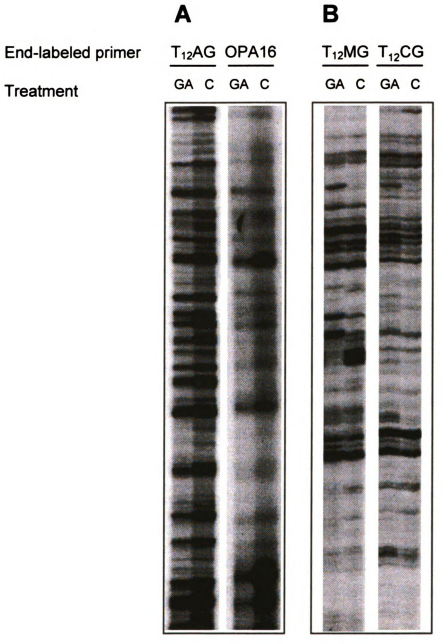

Figure 2.3. Differential display using ^{32}P end-labeled primers. RNA was isolated from the IM of stem sectionstreated for 6.5 h with GA_3, or kept in water as control. (**A**) Comparison of banding patterns obtained using either the oligo dT primer ($T_{12}AG$) or the decamer (OPA16) as end-labeled primer. (**B**) Comparison of banding patterns obtained using either end-labeled degenerate oligo dT primer (T12MG) or end-labeled specific oligo dTprimer (T12CG) and OPA04 as decamer.

under these conditions, both primers contributed equally to the PCR. End-labeling of the oligo dT primer gave the sharpest bands and the most reproducible results and, therefore, this protocol was used in further experiments.

We also compared the banding patterns of degenerate (T_{12}MG) and specific (T_{12}CG) oligo dT primers. As can be seen in Figure 2.3B, the banding pattern obtained with each of the oligo dT primers showed similar as well as different bands. One would expect that more bands will be seen with degenerate than with specific primers. However, this was not the case. With T_{12}MG, more pronounced bands were observed than with T_{12}CG. Therefore, degenerate oligo dT primers were used for the DD I protocol.

The quality of RNA is essential for successful differential display analysis. To test which RNA isolation generated the highest quality RNA for differential display, RNA was isolated by three different methods as decribed in Materials and Methods. Stem sections were treated with GA or kept in water as control, after which differential display was performed with OPA04 and T_{12}MG as primers. In Figure 2.4, the guanidine/acid-phenol method (lanes Gu) is compared to the phenol (lanes Ph) and the TriReagent (lanes Tri) methods. By comparing the amplification products, it is evident that different RNA isolations did not yield differences in banding patterns. This result was not primer-pair specific as the OPA16-T_{12}MG primer pair showed the same results (data not shown).

Besides the quality of RNA, reproducible reverse transcription is also essential in differential display analysis. The banding pattern created by two different reverse transcriptases is shown in Figure 2.4. RNA in the first six lanes was reverse transcribed with Promega M-MLV, while RNA in the second six lanes was reverse transcribed with Gibco-BRL SUPERSCRIPT II RT.

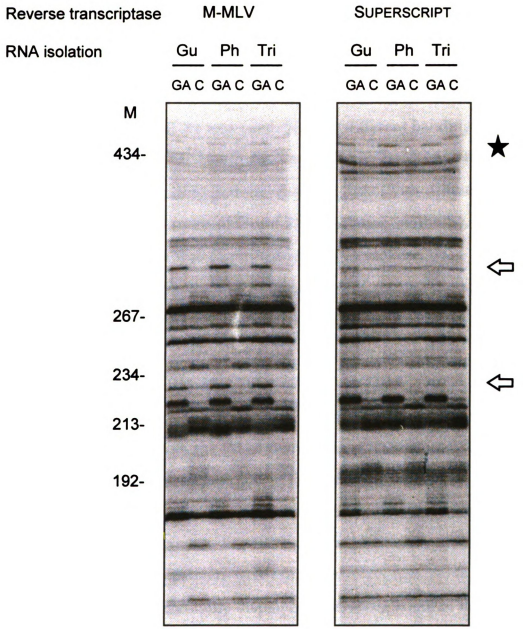

Figure 2.4. Differential display using RNA isolated by different methods and reverse transcriptases. RNA was isolated from the IM of stem sections treated for 6.5 h with GA_3 or kept in water as control, using ^{32}P end-labeled $T_{12}MG$ and OPA04 as primer pair. Gu = Guanidine/acid-phenol method; Ph = phenol method; Tri = TriReagent method as described in Materials and Methods. RNA was reverse transcribed using either M-MLV or SUPERSCRIPT II RT. Star indicates differentially displayed band present preferentially when using SUPERSCRIPT II RT. Arrow indicates displayed band present preferentially when using M-MLV.

As can be seen in Figure 2.4, the two different reverse transcriptases resulted in slightly different banding patterns. For example, two differentially displayed bands, denoted by the arrow, are barely differentially displayed when SUPERSCRIPT II RT was used instead of M-MLV. On the other hand, some differentially displayed bands, denoted by the star, appeared more clearly when SUPERSCRIPT II RT was used. Slightly different banding patterns were observed as well with OPA02-T_{12}MG and OPA10-T_{12}MG as primer pairs (data not shown). Since banding patterns changed little (with different reverse transcriptases) or not at all (with different RNA isolation methods), the differential display analysis was continued with RNA isolated by guanidine/acid-phenol method and Promega M-MLV reverse transcriptase, a technique and enzyme standardly used in our laboratory.

IDENTIFICATION OF GA-REGULATED GENES VIA DD I

RNA was isolated from the IM of stem sections treated for 0.5, 2.5 or 6.5 h with GA or kept for the same amount of time in water as control. To eliminate false positives, each differential display was repeated with RNA isolated in a separate experiment. For DD I, 20 primer combinations using T_{12}MG and OPA1 - OPA20 primers were employed. Very few bands were found to be obviously differentially displayed. Therefore, some of the less convincing bands were also analyzed (Table 2.1). Thirty-eight differentially displayed products were reamplified. Fourteen PCR products were reamplified in the presence of α-[^{32}P]dCTP and used as probe for Northern blot analysis. None were found to contain DNA sequences representing differentially expressed genes. The differential display analysis was repeated using the same primers that led to the identification of those 14 bands. The

Table 2.1. Results of differential display analyses.

	DD I	DD II
Reamplified differentially displayed bands	38	63
Verification of differential expression by Northern blots analysis, with PCR products as probe	14	45
Differentially expressed genes	0	15
GA-regulated differentially expressed genes	0	4
Reproducible differentially displayed bands	4	3
Cloned differentially displayed products	3	3
GA-regulated differentially expressed genes, verified by Northern blot analysis, with cloned insert as probe	3	2

repeat experiment indicated that six of the 14 differentially displayed bands were not reproducibly differentially displayed. In the case of three bands, the labeling intensity on the differential display gel remained constant during GA treatment, while the intensity decreased in the control reaction. For one band, the intensity decreased during GA treatment. The remaining three bands, whose labeling intensity had reproducibly increased during GA treatment, are indicated in Figure 2.5 as *PCR clone 9B*, *dd3* and *dd4*. All three were derived from the same primer pair OPA04-T_{12}MG.

Previously, Northern blot analysis, performed as described above, had failed to show that *dd3* and *dd4* were derived from a gene whose transcript levels had changed during GA treatment. Because *dd3* and *dd4* were consistently differentially displayed, the PCR products were cloned first, after which individual inserts were analyzed. The most convincing differentially displayed product was *PCR clone 9B* (whose PCR product was not used for Northern blot analysis as described above). After reamplification of *PCR clone 9B*, cloning and transformation, 45 colonies were picked and analyzed for plasmid insert. All 45 plasmids contained an insert of the expected size; of these, 38 contained the same insert as verified by dot-blot hybridization (results not shown). One of these inserts was used as hybridization probe on a Northern blot of RNA isolated from the IM of rice stem sections treated with GA, and of RNA isolated from control IM. As shown in Figure 2.6, transcript levels for *PCR clone 9B* had increased during GA treatment. Sequence analysis of *PCR clone 9B* indicated that the clone contained the oligo dT primer at the 3′ end of the gene and OPA04 in the coding region. Except for one unidentified amino acid, the sequence of clone 9B is identical to the corresponding region of histone H3 of rice and other organisms (Van der Knaap and Kende, 1995).

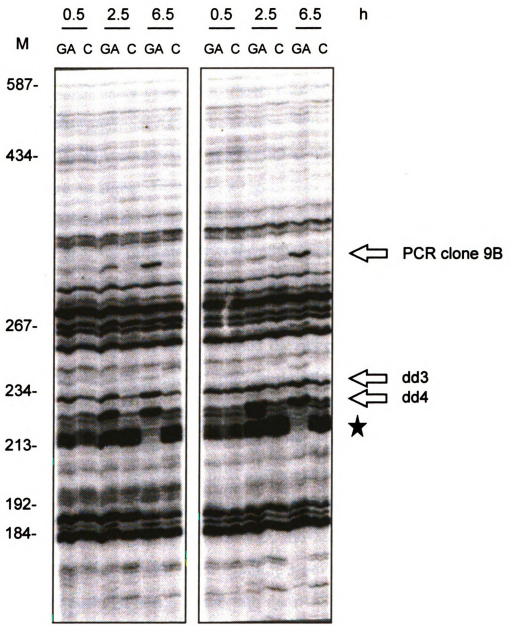

Figure 2.5. Differential display using RNA isolated from the IM of stem sections treated for 0.5 h, 2.5 h and 6.5 h with GA_3 or kept in water. ^{32}P end-labeled $T_{12}MG$ and OPA04 were used as primer pair. The second panel is a repeat of the first one, using RNA isolated in a separate experiment. Star indicates a differentially displayed band which is not reproducibly differentially displayed. Arrows indicate differentially displayed bands which are reproducibly differentially displayed.

After the PCR products corresponding to *dd3* and *dd4* were cloned, a method similar to that described for *PCR clone 9B* was used to identify the most commonly cloned insert. Instead of DNA dot blots, a colony lift identified the most likely insert. This insert was subsequently used as probe for Northern blot analysis. As can be seen in Figure 2.6, the expression of *dd3* increased during GA treatment. For *dd4*, initial Northern blot analysis with total RNA gave no signal. However, a signal was detected on a Northern blot of polyadenylated RNA isolated from GA-treated stem sections. The Northern blot analysis indicated that the transcript levels of the gene encoded by *dd4* increased during GA treatment (data not shown). Figure 2.6 shows the induction pattern of *dd4*, using a longer clone isolated from the cDNA library as probe. Inserts of *dd3* and *dd4* contained the oligo dT primer at the 3′ end of the gene and the OPA04 primer at the 5′ end of the gene. Sequence analysis of *dd3* and *dd4* did not indicate the function of these genes.

Also shown in Figure 2.6 is the signal detected by a cDNA the corresponding mRNA levels of which did not change during the course of the experiment. On a differential display using primer pair $T_{12}MG$ and OPA07, one prominent band, *PCR clone D*, showed equal intensity in all treatments (data not shown). After isolation from the gel, the corresponding cDNA was reamplified and inserted into the pUC19 cloning vector. Sequence analysis indicated 65% amino acid identity to E37, a chloroplast inner-envelope protein isolated from spinach (Dreses-Werringloer *et al.*, 1991; Van der Knaap and Kende, 1995).

IDENTIFICATION OF GA-REGULATED GENES BY DD II

The pilot experiment resulted in the identification of few differentially expressed genes. Further optimization did not increase the number of clear bands per lane, nor reduce the often high background in the lanes. To perform a complete screen, primers and reagents provided in the RNAimage kit were used (GenHunter). To reduce the magnitude of this screen, differential display was performed on RNA isolated at one time point, namely from GA-treated stem sections 2 h after start of treatment and RNA isolated from stem sections incubated for the same amount of time in water as control. Also, instead of using oligo dT primers end-labeled with γ-[^{32}P]rATP, α-[^{33}P]dATP was used in the PCR reaction to label the amplified products. A Genomyx programmable DNA sequencer was purchased, which yielded higher quality sequencing gels and provided cDNA bands of reproducible sharpness. This screen was performed by Dr. Sandrine Jagoueix, and her results are summarized below.

Following the screen with 240 primer combinations, 63 bands were reamplified, 45 of which were tested on Northern blots (Table 2.1). Twenty-six were not differentially expressed, and four gave no signal on Northern blots. The remaining 15 PCR products were differentially expressed, but only four of them had interesting expression patterns: *dd12*, *dd14*, *dd35* and *dd53*. In the case of seven, the intensity of the bands stayed the same in GA-treated stem sections but decreased in water-treated stem sections. For four, the band intensity decreased faster in GA-treated stem sections than in control stem sections. PCR products of *dd12* and *dd14* were purified from agarose gel and inserted into the pGEM-T cloning vector. Northern blot analysis identified inserts from both *dd12* and *dd14* to be clones derived from differentially

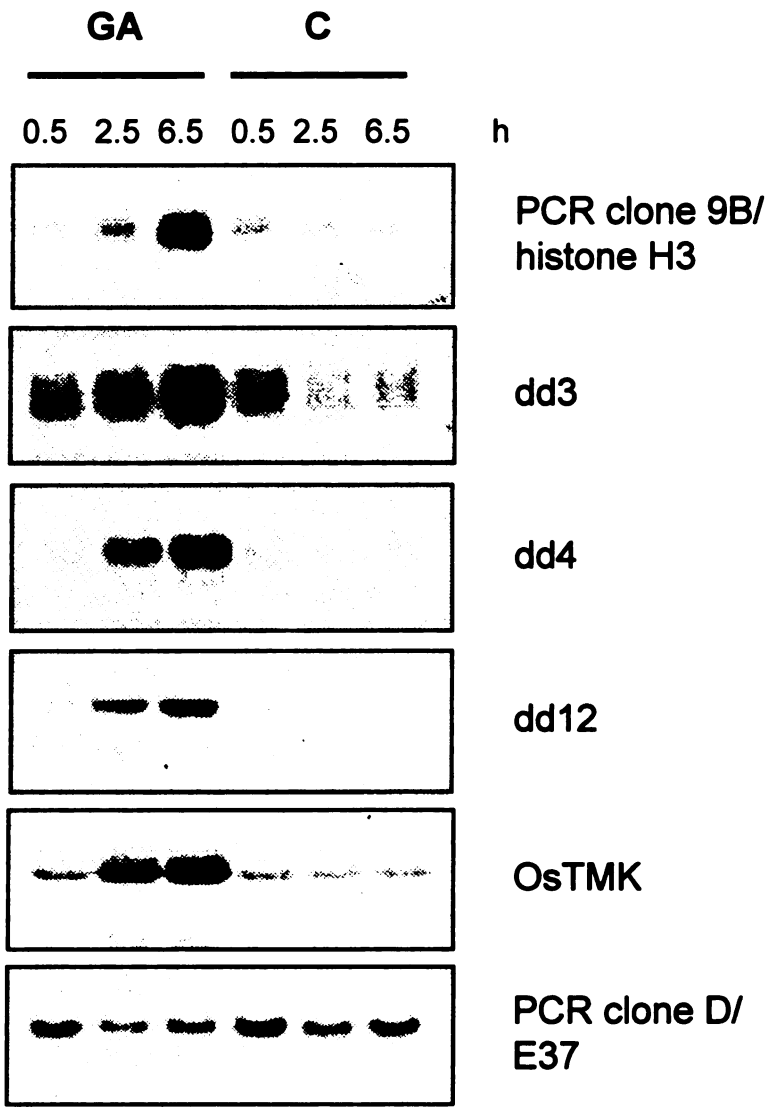

Figure 2.6. Northern blots showing changes in transcript levels of differentially expressed genes in the IM in response to GA. Each lane contains 20 µg of total RNA, isolated from stem sections treated for 0.5 h, 2.5 h and 6.5 h with GA_3 or kept in water as control. Probes for histone H3, *dd12* and *E37* were random prime labeled clones of their respective differentially displayed products. Probes for *dd4* and *OsTMK* were derived from clones isolated from the cDNA library. The probe for *dd3* was riboprobe derived from the 3' UTR as described in Chapter 6.

expressed genes (Fig. 2.6). However, sequence analysis showed that *dd12* and *dd14* were derived from the same gene. They both contained the arbitrary primer H-AP54, but contained different oligo dT primers. The sequence of *dd12* did not identify its function. The PCR product of *dd35* could not be cloned, and repeated differential display failed to show the band again. The PCR product of *dd53* was cloned, but none of the three different inserts tested showed differential expression (data not shown).

The pilot study (DD I) had shown that, if a band is reproducibly differentially displayed, it is mostly likely derived from a gene whose RNA levels have changed. Of the 30 bands that were not differentially expressed or gave no signal on Northern blots, 13 were tested again by differential display with the same primer pairs that had originally identified them. Differential display was reproduced for one band only. After reamplification and cloning, an insert was identified showing differential expression on a Northern blot. However, a time course experiment showed that the transcript levels decreased in control stem sections, but remained constant in GA-treated stem sections. The primer pair that identified *dd12* showed the differentially displayed band *dd12* repeatedly, indicating that its detection was reproducible.

cDNA LIBRARY SCREENS

Inserts, corresponding to the differentially displayed products *dd3*, *dd4* and *dd12*, were used to screen the λgt11 cDNA library. The library was also screened to obtain the full-length clone for *OsTMK*, whose transcript levels increased during GA treatment of stem sections as shown in Figure 2.6. Northern blot analysis had indicated the approximate size of the full-length clones. After the primary phages were identified, PCR with gene-specific

primers was performed to eliminate truncated cDNA clones. Inserts for *dd3* and *dd4* were used to screen the 2.4-kb average size-fractionated library. For *dd3*, four phages were purified to homogeneity that had inserts ranging from 1 to 1.2 kb in size. For *dd4*, ten phages were purified to homogeneity, three of which carried full-length inserts of 1.8 kb. The 3.6-kb average size-fractionated library was screened with inserts corresponding to *dd12* and *OsTMK*. Four phages carrying the *OsTMK* insert, were purified to homogeneity, three of which had full-length inserts of 3.1 kb. For *dd3*, *dd4*, and *OsTMK*, the PCR strategy with gene-specific primers was used to eliminate the purification of severly truncated cDNA clones. It failed, however, to identify full-length clones. For *dd12* PCR analysis identified 12 of 18 primary phages to have full-length inserts. One of these 12 phages was purified to homogeneity and shown to carry a 2.3 kb insert. The sequence analysis of all four clones is given in the following chapters.

2. 5. DISCUSSION

By means of differential display of mRNA, four clones were identified whose transcript levels increased during GA treatment of stem sections. A fifth clone, *OsTMK*, was identified serendipitously by Margret Sauter during a library screen for cyclin genes.

OPTIMIZATION OF DD I

Initial control experiments were necessary to optimize the differential display technique for our purpose. As little as 0.4 µg total RNA gave

reproducible and reamplifiable banding patterns although 0.02 μg of total RNA is sufficient in some systems (Liang *et al.*, 1993). The optimum dNTP concentration in the PCR was 4 μM instead of 2 μM as suggested in the original protocol (Liang and Pardee, 1992, Liang *et al.*, 1993, Liang *et al.*, 1994). This change in concentration was also necessary in DD II to avoid laddering of bands (see below). An often overlooked control is to assess whether the PCR cycling conditions are optimal. Thermal cyclers from different manufacturers have different ramping times and may reach different final temperatures. Using the suggested cycling conditions, we found that 42°C was too stringent an annealing temperature for the anchored oligo dT primer. This was also recently reported by Vielle-Calzada *et al.* (1996). While these authors used an annealing temperature of 35°C to identify differentially displayed bands, for us an annealing temperature of 40°C was sufficient for both primers to contribute equally to the reaction.

After establishing that both primers contributed equally to the amplification of PCR products, the use of ^{32}P end-labeled oligo dT was continued for several reasons. By replacing α-[^{35}S]dATP with γ-[^{32}P]ATP end-labeled oligo dT, severe contamination of the room and the thermal cycler was prevented. α-[^{35}S]dATP forms high levels of volatile ^{35}S -labeled decomposition products during PCR (Trentmann *et al.*, 1995). Also, the use of end-labeled oligo dT primers gave sharper bands than end-labeled decamers (Fig. 2.2). Less sharp bands were observed as well using α-[^{32}P]dCTP in the PCR to label products (Trentmann *et al.*, 1995). Others have found that successful differential display depended on amplification of products derived from the 3' UTR (Tokuyama and Takeda, 1995; Graf *et al.*, 1997). This may be because differentially displayed products from the 3' UTR minimize artifacts arising from variations in cDNA quality. Sequence analysis of many false

positives indicated the presence of the arbitrary primer sequence or an unknown sequence at either end of the fragment, and the absence of the anchored oligo dT primer sequence (Tokuyama and Takeda, 1995). The authors alleviated the problem with ^{33}P end-labeled anchored oligo dT primers and concluded that this modification ensured amplification of the 3' UTR sequences by both the anchored oligo dT primer and the decamer. In another study, far fewer differences were observed than anticipated, and the few differentially displayed products isolated proved to contain the decamer on both ends of the fragment (Graf *et al.*, 1997). By designing arbitrary primers with an A/T content of 60-80%, which corresponds more closely to the A/T content of the 3' UTR, many more differentially expressed genes were identified. In hindsight, this is an additional reason to use end-labeled oligo dT primers to ensure amplification of 3' UTR. Liang *et al.* (1993) found no change in banding pattern whether degenerate or specific anchored oligo dT primers were used. As can be seen in Figure 2.3B, this was not the case in our hands and may be due to using ^{32}P end-labeled oligo dT primers as opposed to α-[^{35}S]dATP in the PCR (Liang *et al.*, 1993).

Further optimization did not lead to improved differential display analysis. For example, different RNA isolation methods did not result in any change in banding patterns as can be seen in Figure 2.4. The guanidine/acid-phenol method used mostly in this thesis resulted in high-quality RNA based on the facts that no degradation products were observed on Northern blots and that several full-length clones of 2 to 3 kb were isolated from the cDNA library. The reverse transcriptases used in this study had different specificities for the template as can be seen in Figure 2.4. Some studies had suggested that the use of two different reverse transcriptases may eliminate false positives (Sung and Denman, 1997). In our case, this would have led to the elimination

of two out of three differentially expressed genes identified during DD I (the arrows in Figure 2.4 correspond to histone H3 and *dd3* respectively). SUPERSCRIPT II RT may be a superior reverse transcriptase for generating cDNA libraries. The rice genome has a high GC content, which can create secondary structure problems in the RNA strand through which reverse transcriptase cannot read. SUPERSCRIPT II RT can perform at higher temperatures and has high processivity through GC-rich sequences. This resulted in long cDNAs as evidenced by the many 2 to 3 kb full-length clones obtained from the library. For differential display, however, amplification of 3' UTR sequences is more preferable (see above). Therefore, the advantage of SUPERSCRIPT II RT over M-MLV was lost.

COMPARISON BETWEEN DD I AND DD II

Although the banding patterns in DD I were reproducible, the bands looked often fuzzy and the lanes contained high background, suggesting suboptimal conditions for running of sequencing gels. Higher quality band patterns were obtained by using a Genomyx programmable sequencer (Averboukh *et al.*, 1996). This resulted in consistenly sharp and reproducible banding patterns, while also being easy to use. The use of longer primers in the differential display (Zhao *et al.*, 1995) yielded more reproducible banding patterns and better separation of longer products on this programmable sequencer (Averboukh *et al.*, 1996). A new generation of GenHunter differential display kits consisted of larger primers (Liang *et al.*, 1994), and this kit was used to perform a complete search for differentially expressed genes.

Both methods for differential display differ in the source of label and in the kind of primers used. DD II made use of RNAimage kits which included

all reaction components except Taq polymerase. During PCR, α-[^{33}P]dATP was incorporated into the reaction products. Compared to DD I using ^{32}P end-labeled oligo dT primer, this may have resulted in a slight increase in number of bands. This is because both strands carried label and may run differently on a denaturing polyacrylamide gel. The advantage of using α-[^{33}P]dATP is that one less manipulation is necessary to complete differential display analysis. The banding pattern in DD I was very reproducible but could vary slightly from day to day. Using DD II, many spurious bands (differentially displayed products between two control RNA samples on the same gel) were obtained with several primer combinations (data not shown). This may be due to the use of only one-base anchored oligo dT primer as compared to two-base anchored oligo dT in DD I. Also, during DD II, a laddering of bands was visible, which was due to either concatemerized primers or concatemerized short PCR products. This concatemerization may be the result of the palindromic *Hind*III site at the very end of both primers. By increasing the dNTP concentration to 4 μM in the PCR, the concatemerization was suppressed, but the spurious bands remained (data not shown). While DD II should have given more efficient cDNA amplification and should have minimized underrepresentation of certain RNA species (Liang *et al.*, 1994), it yielded, in our hands, differential display results that were inferior to those obtained with DD I.

FALSE-POSITIVES IN DIFFERENTIAL DISPLAY

Differential display analysis resulted in the identification of few differentially expressed genes and many false positives. The number of false positives compared to the number of differentially expressed genes was

inflated because, in DD II, 11 more genes were identified to be differentially expressed. However, their transcript level stayed constant during GA treatment but decreased in water-treated control tissue. It is difficult to envision what their role would be in GA-regulated growth. However, a significant number of such 'true' false positives still remained. Since few convincing differentially displayed products were observed, many weak bands were analyzed as well. Initially, *dd3* and *dd4* were identified as false positives. The reamplified and labeled differentially displayed product *dd4* gave no signal on a Northern blot of total RNA (data not shown). However, it was reproducibly differentially displayed and, therefore, reisolated and cloned. With the insert from one of the colonies as probe, a signal could only be detected on blots containing polyadenylated RNA. For *dd3*, at least three different products were contained in the amplified differentially displayed band because three bands were visible on a Northern blot. Two bands were sharp and not differentially expressed. A third band was differentially expressed, but was broad and faint. Therefore, this band was considered background (data not shown). As can be seen in Figure 2.6, the authentic signal for *dd3* is broad and may have been detected on the initial Northern blot.

Although all differential display was repeated side by side (as in Fig. 2.5) with the same primer pair but different batches of RNA, this procedure was not reproducible enough. For example, the band denoted by the star in Figure 2.4 was visible three times with three different RNA isolation methods but was not observed at other times in differential display using the same primer pair. The band was cloned and shown to be a false positive. The bands denoted by the star in Figure 2.5 were false positives also. On repeated

differential display with the same primer pair, the bands were not observed consistently (see Figure 2.4 around 213 bp marker).

In conclusion, instead of chasing down faint bands, it is better to repeat differential display several times. After differentially displayed bands have been identified reproducibly, it is better to clone and to analyze individual inserts instead of using reamplified differentially displayed products as probe for Northern blot analysis. This approach of repeating differentially display and analyzing individual inserts is not feasible when many differential displayed bands have to be evaluated. One approach to deal with this problem is reverse Northern analysis with reverse-transcribed RNA from the different treatments as probe. One can check for true positives either prior to cloning (Zegzouti *et al.*, 1997), or after cloning (Szczyglowski *et al.*, 1997; Poirier *et al.*, 1997). However, differentially displayed products derived from rare transcripts cannot be labeled as true or false positives directly because the signal derived from those RNAs will be too weak.

COMPARISON OF DIFFERENTIAL DISPLAY AND SUBTRACTIVE HYBRIDIZATION: FUTURE ANALYSIS OF DIFFERENTIAL GENE EXPRESSION

Although an extensive search for differentially displayed genes was performed, possibly covering >95% of all genes expressed (Liang and Pardee, 1992; Bauer *et al.*, 1993), not all differentially regulated genes were identified. Transcript levels for two cyclin genes increasing early during GA treatment (Sauter *et al.*, 1995) were not identified. A gene encoding expansin (*Os-EXP4*) was not identified either, although its transcript levels clearly increased 2 h after start of treatment (Cho and Kende, 1997). The reason for not detecting

the cyclin genes and *Os-EXP4* may lay in the fact that differential display cannot always discern between 3- to 6-fold changes in mRNA abundance. Also, differential display may not detect every gene that is differentially expressed. In a study comparing subtractive hybridization to differential display indicated that both methods identified different sets of genes with only two out of 56 clones being identified by both techniques (Wan *et al.*, 1996). Although the differential display was not exhaustive in that case, these authors concluded that amplification in the differential display depended mostly on the primer sequence and the product rather than on abundance, whereas subtractive hybridization mostly dependended on mRNA abundance.

Several new techniques for identifying genes with altered expression patterns have been developed since the start of this work. Although differential display has been a great improvement over differential expression and subtractive hybridization and although this technique can be partially automated (Bauer *et al.*, 1993; Ito *et al.*, 1994; Luehrsen *et al.*, 1997), differential display has its shortcomings (see above). Serial analysis of gene expression (SAGE) can be employed to evaluate the patterns of gene expression in a highly quantitative way with a 97% chance of detecting transcripts as low as one copy per cell (Velculescu *et al.*, 1995). In this method, short sequence tags (11 to 15 base pairs) generated from defined positions within each mRNA molecule are used, and expression patterns are deduced from the abundance of individual tags. The sequence tags generated are long enough to unequivocally determine from which gene they were derived either by database searching (when working with an organism whose genome is extensively studied or entirely sequenced), or by using these tags to identify corresponding cDNA clones by screening a library. SAGE was used in the

analysis of cell-cycle-specific gene expression in yeast (Velculescu *et al.*, 1997), in studying gene expression profiles in normal and cancer cells (Zhang *et al.*, 1997), and in studying the p53-mediated gene regulation in humans (Polyak *et al.*, 1997), and in rat (Madden *et al.*, 1997).

Recent developments made possible by technological improvements and by using whole genome and EST databases have revived the use of differential screening as a tool to identify genes with altered expression patterns (Schena *et al.*, 1995; Chee *et al.*, 1996). Automated scanning for predicted ORFs on each yeast chromosome was used to automatically select PCR primers to amplify each ORF separately. The PCR products were spotted onto microscope slides using high-speed robotics (Lashkari *et al.*, 1997). These so-called microarrays, containing up to 6100 clones or PCR products per 1.8 cm^2, can be used in reverse Northern experiments. RNA isolated from treated and untreated tissue is reverse transcribed and each is labeled with a different fluorescent tag. The probes are hybridized to the same slide, and signals are quantified using laser confocal scanning microscopy, giving a detection limit as high as 1 mRNA molecule in 500,000 (Schena *et al.*, 1996). This technology will allow the identification of all differentially expressed genes in a particular tissue under certain conditions in a matter of hours.

2.6. LITERATURE

Bauer, D., Muller, H., Reich, J., Riedel, H., Ahrenkiel, V., Warthoe, P. and Strauss, M. (1993) Identification of differentially expressed mRNA species by an improved display technique (DDRT-PCR). Nucleic Acids Res **21**:4272-4280.

Bleecker, A.B., Schuette, J.L. and Kende, H. (1986) Anatomical analysis of growth and developmental patterns in the internode of deepwater rice. Planta **169**:490-497.

Chee, M., Yang, R., Hubbell, E., Berno, A., Huang, X.C., Stern, D., Winkler, J., Lockhart, D.J., Morris, M.S. and Fodor, S.P.A. (1996) Accessing genetic information with high-density DNA arrays. Science **274**:610-614.

Cho, H.-T. and Kende, H. (1997) Expression of expansin genes is correlated with growth in deepwater rice. Plant Cell **9**:1661-1671.

Chomczynski, P. and Sacchi, N. (1987) Single-step method of RNA isolation by acid guanidinium thiocyanate phenol chloroform extraction. Anal Biochem **162**:156-159.

Dreses-Werringloer, U., Fischer, K., Wachter, E., Link, T.A. and Fluegge, U.I. (1991) cDNA sequence and deduced amino acid sequence of the precursor of the 37-kDa inner envelope membrane polypeptide from spinach chloroplasts--Its transit peptide contains an amphiphilic alpha-helix as the only detectable structural element. Eur J Biochem **195**:361-368.

Graf, D., Fisher, A.G. and Merkenschlager, M. (1997) Rational primer design greatly improves differential display-PCR (DD-PCR). Nucleic Acids Res **25**:2239-2240.

Ito, T., Kito, K., Adati, N., Mitsui, Y., Hagiwara, H. and Sakaki, Y. (1994) Fluorescent differential display: arbitrarily primed RT-PCR fingerprinting on an automated DNA sequencer. FEBS Letters **351**:231-236.

Lashkari, D.A., DeRisi, J.L., McCusker, J.H., Namath, A.F., Gentile, C., Hwang, S.Y., Brown, P.O. and Davis, R.W. (1997) Yeast microarrays for genome wide parallel genetic and gene expression analysis. Proc Natl Acad Sci USA **94**:13057-13062.

Liang, P., and Pardee, A.B. (1992) Differential display of eukaryotic messenger RNA by means of the polymerase chain reaction. Science **257**:967-971.

Liang, P., Averboukh, L. and Pardee, A.B. (1993) Distribution and cloning of eukaryotic mRNAs by means of differential display: refinements and optimization. Nucleic Acids Res **21**:3269-3275.

Liang, P., Zhu, W., Zhang, X., Guo, Z., O'Connell, R.P., Averboukh, L., Wang, F. and Pardee, A.B. (1994) Differential display using one-base anchored oligo dT primers. Nucleic Acids Res **22**:5763-5764.

Luehrsen, K. R., Marr, L.L., van der Knaap, E. and Cumberledge, S. (1997) Analysis of differential display RT-PCR products using fluorescent primers and GeneScan software. BioTechniques **22**:168-174.

Madden, S.L., Galella, E.A., Zhu, J., Bertelsen, A.H. and Beaudry, G.A. (1997) SAGE transcript profiles for p53-dependent growth regulation. Oncogene **15**:1079-1085.

Métraux, J.P., and Kende, H. (1983) The role of ethylene in the growth response of submerged deepwater rice. Plant Physiol **72**:441-446.

Poirier, G.M.-C., Pyati, J., Wan, J.S. and Erlander, M.G. (1997) Screening differentially expressed cDNA clones obtained by differential display using amplified RNA. Nucleic Acids Res **25**:913-914.

Polyak, K., Xia, Y., Zweier, J.L., Kinzler, K.W. and Vogelstein, B. (1997) A model for p53-induced apoptosis. Nature **389**:300-305.

Raskin, I., and Kende, H. (1984a) Role of gibberellin in the growth response of submerged deep water rice. Plant Physiol **76**:947-950.

Raskin, I., and Kende, H. (1984b) Regulation of growth in stem sections of deep-water rice. Planta **160**:66-72.

Sargent, T.D. and Dawid, I.B. (1983) Differential gene expression in the gastrula of *X. laevis*. Science **222**:135-139.

Sauter, M. and Kende, H. (1992) Gibberellin-induced growth and regulation of the cell division cycle in deepwater rice. Planta **188**:362-368.

Sauter, M., Mekhedov, S.L. and Kende, H. (1995) Gibberellin promotes histone H1 kinase activity and the expression of cdc2 and cyclin genes during the induction of rapid growth in deepwater rice internodes. Plant J **7**:623-632.

Schena, M., Shalon, D., Davis, R.W. and Brown P.O. (1995) Quantitative monitoring of gene expression patterns with a complementary DNA microarray. Science **270**:467-470.

Schena, M., Shalon, D., Heller, R., Chai, A., Brown, P.O. and Davis, R.W. (1996) Parallel human genome analysis: microarray-based expression monitoring of 1000 genes. Proc Natl Acad Sci USA **93**:10614-10619.

St. John, T.P. anf Davis, R.W. (1979) Isolation of galactose-inducible DNA sequences from *S. cerevisiae* by differential plaque filter hybridization. Cell **16**:443-452.

Sung, Y.J., and Denman, R.B. (1997) Use of two reverse transcriptases eliminates false-positive results in differential display. BioTechniques **23**:462-464.

Szczyglowski, K., Hamburger, D., Kapranov, P. and de Bruijn, F.J. (1997) Construction of a *Lotus japonicus* late nodulin expressed sequence tag library and identification of novel nodule-specific genes. Plant Physiol **114**:1335-1346.

Tokuyama, Y. and Takeda, J. (1995) Use of ^{33}P-labeled primer increases the sensitivity and specificity of mRNA differential display. BioTechniques **18**:424-425.

Trentmann, S.M., van der Knaap, E. and Kende, H. (1995) Alternatives to ^{35}S as a label for the differential display of eukaryotic messenger RNA. Science **267**:1186-1187.

Van der Knaap, E. and Kende H. (1995) Identification of a gibberellin-induced gene in deepwater rice using differential display of mRNA. Plant Mol Biol **28**:589-592.

Velculescu, V.E., Zhang, L., Vogelstein, B. and Kinzler, K.W. (1995) Serial analysis of gene expression. Science **270**:484-487.

Velculescu, V.E., Zhang, L., Zhou, W., Vogelstein, J., Basrai, M.A., Bassett Jr, D.E., Hieter, P., Vogelstein, B. and Kinzler, K.W. (1997) Characterization of the yeast transcriptome. Cell **88**:243-251.

Vielle-Calzada, J.P., Nuccio, M.L., Budiman, M.A., Thomas, T.L., Burson, B.L., Hussey, M.A. and Wing, R.A. (1996) Comparative gene expression in sexual and apomictic ovaries of *Pennisetum ciliare* (L.) Link. Plant Mol Biol **32**:1085-1092.

Wan, J.S., Sharp, S.J., Poirier, G.M.-C., Wagaman, P.C., Chambers, J., Pyati, J., Hom, Y.-L., Galindo, J.E., Huvar, A., Peterson, P.A., Jackson, M.R. and Erlander, M.G. (1996) Cloning differentially expressed mRNAs. Nature Biotech **14**:1685-1691.

Zegzouti, H., Marty, C., Jones, B., Bouquin, T., Latche, A., Pech, J.C. and Bouzayen, M. (1997) Improved screening of cDNAs generated by mRNA differential display enables the selection of true positives and the isolation of weakly expressed messages. Plant Mol Biol Rep **15**:236-245.

Zhang, L., Zhou, W., Velculescu, V.E., Kern, S.E., Hruban, R.H., Hamilton, S.R., Vogelstein, B. and Kinzler, K.W. (1997) Gene expression profiles in normal and cancer cells. Science **276**:1268-1272.

Zhao, S., Ooi, S.L. and Pardee, A.B. (1995) New primer strategy improves precision of differential display. BioTechniques **18**:842-850.

CHAPTER 3

Expression of an ortholog of replication protein A1 (RPA1) is induced by gibberellin in deepwater rice

3.1. ABSTRACT

Internodes of deepwater rice are induced to grow rapidly when plants become submerged. This adaptation enables deepwater rice to keep part of its foliage above the rising flood waters during the monsoon season and to avoid drowning. This growth response is, ultimately, elicited by the plant hormone gibberellin (GA). The primary target tissue for GA action is the intercalary meristem of the internode. Using differential display of mRNA, we have isolated a number of genes whose expression in the intercalary meristem is regulated by GA. The product of one of these genes was identified as an ortholog of replication protein A1 (RPA1). RPA is a heterotrimeric protein involved in DNA replication, recombination, and repair and also in regulation of transcription. A chimeric construct, in which the single-stranded DNA-binding domain of rice *RPA1* was spliced into the corresponding region of yeast *RPA1*, was able to complement a yeast *rpa1* mutant. The transcript level of rice *RPA1* is high in tissues containing dividing cells. *RPA1* mRNA levels increase rapidly in the intercalary meristem during submergence and treatment with GA prior to the increase in the level of histone H3 mRNA, a marker for DNA replication.

3.2. INTRODUCTION

Deepwater rice (*Oryza sativa* L.) is a subsistence crop in regions of Southeast Asia that are flooded during the monsoon season (Catling, 1992). To avoid drowning, it has evolved the capacity to elongate very rapidly when it becomes submerged. This adaptation permits deepwater rice to keep part of its foliage above the rising flood waters. In the flood plains of Bangladesh, elongation rates of up to 25 cm day^{-1} have been reported (Vergara *et al.*, 1976); in our laboratory, we have measured growth rates of up to 5 mm h^{-1} (Stünzi and Kende, 1989). Understanding the physiological and molecular basis of the growth response in deepwater rice is important for two reasons. It may help in identifying the gene(s) that could confer elongation capacity onto modern, high-yielding rice cultivars. Deepwater rice is also an excellent object in which to study basic aspects of plant growth because of its unusually high growth rate, which is under environmental and hormonal control.

In earlier work, we examined the environmental and hormonal regulation of the growth response in deepwater rice and the cellular basis of rapid internodal elongation. The plant hormone ethylene accumulates in submerged internodes because of enhanced synthesis under reduced partial pressures of O_2 and because of its low rate of diffusion from the plant into the surrounding water (Raskin and Kende, 1984a). The interaction of ethylene and two other plant hormones *i.e.* abscisic acid, and gibberellin (GA), determines the growth rate of the plant. Ethylene renders the internode more responsive to GA (Raskin and Kende, 1984b), at least in part by lowering the level of endogenous abscisic acid, a potent antagonist of GA action in rice (Hoffmann-Benning and Kende, 1992). Growth of the internode is, ultimately, promoted by GA (Raskin and Kende, 1984b).

The primary target tissue of GA is the intercalary meristem of the internode, where GA enhances cell division activity and cell elongation (Raskin and Kende, 1984b; Sauter and Kende, 1992b; Sauter *et al.*, 1993). The intercalary meristem is a zone of about 3 mm in length and is located at the base of the internode (Bleecker *et al.*, 1986). Cells are displaced from the intercalary meristem into the elongation zone, where they reach their final size. In GA-treated internodes, the final cell length is about three to four times longer than in control internodes (Raskin and Kende, 1984b; Sauter and Kende, 1992b). Correspondingly, the length of the elongation zone expands from about 10 to 35 mm upon treatment with GA (Sauter *et al.*, 1993). Growth stops above the elongation zone in the differentiation zone, where lignification of developing metaxylem and cortical sclerenchyma takes place (Bleecker *et al.*, 1986; Sauter and Kende, 1992a).

We have investigated the effect of GA on cell division activity in the intercalary meristem and have correlated the progression of cells through the cell cycle to molecular events that regulate it. The fraction of meristematic cells in the G2 phase declined within 4 h of GA treatment, indicating that these cells had entered mitosis (Sauter and Kende, 1992b). The expression of two cyclin genes in the intercalary meristem was enhanced by GA, and the time course of induction was compatible with a role for both cyclins in regulating the transition from the G2 to M phase (Sauter *et al.*, 1995). Between 4 and 7 h of incubation in GA, the rate of [^{3}H]thymidine incorporation into DNA doubled, showing an increase in DNA synthesis (Sauter and Kende, 1992b). In a screen for GA-regulated gene expression using differential display of mRNA (Liang and Pardee, 1992), we identified a histone H3 gene whose transcript level increased in parallel with the GA-induced rise in DNA synthesis (Van der Knaap and Kende, 1995). In this report, we are describing

the results of further screening, which led to the identification of a gene that encodes an ortholog of replication protein A1 (RPA1). In the internode, this gene is expressed in the intercalary meristem, and its transcript level increases as a result of GA treatment and submergence.

3.3. MATERIALS AND METHODS

PLANT MATERIAL

Deepwater rice (*Oryza sativa* L., cv. Pin Gaew 56) was obtained from the International Rice Research Institute, Los Baños, Philippines, and grown as described (Stünzi and Kende, 1989). For submergence experiments, 12-week-old plants were partially immersed in deionized water (Métraux and Kende, 1983) and kept under continuous light. Stem sections containing the growing internode were excised and treated with 50 µM gibberellin A_3 (gibberellic acid, GA_3) for the periods indicated (Raskin and Kende, 1984a).

DIFFERENTIAL DISPLAY OF mRNA

RNA was isolated according to Puissant and Houdebine (1990) from the intercalary meristem of internodes treated for 2 h with GA_3 or distilled water as control. Prior to reverse transcription, the RNA was treated with DNase I (Boehringer Mannheim) to remove residual DNA. Differential display (Liang and Pardee, 1992) was performed with RNAimage^{TM} kits (GenHunter, Nashville, TN) with slight modifications of the manufacturer's specifications. Briefly, 0.2 µg of RNA was reverse transcribed in a total volume of 20 µl in

the presence of 20 μM dNTP and 0.2 μM H-T_{11}M for 1 h. Two μl of cDNA was amplified with the same H-T_{11}M (0.2 μM) primer and 0.2 μM H-AP primer in the presence of 4 μM dNTP and 0.25 μl α-[^{33}P]dATP (2000 Ci/mmol, New England Nuclear) in a total volume of 20 μl. PCR conditions were: 95°C for 30 sec, 40°C for 2 min, 72°C for 1 min over 40 cycles. PCR products were separated on a 6% DNA sequencing gel in a Genomyx$_{LR}$ programmable DNA sequencer (Foster City, CA) and visualized by autoradiography. Using the primers 5'-AAGCTTTTTTTTTTA-3' and 5'-AAGCTTTTGAGGT-3', a differentially displayed cDNA band, *dd12*, was identified. After re-amplification using the above PCR conditions but at a dNTP concentration of 20 μM in a total volume of 40 μl, the *dd12* cDNA was ligated into the pGEM-T vector (Promega). Differential expression of the *dd12* transcript was confirmed by Northern blotting.

NORTHERN BLOT ANALYSIS

Twenty μg of total RNA was loaded on 1.2% agarose-formaldehyde gels (Ausubel *et al.*, 1987) and transferred to Hybond N membrane (Amersham). Blots were prehybridized in 5x SSC, 10x Denhardt's solution (Sambrook *et al.*, 1989), 0.1% SDS, 0.1 M K-phosphate, pH 6.8, and 100 μg/ml denatured salmon sperm DNA for 4 h at 42°C, and hybridized in 5x SSC, 10x Denhardt's solution, 0.1 M K-phosphate, pH 6.8, 10% dextran sulphate, 30% formamide, and 100 μg/ml denatured salmon sperm DNA overnight at 42°C with a probe prepared in the presence of α-[^{32}P]dCTP (New England Nuclear) using a random prime labeling kit (Boehringer Mannheim). High-stringency washes were performed with 0.1x SSC and 0.1% SDS at 65°C twice for 30 min. The radioactivity on blots was quantified by PhosphorImager analysis (Molecular

Dynamics, Sunnyvale, CA). All values were normalized for equal loading with *E37*, a cDNA corresponding to a transcript whose expression does not change during treatment with GA_3 (Van der Knaap and Kende, 1995).

SEQUENCE ANALYSIS

A full-length cDNA clone corresponding to the PCR product *dd12* and henceforth called *DD12* was isolated from a rice intercalary meristem cDNA library and cloned into the *Eco*RI site of pBluescript SK(-) phagemid (Stratagene). Sequence analysis was performed at the W.M. Keck facility at Yale University.

IN VITRO MUTAGENESIS

DD12 was subcloned into the *Eco*RI-*Sph*I site of pALTER^R-1 (Promega). The *Sph*I site of *DD12* was located 150 bp from the 3' end of *DD12* within the 3' untranslated region. To create an *Nde*I cloning site at the 5' end of the nucleotide sequence encoding the single-stranded DNA-binding domain SBD-A and a *Bam*HI site at the 3' end of the nucleotide sequence encoding SBD-B, 5'-GGCGCGGTTGCATATGACGAGAAGAGTT-3' and 5'-GCTTGGTATGACGGATCCGGCAAGGGTACT-3', respectively, were used as primers for mutagenesis (Fig. 3.1A). The internal *Nde*I site was eliminated by mutagenesis using 5'-AGCTAGGGCCTTATGTTGGTG-3' as primer. The construct thus formed was called pALTER-S1. *In vitro* mutagenesis was performed according to manufacturer's (Promega) specifications. Mutagenesis over the primer regions was verified by sequence analysis.

YEAST COMPLEMENTATION

p*DS1*, a yeast shuttle vector containing wild-type yeast *RPA1* on p*RS415* (LEU2) (Philipova *et al.*, 1996) was digested with *Nde*I and *Bam*HI to release the region of the yeast SBD-A and SBD-B domains. pALTER-S1 was digested with *Nde*I and *Bam*HI, and the rice SBD-A and SBD-B region was cloned into the *Nde*I-*Bam*HI site of p*DS1*. This resulted in the replacement of the yeast SBD-A and SBD-B with the rice SBD-A and SBD-B, and this construct was called p*DS9*. The yeast strain SBY102 (*MATα, ade2-1, can1-100, leu2-3,112, his3-11, ura3-1, Δrpa1::TRP1;*) (Philipova *et al.*, 1996) containing wild-type *RPA1* on the shuttle vector YCp50 (URA3) was transformed with the appropriate construct by a modified LiAc method (Schiestl and Gietz, 1989) and selected on synthetic complete medium without leucine (Sherman, 1991). To remove the wild-type yeast *RPA1* on YCp50, the colonies were selected on the same medium containing 5-fluoroorotic acid (Boeke *et al.*, 1987).

3.4. RESULTS

IDENTIFICATION OF A GA-REGULATED GENE

We employed differential display of mRNA (Liang and Pardee, 1992; Van der Knaap and Kende, 1995) to identify genes whose transcript level in the intercalary meristem was altered within 2 h of GA treatment. A 239-bp differentially displayed PCR product, *dd12*, appeared in GA-treated tissue and was further investigated. The cDNA was reamplified, cloned, and used as probe to verify by Northern blot analysis that the corresponding transcript

A

```
MDSDAAPSVTPGAVAFVLENASPDAATGVPVPEIVLQVVDLKPIGTRFTFLASDGKDKIK   60
TMLLTQLAPEVRSGNIQNLGVIRVLDYTCNTIGEKQEKVLIITKLEVVFKALDSEIKCEA  120
EKQEEKPAILLSPKEESVVLSKPTNAPPLPPVVLKPKQEVKSASQIVNEQRGNAAPAARL  180
AMTRRVHPLISLNPYQGNWIIKVRVTSKGNLRTYKNARGEGCVFNVELTDVDGTQIQATM  240
FNEAAKKFYPMFELGKVYYISKGSLRVANKQFKTVHNDYEMTLNENAVVEEAEGETFIPQ  300
IQYNFVKIDQLGPYVGGRELVDVIGVVQSVSPTLSVRRKIDNETIPKRDIVVADDSSKTV  360
TISLWNDLATTTGQELLDMVDSAPIIAIKSLKVSDFQGLSLSTVGRSTIVVNPDLPEAEQ  420
LRAMYDSEGKGTSMASIGSDMGASRVGGARSMYSDRVFLSHITSDPNLGQDKPVFFSLNA  480
YISLIKPDQTMWYRA[redacted]QKNDAECSLRYIMVIKVSDPTGEA  540
WLSLFNDQAERIVGCSADELDRIRKEEGDDSYLLKLKEATWVPHLFRVSVTQNEYMNEKR  600
QRITVRSEAPVDHAAEAKYMLEEIAKLTGC                                 630
```

B

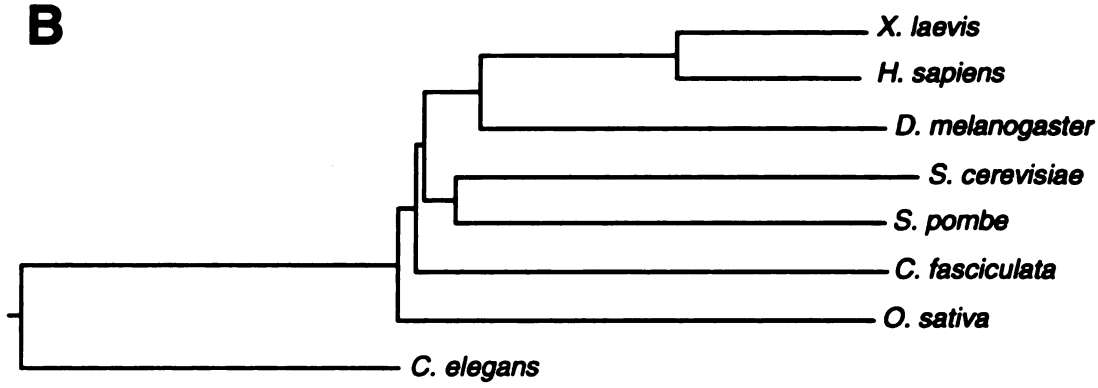

Figure 3.1. Amino acid sequence and phylogenetic analysis of DD12 (Os-RPA1). (**A**) The lightly shaded amino acid sequences comprise SBD-A and SBD-B, the darker shaded sequence the zinc finger domain. The location of the primers used for *in vitro* mutagenesis are underlined. (**B**) Phylogenetic analysis of RPA1 proteins from the species indicated. The dendogram was constructed using the Clustal method with the PAM250 residue weight table. The accession numbers are: Q01588 (*Xenopus laevis*), P27694 (*Homo sapiens*), Z70277 (*Drosophila melanogaster*), P22336 (*Saccharomyces cerevisiae*), U59385 (*Schizosaccharomyces pombe*), S38458 (*Crithidia fasciculata*), AF009179 (*Oryza sativa*), U41535 (*Caenorhabditis elegans*).

indeed accumulated as a result of GA treatment (results not shown, see also Fig. 3.4). A rice internode-specific cDNA library was screened with the differentially displayed and subcloned *dd12* PCR product. A full-length clone of 2.3 kb was isolated whose sequence showed an open reading frame from position 55 to 1944, encoding a protein of 69.6 kDa predicted molecular mass (Fig. 3.1A). Database searches indicated amino acid similarity to RPA1 from other organisms. RPA complexes are heterotrimers with subunits of approximately 70 (RPA1), 30 (RPA2), and 14 (RPA3) kDa (Wold, 1997). RPA was first identified as a factor necessary to support SV40 replication (Wobbe *et al.*, 1987; Fairman and Stillman, 1988; Wold and Kelly, 1988). Later, it was also found to be necessary for recombination (Heyer *et al.*, 1990; Moore *et al.*, 1991) and for DNA repair (Coverley *et al.*, 1991; 1992). *DD12* encodes a protein containing two contiguous single-stranded DNA-binding domains, SBD-A and SBD-B (Fig. 3.1A, lightly shaded amino acid sequences), which share similarity with *E. coli* single-stranded DNA-binding domains (Philipova *et al.*, 1996). *DD12* also encodes a zinc finger motif (Fig. 3.1A, dark-shaded amino acid sequences), which is conserved in all RPA1 proteins but whose function is unknown. The phylogenetic relationships between all known *RPA1* genes in the data base are given in Figure 3.1B. The percentage amino acid identity between rice and other RPA1 proteins ranges from 33.3% (*H. sapiens*) to 24.5% (*C. fasciculata*) based on pairwise comparisons using ALIGN. The percentage amino acid identity of the SBD-A and SBD-B region varies from 44.9% (*H. sapiens*) to 33.1% (*C. elegans*).

YEAST COMPLEMENTATION.

It has been suggested that species-specific interactions between RPA and

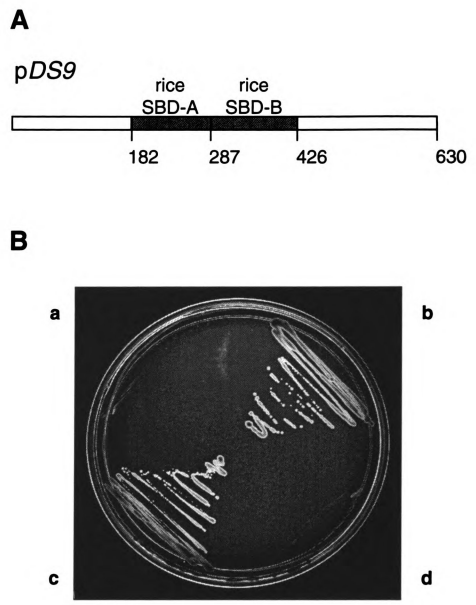

Figure 3.2. Complementation of a yeast *rpa1* mutant with p*DS9*. (**A**) Schematic representation of the chimeric protein encoded by p*DS9* containing the rice SBD-A and SBD-B domains (shaded) between the yeast N-terminal and C-terminal regions. The numbers above the diagram represent the amino acid positions of Os-RPA1. (**B**) Transformed yeast was plated out on complete synthetic medium (minus leucine, plus 5-fluorootic acid). Sector a, SBY102 non-transformed; sector b, SBY102 transformed with p*DS1*, which contains the wild-type *RPA1* of yeast; sector c, SBY102 transformed with p*DS9*; sector d, SBY102 transformed with p*JM241*; which contains the wild-type *RPA2* of yeast on p*RS415* (LEU2).

other cellular components account for the inability of yeast RPA to function in SV40 DNA replication (Brill and Stillman, 1989) and for the failure of human *RPA2* to complement a yeast *rpa2* mutant (Brill and Stillman, 1991). The C-terminal and N-terminal regions of RPA1 interact with other cellular factors (see below) and are less conserved among each other than are SBD-A and SBD-B. Replacement of yeast SBD-A and SBD-B with human SBD-A and SBD-B was shown before to rescue a yeast *rpa1* mutant (Philipova *et al.*, 1996). We constructed a chimeric clone, p*DS9*, encoding a protein with the rice SBD-A and SBD-B domains between the yeast N-terminal and C-terminal domains (Fig. 3.2A). Figure 3.2B shows the result of the complementation experiment. Both p*DS1* containing the wild-type yeast *RPA1* (sector b), and p*DS9* containing the rice-yeast chimera (sector c) rescued the yeast mutant, whereas p*JM241* containing yeast *RPA2* (sector d) did not. After selection, the colonies in sectors b and c were not able to grow on synthetic complete medium without uracil, which indicates loss of the original yeast *RPA1* gene on the YCp50 vector (data not shown). Also, dot blot analysis showed the presence of the yeast-rice chimera in colonies from sector c (data not shown). These results confirmed that the protein encoded by *DD12* is an ortholog of RPA1. Therefore, *DD12* will henceforth be called *Os-RPA1*.

TISSUE-SPECIFIC EXPRESSION OF *Os-RPA1*

Os-RPA1 mRNA was detected in tissues that contain dividing cells, namely in the highest node, which includes the apical meristem; in the sheath of the second youngest leaf; in the youngest leaf; in root tips; and in the coleoptile (Fig. 3.3). *Os-RPA1* transcript was also expressed in the intercalary meristem of the internode; a trace of *Os-RPA1* mRNA was also

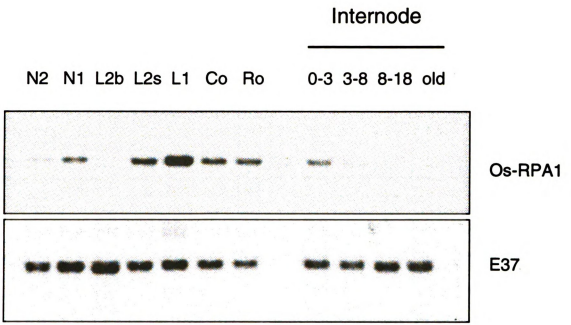

Figure 3.3. Tissue-specific expression of *Os-RPA1* in rice. N2, second highest node; N1, highest node containing the shoot apex; L2b, basal 2 cm of second youngest leaf blade; L2s, basal 2 cm of second youngest leaf sheath; L1, youngest leaf; Co, coleoptile 3 days after germination; Ro, root 3 days after germination; 0-3, internodal region 0-3 mm above N2 containing the IM; 3-8, internodal region 3-8 mm above N2 containing mostly the EZ; 8-18, internodal region 8-18 mm above N2 containing the upper part of the EZ and the DZ; old, oldest part of the internode. The upper panel shows hybridization signals with *Os-RPA1* as probe and the lower panel shows hybridization signals with *E37* as internal loading control.

evident in the internodal region just above it, which probably still contains some meristematic cells at its base but which, otherwise, consists of elongating cells. No *Os-RPA1* transcript was detected in the differentiation zone and in the oldest part of the internode.

THE TIME COURSE OF *Os-RPA1* EXPRESSION AND ITS CORRELATION WITH THE CELL CYCLE.

The level of *Os-RPA1* transcript in the intercalary meristem increased after 2 to 3 h of treatment with GA_3 and reached a maximum after 8 h (Fig. 3.4A, top panel). The increase in transcript level of *Os-RPA1* was not observed in control stem sections (data not shown). Submergence of whole plants also caused an increase in accumulation of *Os-RPA1* mRNA (Fig. 3.4B, top panel). These same blots were also hybridized to *E37* as loading control (Fig. 3.4A and B; bottom panels).

Because RPA is involved in DNA replication, we were interested in correlating the increase in transcript level of *Os-RPA1* to that of histone H3, which is a marker for the S-phase of the cell cycle (Van der Knaap and Kende, 1995). For this purpose, the Northern blots shown in Figure 3.4A and B were hybridized to the histone H3 probe (Fig. 3.4A and B, center panels). The signals were quantified by PhosphorImager analysis and normalized for equal loading using *E37* as internal standard. Taking a three-fold higher mRNA level over the 0-h time point as a significant increase, we found that the rise in *Os-RPA1* transcript level preceded that of histone H3 by 2 h in GA-treated internodes (Fig. 3.4C) and by 4 h in internodes of submerged plants (Fig. 3.4D).

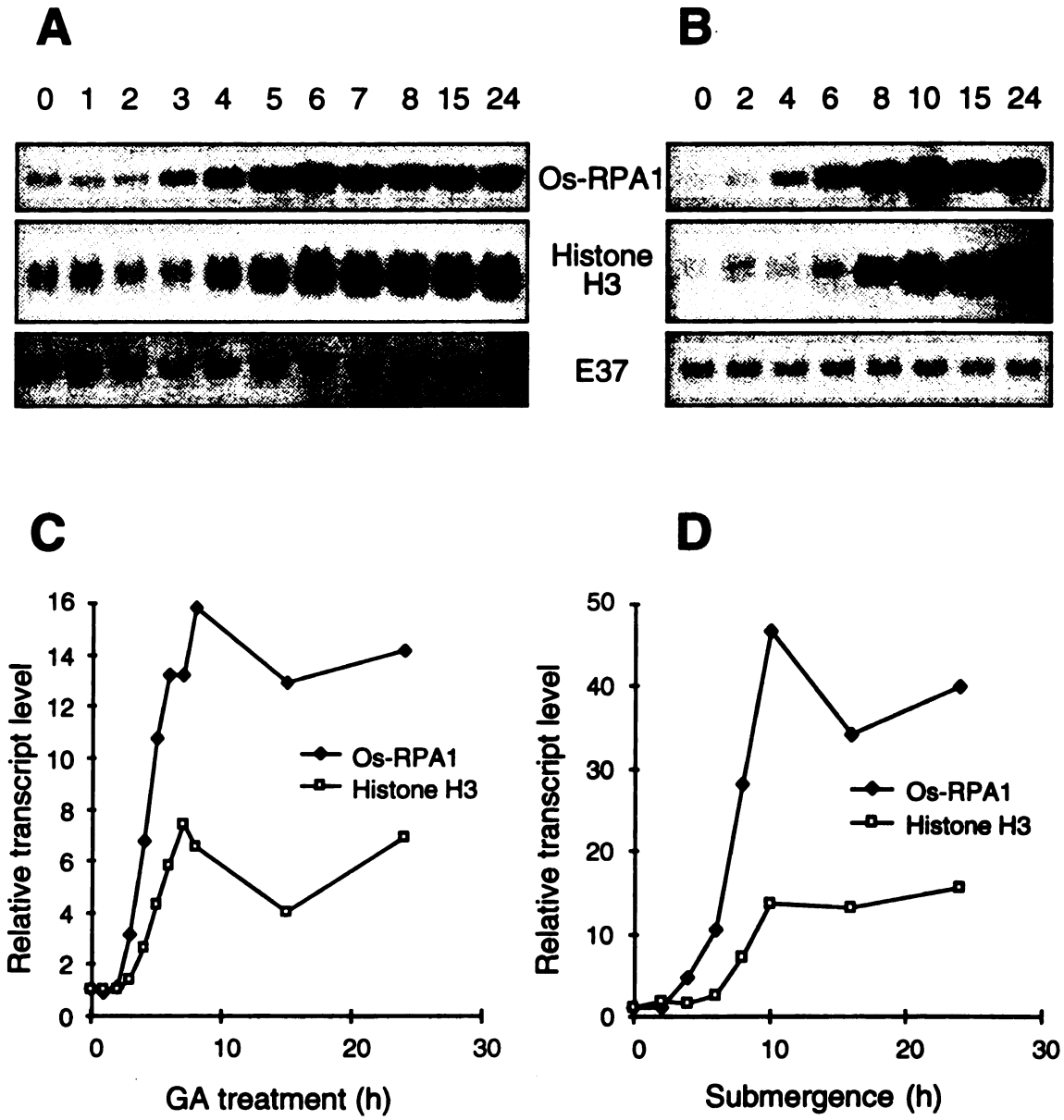

Figure 3.4. Change in *Os-RPA1* transcript levels during GA treatment of rice stem sections and during submergence of whole plants. (**A**) Northern blot analysis of RNA from the intercalary meristem of stem sections treated with GA_3 for the periods in hours indicated above the lanes. The same blot was hybridized to *Os-RPA1*, the histone H3 cDNA probe, and *E37*. (**B**) Northern blot analysis of RNA from the intercalary meristem of plants submerged for the periods in hours indicated above the lanes. The same blot was hybridized to *Os-RPA1*, the histone H3 cDNA probe, and *E37*. (**C**) Quantitative analysis of the Northern blot shown in (A) using a PhosphorImager. All values were normalized to the *E37* loading control. (**D**) Quantitative analysis of the Northern blot shown in (A).

3.5. DISCUSSION

In our search for GA-regulated genes in deepwater rice, we identified a gene, *DD12*, whose transcript level increased early in response to GA treatment and submergence. Sequence analysis of *DD12* indicated similarity to *RPA1* genes from several organisms. Replacement of the SBD domain of yeast *RPA1* with the homologous domain from *DD12* yielded a construct that was used successfully to complement a yeast *rpa1* mutant. Based on these results, we concluded that *DD12* is an ortholog of *RPA1* and called it *Os-RPA1*. To date, *Os-RPA1* is the only identified plant *RPA1* gene in the database, although apparent *Arabidopsis* and maize homologs exist in the EST database.

In synchronized yeast cells, increased transcript levels of *RPA1* correlated with the late G1 to S-phase (Brill and Stillman, 1991). This is also the case for the expression of several other yeast replication genes whose transcript levels increased prior to the accumulation of histone H2A-H2B mRNA (Lowndes *et al.*, 1991). We found a similar trend in the intercalary meristem of rice internodes. Particularly during submergence (Fig. 3.4B and D), the increase in *Os-RPA1* mRNA levels preceded the onset of DNA replication, as indicated by the accumulation of histone H3 mRNA (Van der Knaap and Kende, 1995). On the basis of these results, it appears that in rice, as in yeast, expression of replication proteins is regulated differently than that of histones.

RPA1 encodes the largest subunit of the heterotrimeric complex RPA and contains three functional domains (Figs. 3.1A and 3.2A). The C-terminal region mediates the interaction with the other two subunits, RPA2 and RPA3 (33-35). The primary function of SBD-A and SBD-B is to bind single-stranded

DNA (Philipova *et al.*, 1996; Kim *et al.*, 1996; Lin *et al.*, 1996; Bochkarev *et al.*, 1997); however SBD is also able to bind to damaged and double-stranded DNA (see below, and Clugston *et al*, 1992; He *et al.*, 1995; Burns *et al.*, 1996). The N-terminal domain is important for protein-protein interactions, e.g., with the transcriptional activators GAL4 and VP16 (He *et al.*, 1993; Li and Botchan, 1993), with the tumor suppressor p53 (Dutta et al., 1993), and possibly with other proteins of DNA metabolism. However, the precise role of RPA in these interactions is unclear (for a recent comprehensive review of RPA structure and function, see Wold, 1997).

In addition to its role in DNA replication, repair, and recombination, RPA is implicated in transcriptional regulation of several genes. RPA was identified as a protein factor that bound specifically to the upstream repression sequence (URS) of the promoter of the yeast *CAR1* gene, which is involved in nitrogen metabolism (Luche *et al.*, 1993), to a similar element in the promoter of the yeast *MAG* gene involved in DNA repair (Singh and Samson, 1995), and to a similar element in the promoter of the yeast *FOX3* gene, which is required for peroxisome functioning (Einderhand *et al.*, 1995). Based on sequence similarity, several *cis* elements, to which RPA binds, were identified in the promoters of many more genes involved in basic cell metabolism. Functional analysis of these *cis* elements showed that most of them act as upstream repression sequences, and some as upstream activation sequences. This indicates a role for RPA in both transcriptional repression and activation and in coordination of gene expression. The involvement of RPA in transcriptional regulation is found not only in yeast. The transcription of the human metallothionine IIA gene is repressed by RPA both *in vitro* and *in vivo* (Tang *et al.*, 1996).

In conclusion, rice RPA is probably involved in submergence- and GA-

enhanced DNA replication. In addition, it may also play a role in coordinating general transcription that accompanies accelerated growth.

3.6. LITERATURE

Ausubel, F.M., Brent, R., Kingston, R.E., Moore, D.D., Seidman, J.G., Smith, J.A. & Struhl, K. (1987) Current Protocols in Molecular Biology. Wiley, New York, pp. 4.9.1.-4.9.8.

Bleecker, A.B., Schuette, J.L. and Kende, H. (1986) Anatomical analyisis of growth and developmental patterns in the internode of deepwater rice. Planta **169**:490-497.

Bochkarev, A., Pfuetzner, R.A., Edwards, A.M. and Frappier, L. (1997) Structure of the single-stranded-DNA-binding domain of replication protein A bound to DNA. Nature **285**:176-181.

Boeke, J.D., Trueheart, J., Natsoulis, G. and Fink, G.R. (1987) 5-Fluoroorotic acid as a selective agent in yeast molecular genetics. Methods Enzymol **154**:164-175.

Brill, S.J. and Stillman, B. (1991) Replication factor-A from *Saccharomyces cerevisiae* is encoded by three essential genes coordinately expressed at S phase. Genes Dev **5**:1589-1600.

Brill, S.J. and Stillman, B. (1989) Yeast replication factor-A functions in the unwinding of the SV40 origin of DNA replication. Nature **342**:92-95.

Burns, J.L., Guzder, S.N., Sung, P., Prakash, S. and Prakash, L. (1996) An affinity of human replication protein A for ultraviolet-damaged DNA. Implications for damage recognition in nucleotide excision repair. J Biol Chem **271**:11607-11610.

Catling, D. (1992) Rice in Deep Water. The MacMillan Press Ltd, London and Basingstoke, UK.

Clugston, C.K., McLaughlin, K., Kenny, M.K. and Brown, R. (1992) Binding of the human single-stranded-DNA binding-protein to DNA damaged by the anticancer drug cis-diamminedichloroplatinum (II). Cancer Res **52**:6375-6379.

Coverley, D., Kenny, M.K., Munn, M., Rupp, W.D., Lane, D.P. and Wood, R.D. (1991) Requirement for the replication protein SSB in human excision

repair. Nature **349**:538-541.

Coverley, D., Kenny, M.K., Lane, D.P. and Wood, R.D. (1992) A role for the human single-stranded-DNA binding-protein HSSB/RPA in an early stage of nucleotide excision repair. Nucleic Acids Res **20**:3873-3880.

Dutta, A., Ruppert, J.M., Aster, J.C. and Winchester, E. (1993) Inhibition of DNA replication factor RPA by p53. Nature **365**:79-82.

Einerhand, A.W., Kos, W., Smart, W.C., Kal, A.J., Tabak, H.F. and Cooper, T.G. (1995) The upstream region of the FOX3 gene encoding peroxisomal 3-oxoacyl-coenzyme A thiolase in *Saccharomyces cerevisiae* contains ABF1- and replication protein A-binding sites that participate in its regulation by glucose repression. Mol Cell Biol **15**:3405-3414.

Fairman, M.P. and Stillman, B. (1988) Cellular factors required for multiple stages of SV40 DNA-replication *in vitro*. EMBO J **7**:1211-1218.

Gomes, X.V. and Wold, M.S. (1995) Structural analysis of human replication protein A. Mapping fucntional domains of the 70-kDa subunit. J Biol Chem **270**:4534-4543.

He, Z.G., Brinton, B.T., Greenblatt, J., Hassell, J.A. and Ingles C.J. (1993) The transactivator proteins VP16 and GAL4 bind replication factor A. Cell **73**:1223-1232.

He, Z.G., Henricksen, L.A., Wold, M.S. and Ingles, C.J. (1995) RPA involvement in the damage-recognition and incision steps of nucleotide excision-repair. Nature **374**:566-569.

Heyer, W.-D., Rao, M.R.S., Erdile, L.F., Kelly, T.J. and Kolodner, R.D. (1990) An essential *Saccharomyces cerevisiae* single-stranded DNA binding protein is homologous to the large subunit of human RP-A. EMBO J **9**:2321-2329.

Hoffmann-Benning, S. and Kende, H. (1992) On the role of abscisic acid and gibberellin in the regulation of growth in rice. Plant Physiol **99**:1156-1161.

Kim, D.K., Stigger, E. and Lee, S.H. (1996) Role of the 70-kDa subunit of human replication protein A (I). Single-stranded DNA binding activity, but not polymerase stimulatory activity, is required for DNA replication. J Biol Chem **271**:15124-15129.

Li, R. and Botchan, M.R. (1993) The acidic transcriptional activation domains of VP16 and p53 bind the cellular replication protein A and stimulate *in vitro* BPV-1 DNA replication. Cell **73**:1207-1221.

Liang, P., and Pardee, A.B. (1992) Differential display of eukaryotic messenger RNA by means of the polymerase chain reaction. Science **257**:967-971.

Lin, Y.L., Chen, C., Keshav, K.F., Winchester, E. and Dutta, A. (1996) Dissection of functional domains of the human DNA replication protein complex Replication Protein A. J Biol Chem 271:17190-17198.

Lowndes, N.F., Johnson, A.L. and Johnston L.H. (1991) Coordination of expression of DNA synthesis genes in budding yeast by a cell-cycle regulated *trans* factor. Nature **350**:247-250.

Luche, R.M., Smart, W.C., Marion, T., Tillman, M., Sumrada, R.A. and Cooper, T.G. (1993) *Saccharomyces cerevisiae* BUF protein binds to sequences participating in DNA replication in addition to those mediating transcriptional repression (URS1) and activation. Mol Cell Biol **13**:5749-5761.

Métraux, J.-P. and Kende, H. (1983) The role of ethylene in the growth response of submerged deepwater rice. Plant Physiol **72**:441-446.

Moore, S.P., Erdile, L., Kelly, T. and Fishel, R. (1991) The human homologous pairing protein HPP-1 is specifically stimulated by the cognate single-stranded binding-protein hRP-A. Proc Natl Acad Sci USA **88**:9067-9071.

Philipova, D., Mullen, J.R., Maniar, H.S., Lu, L., Gu, C. & Brill S.J. (1996) A hierarchy of SSB protomers in replication protein A. Genes Dev **10**:2222-2233.

Puissant, C. and Houdebine, L.M. (1990) An improvement of the single-step method of RNA isolation by acid guanidium thiocyanate-phenol-chloroform extraction. BioTechniques **8**:148-149.

Raskin, I. and Kende, H. (1984a) Regulation of growth in stem sections of deepwater rice. Planta **160**:66-72.

Raskin, I. and Kende, H. (1984b) Role of gibberellin in the growth response of submerged deepwater rice. Plant Physiol **76**:947-950.

Sambrook, J., Fritsch, E.F. & Maniatis, T. (1989) Molecular Cloning: A Laboratory Manual. Cold Spring Harbor Lab. Press, Plainview, N.Y., 2nd Ed., p. B15.

Sauter, M. and Kende, H. (1992a) Levels of β-glucan and lignin in elongating internodes of deepwater rice. Plant Cell Physiol **33**:1089-1097.

Sauter, M. and Kende, H. (1992b) Gibberellin-induced growth and regulation of the cell division cycle in deepwater rice. Planta **188**:362-368.

Sauter, M., Seagull, R.W. and Kende, H. (1993) Internodal elongation and orientation of cellulose microfibrils and microtubules in deepwater rice. Planta **190**:354-362.

Sauter, M., Mekhedov, S.L. and Kende, H. (1995) Gibberellin promotes histone H1 kinase activity and the expression of cdc2 and cyclin genes during the induction of rapid growth in deepwater rice internodes. Plant J **7**:623-632.

Schiestl, R.H. and Gietz, R.D. (1989) High efficiency transformation of intact yeast cells using single stranded nucleic acids as a carrier. Curr Genet **16**:339-346.

Sherman, F. (1991) Getting started with yeast. Methods Enzymol **194**:3-21.

Singh, K.K. and Samson, L. (1995) Replication protein A binds to regulatory elements in yeast DNA repair and DNA metabolism genes. Proc Natl Acad Sci USA **92**:4907-4911.

Stünzi, J.T. and Kende, H. (1989) Gas composition in the internal air spaces of deepwater rice in relation to growth induced by submergence. Plant Cell Physiol **30**:49-56.

Tang, C.M., Tomkinson, A.E., Lane, W.S., Wold, M.S. and Seto, E. (1996) Replication protein A is a component of a complex that binds the human metallothionein IIA gene transcription start site. J Biol Chem **271**:21637-21644.

Van der Knaap, E. and Kende, H. (1995) Identification of a gibberellin-induced gene in deepwater rice using differential display of mRNA. Pl Mol Biol **28**:589-592.

Vergara, B.S., Jackson, B. & De Datta S.K. (1977) Deep water rice and its response to deep water stress. *In* Climate and Rice: proceedings of the 1976 symposium. International Rice Research Institute, Los Baños, Philippines, pp. 301-319.

Wobbe, C.R., Weissbach, L., Borowiec, J.A., Dean, F.B., Murakami, Y., Bullock, P. and Hurwitz. J. (1987) Replication of simian virus-40 origin-containing DNA *in vitro* with purified proteins. Proc Natl Acad Sci USA **84**:1834-1838.

Wold, M.S. and Kelly, T. (1988) Purification and characterization of replication protein-A, a cellular protein required for *in vitro* replication of

simian virus-40 DNA. Proc Natl Acad Sci USA **85**:2523-2527.

Wold, M.S. (1997) Replication Protein A1: a heterotrimeric, single-stranded DNA-binding protein required for eukaryotic DNA metabolism. Annu Rev Biochem **66**:61-91.

CHAPTER 4

Identification of a gibberellin-induced leucine-rich-repeat receptor-like kinase in deepwater rice and its interaction with a kinase-associated protein phosphatase

4.1. ABSTRACT

A leucine-rich-repeat receptor-like kinase, OsTMK, was identified in deepwater rice. The transcript levels of *OsTMK* increased in response to gibberellin (GA) in the internode of rice. Furthermore, the expression was high in regions undergoing cell division and elongation, suggesting a role for this gene in growth. The kinase domain of OsTMK constituted an active kinase, autophosphorylating on serine and threonine residues. A putative downstream signal transduction component is the rice homolog of kinase-associated protein phosphatase (KAPP). The kinase interaction domain of OsKAPP was efficiently phosphorylated by the kinase domain of OsTMK. In rice, the expression patterns of *OsKAPP* and *OsTMK* were found to be similar, suggesting an *in vivo* interaction.

4.2. INTRODUCTION

The succesful existence of all plants is dependent upon their ability to coordinate complex developmental changes and to sense and respond to fluctuations in their environment. A stimulus is perceived by the cell, a signal is generated and transmitted (signal transduction), and a biochemical change is elicited (the response). Deepwater rice belongs to a group of rice cultivars whose survival during flooding is based on its capacity for rapid increase of internodal elongation when it becomes submerged. Under field conditions growth rates of up to 25 cm/day have been reported which result in plants that are up to 6 m tall (Catling, 1992). The signal for accelerated growth is an increase in ethylene levels which, via a decrease in abscisic levels (Hoffman-Benning and Kende, 1992), enhances the responsiveness of the internode to GA (Raskin and Kende, 1984a). While ethylene, in part, signals the change in the environment, the growth response is, ultimately, elicited by GA. Recently, several signal transduction components have been identified that mediate responses to GA. Two putative transcription factors with high sequence similarity to each other, GAI (Peng *et al.*, 1997) and RGA (Silverstone *et al.*, 1998), were shown to mediate responses to GA. Epistasis experiments have indicated that downstream of *GAI* is *SPY*. *SPY* encodes a protein with O-linked N-acetylglucosamine transferase activity which may modify post-translationally target proteins in the GA signaling pathway (Jacobsen *et al.*, 1996; Olszewski, 1997). As of yet, no specific receptor, kinase, phosphatase, channel protein, or heterotrimeric G-protein has been identified and shown to mediate responses to GA. However, in the cereal aleurone system, studied extensively to understand the role of GA and ABA in synthesis and secretion of hydrolytic enzymes, several signal transduction

components have been implicated (Bethke *et al.*, 1997; Ritchie and Gilroy, 1998; Jones *et al.*, 1998). Furthermore, circumstantial evidence has pointed to the plasma membrane as the site of GA perception (Hooley *et al.*, 1991; Gilroy and Jones, 1994).

Many signals are initially perceived by transmembrane receptors, a large number of which function by activation of an intrinsic protein kinase domain. In recent years, many plant receptor-like kinases (RLK) have been identified. While the majority of animal receptor kinases autophosphorylate on tyrosine residues, the majority of plant RLKs autophosphorylate on serine and/or threonine residues (Braun and Walker, 1996), and to date no plant kinase has been identified that exclusively autophosporylates on tyrosine residues. One RLK however, PRK1 (Mu *et al.*, 1994), confers dual-specificity, phosphorylating on tyrosine as well as serine residues. A related group of plant RLKs shows sequence similarity to members of the two-component signal transduction systems from bacteria. The intracellular domain of these RLKs shows sequence similarity to histidine kinases, and this group comprises the ethylene receptors (Chang *et al.*, 1992; Schaller and Bleecker, 1995; Wilkinson *et al.*, 1995) and a gene, *CKI1*, whose encoded protein is involved in cytokinin signaling (Kakimoto, 1996). The red/far-red light-absorbing phytochromes are not transmembrane receptors but are located in the cytosol. However, they also show limited sequence similarity to histidine kinases (Elich and Chory, 1997). Autophosphorylation of these receptor-like histidine kinases has not been conclusively shown and, in the case of phytochrome, may not be at a conserved histidine residue (Elich and Chory, 1997).

The group of RLKs, which, based on sequence similarity, are predicted or have been shown to have substrate specificity for serine and threonine

residues, can be classified according to the amino acid sequence features in the proposed extracellular domains. The two largest subclasses are: (i) RLKs whose extracellular domain contain leucine-rich repeats (LRR), and (ii) RLKs whose extracellular domain shows sequence similarity to the *S*-locus glycoprotein. The extracellular domain of several other plant RLKs identified are unique.

We are interested in the role of GA in vegetative growth in the internodes of deepwater rice. In a search for GA-regulated transcripts, a leucine-rich repeat receptor-like kinase (LRR-RLK), *OsTMK*, was identified. Direct involvement of this RLK in GA signaling cannot be confirmed at this time. However, the expression of *OsTMK* increased during GA treatment of rice stem sections, which suggests a role for this gene in plant growth. A potential downstream signal transduction component is a kinase-associated protein phosphatase (KAPP), originally identified in *Arabidopsis* by its *in vitro* interaction with RLK5, a LRR-RLK (Stone *et al.*, 1994). Interaction between the kinase domain of OsTMK and the kinase interaction domain of OsKAPP was, therefore, also investigated.

4.3. MATERIALS AND METHODS

PLANT MATERIAL

Seeds of deepwater rice (*Oryza sativa* L., cv. Pin Gaew 56) were obtained from the International Rice Research Institute (Los Baños, Philippines). Plants were grown as described in Stünzi and Kende (1989). Twenty-cm-long stem sections containing the growing internode were excised and treated with 50 μM GA_3

(Raskin and Kende, 1984b). Incubation was allowed to proceed for the periods indicated, after which the different regions were excised, frozen immediately, and stored at -80°C until use.

IDENTIFICATION OF OsTMK

A partial cDNA clone, *OsKIN* of 913 bp, was serendipitously identified in our laboratory by Margret Sauter during a library screen for cyclin genes. This clone had no similarity to cyclins but had similarity to protein kinases. A 305-bp fragment at the 5'-end of *OsKIN* was used to screen a intercalary meristem-specific, unamplified cDNA library to obtain a full-length clone, *OsTMK*. The phage insert was inserted into the *Not*I site of pBluescript SK(-) phagemid (Stratagene) and the sequence was determined by the Biochemistry Facility of the Plant Research Laboratory at Michigan State University, East Lansing, MI; by the WM Keck Facility at Yale University, New Haven, CT; and by Genomyx, Fostercity, CA. The sequences were aligned using Sequencher, version 3.0 (Gene Codes Corporation).

NORTHERN BLOT ANALYSIS

Twenty μg of total RNA, isolated according to Puissant and Houdebine (1990), was electrophoretically separated in a 1.2% formaldehyde-agarose gel (Ausubel *et al.*, 1987) and transferred to Hybond-N membrane (Amersham). DNA fragments containing the *OsKIN* insert, the ribosomal 5S RNA binding protein insert (*RL5*; Kim and Wu, 1993), or the *E37* insert (Van der Knaap and Kende, 1995) were isolated from agarose gels by digestion with β-agarase (NEB). Fifty ng of template DNA was labeled in the presence of α-[^{32}P]dCTP

(3000 Ci/mmol, NEN), using a random prime labeling kit (BMB). Northern blots were prehybridized for 4 h at 42°C in 5x SSC, 10x Denhardt's solution, 0.1% SDS, 0.1 M K-PO_4, pH 6.8, and 100 µg/ml denatured salmon sperm DNA and hybridized overnight at 42°C in 5x SSC, 10x Denhardt's solution, 0.1 M K-PO_4, pH 6.8, 100 µg/ml denatured salmon sperm DNA, 10% dextrane sulfate, and 30% formamide (BMB). The blots were washed twice in 2x SSC and 0.5% SDS and twice in 0.1x SSC and 0.1% SDS at 65°C for 30 min each. For *OsKAPP*, an RNA probe was made from the region encoding the kinase interaction domain (KID; Song *et al.*, 1998), in the presence of α-[^{32}P]UTP (NEN). Blots were prehybridized and hybridized in 3x SSPE, 10x Denhardt's solution, 0.5% SDS, 50 µg/ml denatured salmon sperm DNA, and 50% formamide at 65°C overnight. Blots were washed twice for 5 min each in 2x SSC and 0.5% SDS at 65°C followed by twice in 0.1x SSC and 0.5% SDS for 30 min each. The radioactivity on blots was quantified by PhosphorImager analysis (Molecular Dynamics).

SOUTHERN BLOT ANALYSIS

Rice genomic DNA was isolated from a CsCl gradient according to Ausubel *et al.* (1987). Four µg of genomic DNA was digested with the appropriate restriction enzyme, and the fragments were separated on a 0.8% agarose gel for 20 h at 30 V. The gel was treated for 15 min in 0.25 N HCl, 30 min in 0.5 N NaOH and 1.5 M NaCl and 15 min in 1 M Tris-HCl, pH 8 and 1.5 M NaCl, after which the DNA was transferred to Hybond N+ (Amersham). A probe was made using the insert of *OsKIN* in the presence of α-[^{32}P]dCTP (NEN) using a random prime labeling kit (BMB). Blots were prehybridized and hybridized in 6x SSC, 5x Denhardt's solution, and 1% SDS overnight at 65°C.

Non-specific hybridization was removed by stringent washes in 0.1x SSC and 0.1% SDS at 65°C.

OVEREXPRESSION OF THE KINASE DOMAIN OF OsTMK IN *E. coli*

To facilitate the cloning of the kinase domain of OsTMK in frame to maltose binding protein (MBP), a restriction enzyme site was introduced via PCR. The primers used were 5'-ATGGAATTCTCAATTCAAGTCCTC-3' and the reverse primer present in pBluescript SK (-). The product was amplified from a plasmid containing the full-length clone with Pwo polymerase (BMB). The PCR product was digested with *Eco*RI and *Hind*III and inserted directionally in the same sites of p*MAL-cRI* (NEB). The construct thus created, p*MBP-OsTKD*, was sequenced over the primer region to verify that the proper fusion construct had been obtained. p*MBP-OsTKD* was introduced in *E. coli* host ER2508 (NEB). The cells were grown in rich medium (10 g bacto tryptone, 5 g yeast extract, 5 g NaCl, and 2 g glucose per liter) supplemented with 1 mM $MnCl_2$ and 50 μg/ml carbenicillin (Sigma) at 37°C until an OD_{600} of 0.6 was reached. The cells were induced by addition of 50 μM isopropyl β-D-thiogalactoside for 2 h at room temperature, after which the cells were harvested by centrifugation. The bacterial pellet was resuspended in lysis buffer (10 mM Tris-HCl, pH 7.3, 150 mM NaCl, 1 mM DTT, 0.1% Tween-20, and 1mM phenylmethylsulfonyl fluoride), and stored at -20°C overnight. The cells were lysed with a cup sonicator at 30% duty cycle, 4-5 probe setting, or with a French press. MBP-OsTKD fusion protein (83 kD) was allowed to bind to amylose resin (NEB) for 20 min, and the resin was washed several times with lysis buffer. The final wash was performed in lysis buffer without Tween-20, and the fusion proteins were eluted in 10 mM maltose and 10 mM

Tris-HCl, pH 7. The GST-OsKID fusion construct was kindly provided by W.-Y. Song and P.C. Ronald (University of California at Davis) and contained the rice KID fused in-frame to GST (Song *et al.*, 1998). Overexpression of GST-OsKID (55 kD) was performed essentially the same as described for MBP-OsTKD, except that $MnCl_2$ was omitted from the rich medium. After lysis of the cells, the fusion proteins were purified by affinity binding to glutathione agarose resin (Sigma). After several washes, the fusion protein was eluted in 10 mM reduced glutathione and 10 mM Tris-HCl, pH 7. Protein concentrations were determined by comparison of band intensity to known standards on a Coomassie blue-stained polyacrylamide gel.

AUTO- AND TRANSPHOSPHORYLATION ASSAYS AND PHOSPHOAMINO ACID ANALYSIS

Purified MBP-OsTKD in the presence or absence of GST-OsKID, was incubated in a total volume of 15 µl with 10 µCi γ-[^{32}P]ATP (6000 Ci/mmol, NEN) + 20 µM non-radioactive ATP, 50 mM Tris-HCl, pH 7.3, 1 mM DTT, and 10 mM $MnCl_2$. The reaction was allowed to proceed for the appropriate time at room temperature or at 30°C, after which the reaction was stopped by addition of 35 µl of ice-cold 10% trichloroacetic acid (TCA). The radiolabeled proteins were collected by centrifugation, washed with 50 µl of ice-cold 10% TCA, and resuspended in 4 µl Tris-base and 5 µl 2x SDS sample buffer (BioRad). The resuspended proteins were directly loaded on a 10 or 12% polyacrylamide gel and electrophoretically separated with a constant current of 15 mA. The gel was stained in Coomassie blue to verify equal loading, dried, and X-ray film was exposed to the gel at room temperature. The radioactivity was quantified by PhosphorImager analysis. For phosphoamino acid analysis, the

autophosphorylated MBP-OsTKD was eluted from polyacrylamide gel overnight in 50 mM NH_4HCO_3. The sample was precipitated by TCA and acid hydrolyzed in 6 N HCl at 110°C for 1 h. The HCl was evaporated, and the pellet was resuspended in pH 1.9 electrophoresis buffer (2.2% formic acid and 7.8% acetic acid) containing phosphoamino acid standards, and applied to a thin-layer cellulose plate (TLC, Merck) as described by Boyle *et al.* (1991). Samples were subjected to electophoresis at 1.5 kV for 20 min in pH 1.9 buffer in the first dimension followed by electrophoresis in pH 3.5 buffer (5% acetic acid and 0.5% pyridine) at 1.3 kV for 16 min in the second dimension. Phosphoamino acids standards were visualized by spraying the plate with 0.25% ninhydrin in acetone and incubating the plate at 65°C for 30 min. X-ray film was exposed to the TLC plate for 2 days at -80°C.

4. 4 RESULTS

SEQUENCE ANALYSIS OF OsTMK

Screening of the rice cDNA library with the partial clone *OsKIN* resulted in the isolation of three independent inserts of approximately 3100 bp. This size was similar to the size expected from Northern blot analysis, indicating that a full-length clone was isolated. DNA sequence analysis of the longest cDNA insert (3123 bp) showed an ORF from position 50 to 2935, yielding a predicted protein of 101.6 kD (see Fig. 4.1). No in frame stop codon was observed upstream of the putative start methionine. However, one rice EST, identical to *OsTMK* (D41598), was found to be extended by 5 nucleotides at the 5' end and showed an in frame stopcodon. The putative signal

sequence is followed by an extracellular leucine-rich repeat (LRR) domain containing eleven complete and two incomplete repeats (see Fig. 4.2A), and eight potential N-glycosylation sites (consensus N-X-S/T). The first ten LRRs are flanked by two cysteine residues spaced eleven and eight amino acids apart, respectively. One cysteine pair (spaced eight amino acids apart) is found at the N-terminal side of the last three LRRs. LRRs are believed to play a role in protein-protein interaction, and several LRR domains are flanked by cysteine clusters (Kobe and Deisenhofer, 1994; see Fig. 4.2B). The extracellular domain is followed by a putative transmembrane region, and the C-terminal intracellular portion of the protein containing the 12 characteristic kinase subdomains; the conserved residues of which indicate serine/threonine kinase activity (Hanks and Quinn, 1991). Database searches with the BLAST program (Altschul *et al.*, 1990) indicated high amino acid similarity to RLKs from plants. The highest similarity was to TMK1 from *Arabidopsis* (Chang *et al.*, 1992), followed by an ORF (locus 2213607 on BAC F21J9) with accession number AC000103. We, therefore, named the gene encoded by this insert *OsTMK*. As can be seen in Figure 4.1, the alignment of OsTMK and TMK1 shows high amino acid identity and almost no gaps. In contrast, the alignment of AC000103 to OsTMK and to TMK1 shows gaps. The serine/glycine-rich stretch between the last LRRs and the transmembrane region is missing. Also, less amino acid sequence similarity is found immediately outside the conserved kinase domains. The spacing of the LRRs and the presence of the cysteine pairs is conserved in all three proteins. Figure 4.2A shows the alignment of the LRRs in the three proteins. The consensus, which is shown below the alignment, is commonly found in other plant proteins containing LRRs (Li and Chory, 1997), except for the presence of S/T and S at position 5 and 6, respectively. Figure 4.2B shows the alignment of the


OsTMK MWRRRGGGGGGGGGGVAVAVALAVMLVVGAAAGDTAASDAAAMRAVARALGADKALGWSTGDPCSSPRAWAGVTCDSAGRVTAVQVGNR 90
TMK1 -KK-- TFLLFSFTFLL-LSLSK- -SDG -LS--LSLKKS-NPPSSF---DP---K -THIV-TGTK---RI-I-HS 74
AC000103 MI-KNFL-LLCFIALVNV ESSP-E-V-I-LRDS-KLSGNPN--GS---KWS MFIK--ASN---I-I-D- 70
OsTMK SLTGRLAFEVRNLTALARLELFDNSISGELPSLAGLSSLQYLLVHNNGFTRIPPDFFKGLTALAAVSLDNNPFDPWPLPADLADCTSLTN 180
TMK1 G-Q-T-S-DL---SE-E----QW-N---PV---S--A---V-MLS--N-DS--S-V-Q---S-QS-EI-----KS-EI-ES-RNASA-Q- 164
AC000103 GIS-K-P-DLGK--S-TKF-VMR-RLT-PI------K--VTVYAND-D--SV-E---S--SS-QH---------S-VI-PS-ENA---VD 160
OsTMK FSANTANVTGALPDFFS TALPSLQRLSLAFNKMSGPVPASLATAPLQALWLNNQIGENQFNGSISFISNMTSLQELWLHSNDFTGPLP 268
TMK1 ----S---S--S--G-L-P DEF-G-SI-H----NLE-EL-M---GSQV-S----G-K LT-D-TVLQ---G-K-V-----K-S---- 249
AC000103 ---VNC-LS-KI--YLFEGKDFS--TT-K-SY-SLVCEF-MNFSDSRV-V-M--G-K-REKLH-----LQK----TNVT-QG-S-S---- 250
OsTMK DFSGLASLSDLELRDNQLTGPVPDSLLKLGSLTKVPLTNNLLQGPIPKFADKVKADVVPTTERFCLSTPGQPCDPRVSLLLEVAAGFQYP 358
TMK1 -----KE-ES-S----SF-----A---S-E--KV-N----H-----V-V-KSS-SV-LDKDSNS----S--E -----KS--LI-SS-D-- 338
AC000103 -----V--KSFNV-E---S-L--S--FE-Q--SD-A-G---------N-TAPDIKPDLNGLNS---D---TS-----NT--SIVEA-G-- 340
OsTMK AKLADNWKGNDPCDGYIGVGCDAGNITVLNFARMGFSGSISPAIGKITTLQKLILADNNITGTVPKEVAALPALTEVDLSNNNLYGKLPT 448
TMK1 PR--ES-------TNW--IA-SN-----ISLEK-ELT-T---EF-A-KS--RI--GI--L--MI-Q-LTT--N-KTL-V-S-K-F--V-G 428
AC000103 VNF-EK-------S-WV-IT-TGTD---I--KNL-LN-T---RFADFAS-RVIN-SQ--LN--I-Q-L-K-SN-KTL-V-K-R-C-EV-R 430
OsTMK FAAKNVLVKANGNPNIGKDAPAPSGSGGSGGSNAPDGGNGGDGSN GSPSPSSAGIIAGSVVGAIAGVGLLAALGFYCYKRKQKPFGRVQ 537
TMK1 -RS --V-NT----D----KSSL-SP-S-SP-GGSGS-IN--KDRR-MK-STFI---V---L-GLLSIF-IGL-V-CW--KR--R-SGSE 517
AC000103 -NTTI-NTTG-FE DCPN-NA -KKAS-N--K-V---I-ILLALL-IGVAI-FLV-K-MQYHK 488
OsTMK SPHAMVVHPRHSGSDPDMVKITVAGGNVN GGAAASETYSQASSGPRDIHVVETGNMVISIQVLRNVTNNFSDENVIGKGGFGTVYKGEL 626
TMK1 -SN-V----------NES-------SS-SV---ISDTY-LPGT-EVGDN-QM--A---L-------S------SD-I---I-----V----- 607
AC000103 M--QQQS--Q-AF---IENLCTG V--SGFS GN-A-LG-A--I--------DA-Y--DEK-I-----I-----I----- 566
OsTMK HDGTKIAVKRMEAGVMGNKGLNEFKSEIAVLTKVRHRNLVSLLGYCLDGNERILVYEYMPQGTLSQHLFEWKEHNLRPLEWKKRLSIALD 716
TMK1 -------I---N--IAG--FA---I----------H--T----------KL-----------R-----S-EG-K--L--Q--TL--- 697
AC000103 -------I---SSIISG---D---I-----R-------V-H----E----L---Q--------R-I-Y---EG------TR--I---- 656

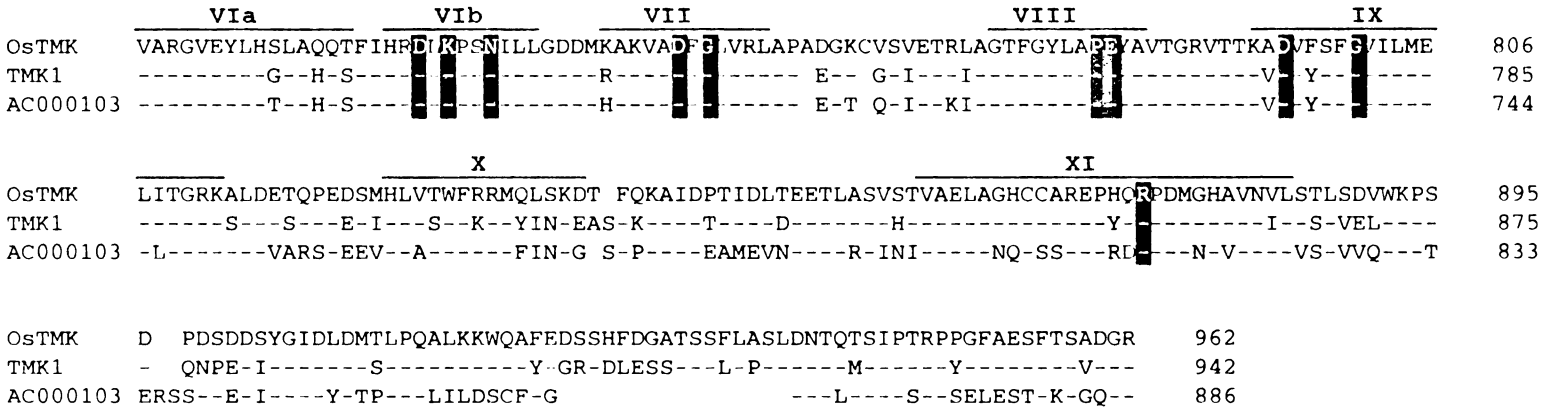

Figure 4.1. Sequence comparison between OsTMK, TMK1 and AC000103. The sequences were aligned by Clustal W 1.7. Identical amino acids are indicated by a dash; open spaces indicate gaps in the alignment. The blue boxes are the putative signal sequence and the predicted transmembrane spanning domain, respectively. The LRR domain is indicated in orange. The 3 cysteine pairs are double underlined. The roman numerals in green refer to the 12 subdomains found in protein kinases. The conserved sequences in the kinase domains are indicated in green (Hanks and Quinn, 1991)

A

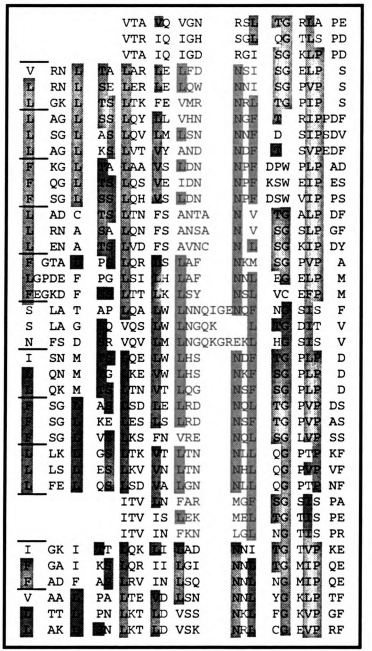

consensus: L/F xx L SS/T Lxx Lx/V Lxx NxL/F SG/T xaP xx

Figure 4.2. Comparison of conserved features in the putative extracellular domains of OsTMK, TMK1, and AC000103.

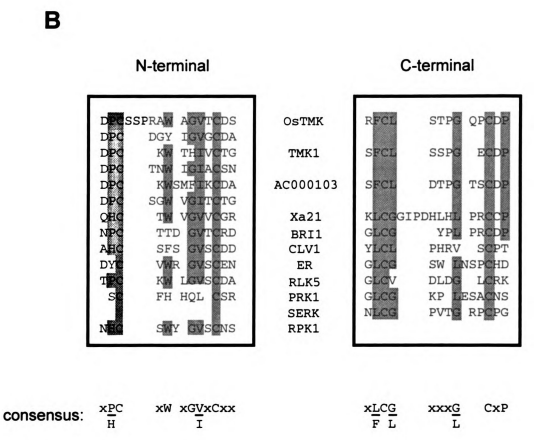

Figure 4.2. Comparison of conserved features in the putative extracellular domains of OsTMK, TMK1, and AC000103. Amino acid residues with identity to the consensus are indicated by the grey boxes. The "x" in the consensus indicates any amino acid; the "a" indicates an aliphatic amino acid. (**A**) Alignment of the eleven complete and two incomplete LRRs in OsTMK, TMK1, and AC000103. The first LRR of all three proteins are grouped as indicated by the horizontal bar and the number behind the repeat. The alignment is followed by the second LRR and so forth. The gap between LRR 10 and 11 is not shown. (**B**) On the left, alignment of the cysteine pairs present N-terminal of the LRRs; on the right, alignment of the cysteine pairs present C-terminal of the LRRs. The references are: TMK1, Chang *et al.*, 1992; AC000103, accession number for genomic sequence of *Arabidopsis* BAC F21J9; Xa21, Song *et al.*, 1995; BRI1, Li and Chory, 1997; CLV1, Clark *et al.*, 1997; ER, Torii *et al.*, 1996; RLK5, Walker, 1993; PRK1, Mu *et al.*, 1994; DcSERK, Schmidt *et al.*, 1997; RPK1, Hong *et al.*, 1997. The cysteine pair in RPK1 is located between the first and second LRR.

Table 4.1. Amino acid identity between leucine-rich repeat receptor-like kinases. The numbers indicate overall percent identity between the pairs, based on pairwise comparisons using ALIGN. The last column shows the number of repeats found in the presumed extracellular domain of the kinases. The references are: TMK1, Chang *et al.,* 1992; AC000103, accession number for genomic sequence of *Arabidopsis* BAC F21J9; Xa21, Song *et al.,* 1995;BRI1, Li and Chory, 1997; CLV1, Clark *et al.,* 1997; ERECTA, Torii *et al.,*1996; RLK5, Walker, 1993; DcSERK, Schmidt *et al.,* 1997; PRK1, Mu *et al.,* 1994.

	OsTMK	**TMK1**	**number of LRR**
OsTMK			13
TMK1	59.0		13
AC000103	49.2	53.3	13
Xa21	24.9	26.5	23
BRI1	24.4	25.2	25
CLV1	25.6	27.9	21
ERECTA	25.6	28.2	19
RLK5	25.8	27.2	21
DcSERK	23.3	22.6	5
PRK1	20.9	21.2	5

sequences surrounding the two cysteine residues located either N-terminal or C-terminal of the LRRs in the different LRR-RLKs. Often, the cysteines are spaced seven amino acids apart; for OsTMK, TMK1 and AC000103 they are predominantly eight amino acids apart. The percent amino acid identity, which includes the signal sequences and the transmembrane regions, between several LRR-RLKs is shown in Table 4.1. While the amino acid identity between OsTMK, TMK1 and AC000103 is approximately 55%, the identity between all other LRR-RLKs is around 25%. The kinase domain of OsTMK is 79% identical to TMK1 and 63% to AC000103, while the LRR domain of OsTMK is 49% identical to TMK1 and 40% to AC000103. This indicates that OsTMK, TMK1 and AC000103 belong to a subgroup within the larger LRR-RLK family.

EXPRESSION OF OsTMK IN GA-TREATED RICE INTERNODES AND SOUTHERN BLOT ANALYSIS

We were interested to know whether this gene plays a role in GA-mediated growth. In rice stem sections, GA was shown to increase cell size and the rate of cell production in the intercalary meristem (IM), which is located at the base of the growing internode. GA also resulted in a 3- to 4-fold increase in final cell size of cells in the elongation zone (EZ) after cells emerge out of the IM (Bleecker *et al.*, 1986; Sauter and Kende, 1992). Northern blot analysis shown in Figure 4.3, indicated that the transcript levels for *OsTMK* changed in response to GA in different regions of the internode. Figure 4.3A shows a Northern blot containing RNA from the IM and the lower part of the EZ of GA-treated stem sections. The top panel shows a blot hybridized to *OsTMK*, while in the bottom panel the same blot was hybridized to a gene

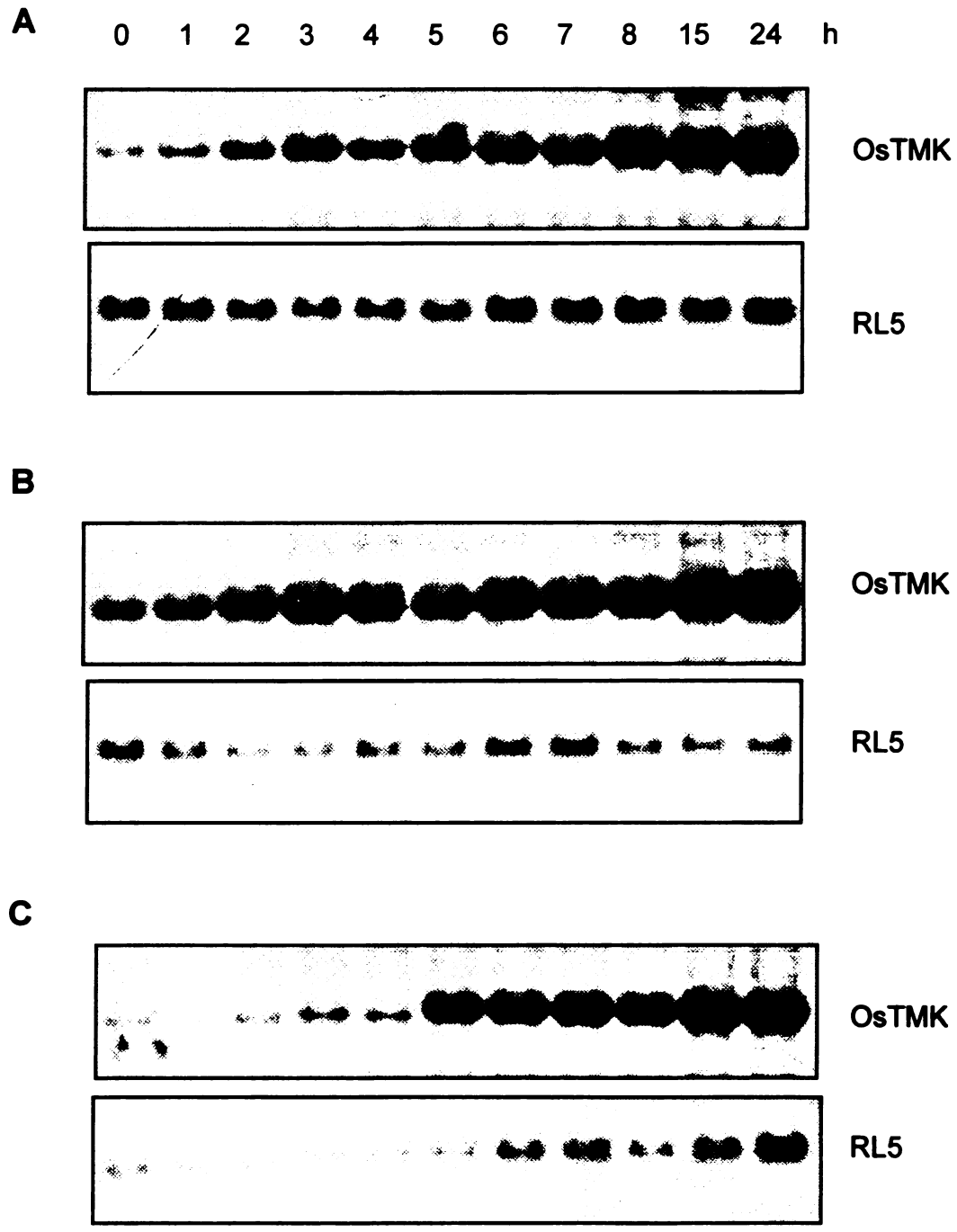

Figure 4.3. Expression of *OsTMK* in GA-treated stem sections. Stem sections were incubated in 50 μM GA_3 for the times indicated above the lanes. (**A**) Northern blot containing RNA isolated from the 0-5 mm region above the second highest node, including the IM and the lower part of the EZ. (**B**) 5-10 mm above the second highest node, including the EZ. (**C**) 10-20 mm above the second highest node, including the upper part of the EZ and DZ. To verify equal loading, all blots were hybridized to *RL5*.

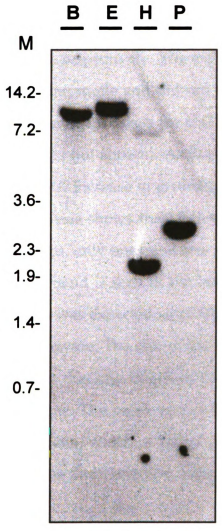

Figure 4.4. Southern blot analysis of *OsTMK* in rice. Blot containing genomic DNA, digested with either *Bam*HI (B), *Eco*RI (E), *Hind*III (H), or *Pst*I (P). The blot was probed with random prime labeled *OsKIN* insert, which corresponds to the kinase domain of the gene.

whose expression did not change significantly during treatment, *RL5*. The signals were quantified by PhosphorImager analysis and normalized for equal loading with the signals derived from *RL5*. *OsTMK* transcript levels increased after 3 h and continued to increase 9-fold, 15 h after the start of treatment. Figure 4.3B and C show Northern blots containing RNA from the EZ and the differentiation zone (DZ), respectively. The expression of *OsTMK* is very low in the oldest part of the internode and did not change during GA treatment (data not shown). The transcript levels for *OsTMK* did not increase either in control stem sections (data not shown). As is evident from these analyses, the transcript levels of *OsTMK* increase in growing tissues in response to GA.

Southern blot analysis shows that, following high stringency hybridizations and washes, only one band was detected in each lane (see Fig. 4.4). An additional faint band is seen in the lane containing genomic DNA digested by *Hind*III. This was expected since the probe used had an internal site for this restriction enzyme. The size of the smallest band is 2 kb, which eliminated the possibility that one fragment contained two linked copies of *OsTMK* in the rice genome. The probe used was derived from the region encoding the kinase domain, which, together with the presence of a single band in each digest on the Southern blot, indicated the presence of a single gene in the rice genome.

PHOSPHORYLATION ASSAYS WITH THE KINASE DOMAIN OF OsTMK

To examine whether OsTMK constituted an active kinase and to determine which amino acid residues were phosphorylated, the kinase domain was cloned in frame to MBP, and overexpressed in *E. coli*. The fusion protein was purified and subjected to a phosphorylation assay. As can be seen

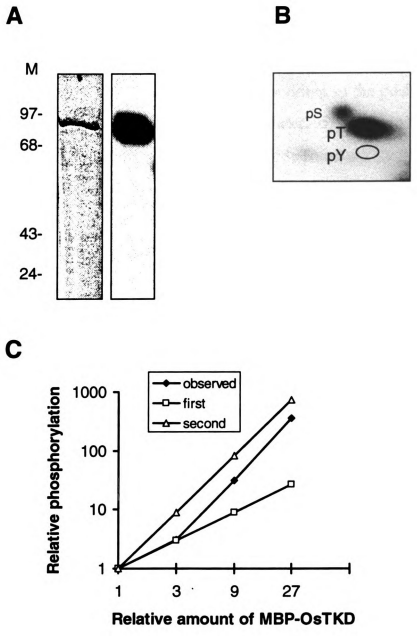

Figure 4.5. Autophosphorylation of MBP-TKD. (**A**) Purified MBP-OsTKD (500 ng) was allowed to autophosphorylate for 20 min at room temperature. The right panel is an autoradiogram of the Coomassie blue-stained gel in the left panel. (**B**) Phosphoamino acid analysis of autophosphorylated MBP-OsTKD. (**C**) Autophosphorylation as a function of enzyme concentration. The amount of MBP-OsTKD used ranged from 10 to 810 nM (12.5 ng to 1 μg per 15 μl reaction). The phosphorylation reaction was performed at 30ºC for 20 min. The open symbols reflect a curve expected for a first or second order reaction, respectively. The closed symbols reflect the curve that was observed.

in Figure 4.5A, the overexpressed protein was purified to homogeneity and was able to autophosphorylate. The autophosphorylated fusion protein was eluted from the acrylamide gel and acid hydrolyzed to determine the substrate specificity (Fig. 4.5B). ^{32}P labeled spots corresponding to the positions of phosphothreonine and phosphoserine were detected, while no label corresponding to phosphotyrosine was detected. This indicated that OsTMK, like TMK1, is a serine/threonine protein kinase. Most RLKs undergo intermolecular phosphorylation (second order with respect to enzyme concentration; Horn and Walker, 1995). A first order reaction, or intramolecular phosphorylation mechanism, would result in a linear increase of phosporylation depending on enzyme concentration. As shown in Figure 4.5C, MBP-OsTKD can phosphorylate itself via an intermolecular mechanism. At low enzyme concentrations, the level of autophosphorylation displayed a first order reaction mechanism, while at higher enzyme concentrations, the level of autophosphorylation increased more than the increase in MBP-OsTKD concentration. This suggests that the autophosphorylation of OsTMK is dependent on receptor concentration and is accomplished via a higher order reaction mechanism.

A potential downstream component of several RLKs in plants is KAPP, originally identified in *Arabidopsis* as a protein that interacts *in vitro* with the kinase domain of RLK5 (Stone *et al.*, 1994). *Arabidopsis* and maize KAPP have been shown to interact with TMK1 (Braun *et al.*, 1997) via the kinase interaction domain (KID). We were interested to find out whether the KID of OsKAPP is a substrate for phosphorylation by OsTMK. As shown in Figure 4.6, MBP-OsTKD phosphorylated GST-OsKID, while it did not phosphorylate GST. GST or GST-OsKID did not autophosphorylate or phosphorylate each

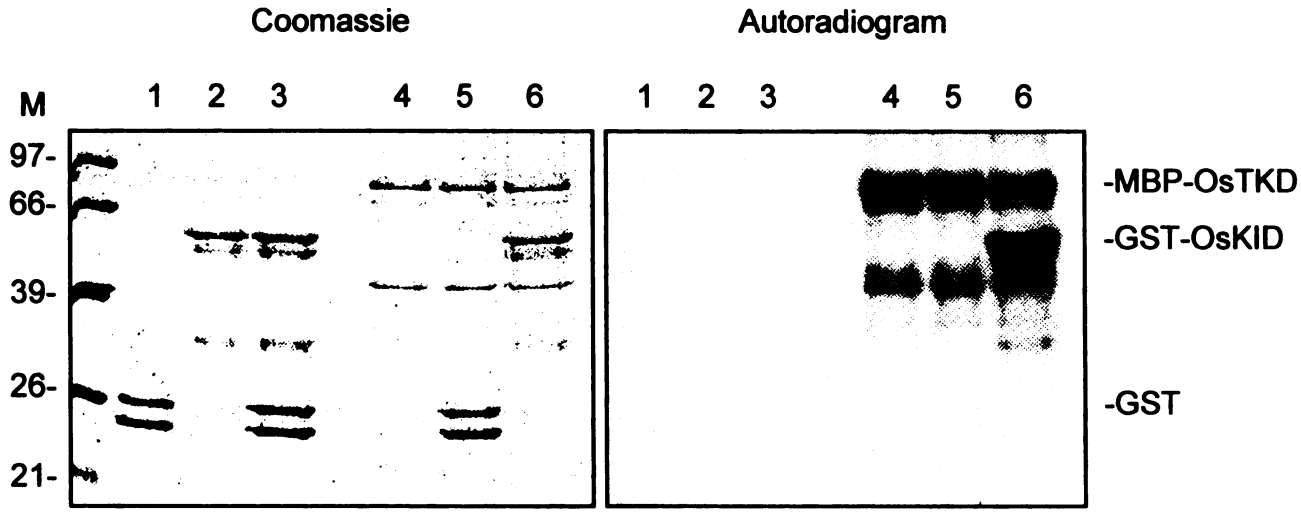

Figure 4.6. Phosphorylation assay using GST-OsKID as substrate. The right panel is an autoradiogram of the Coomassie blue-stained gel in the left panel. The reaction was allowed to proceed for 20 min at room temperature and contained: lane 1, 1.5 μg GST; lane 2, 0.5 μg GST-OsKID; lane 3, GST-OsKID and GST; lane 4, 0.5 μg MBP-OsTKD; lane 5, MBP-OsTKD and GST; lane 6, MBP-OsTKD and GST-OsKID. The lower bands are proteolytic degradation products.

other. This indicates that GST-OsKID is a substrate for MBP-OsTKD and that these proteins interact *in vitro*.

MBP-OsTKD and GST-OsKID are both substrates for phosphorylation. Therefore, the level of phosphorylation was determined by using increasing amount of fusion proteins. As shown in Figure 4.7A, increasing amounts of MBP-OsTKD led to increase in autophosphorylation of MBP-OsTKD and increase in phosphorylation of GST-OsKID. However, the level of autophosphorylation was greatly increased by decreasing amounts of GST-OsKID. Decrease in levels of autophosphorylation may be due, in part, to a transfer of phosphate from enzyme to substrate. After MBP-OsTKD was fully autophosphorylated, free ATP was removed. MBP-OsTKD was allowed to further incubate in the presence of GST-OsKID. As can be seen in Figure 4.7B, no phosphate turnover of MBP-OsTKD was observed (compare lane 1 with lanes 2 to 5 in Fig. 4.7B). Also, no transfer of phosphate from MBP-OsTKD to GST-OsKID was detected. OsKID became only labeled when it was incubated in the presence of γ-[^{32}P]ATP, as shown in lane 5 of Figure 4.7B. Autophosphorylation can be inhibited by increasing amounts of inactive kinase (Horn and Walker, 1995; Williams et al., 1997). To investigate whether inhibition of *in vitro* autophosphorylation of MBP-OsTKD was specific to its substrates, a phosphorylation assay with MBP-OsTKD either in the presence of OsKID, GST, or BSA was performed. As shown in Figure 4.7C, autophosphorylation of MBP-OsTKD and phosphorylation of GST-OsKID were inhibited at high protein concentrations, whether the proteins were substrates or not.

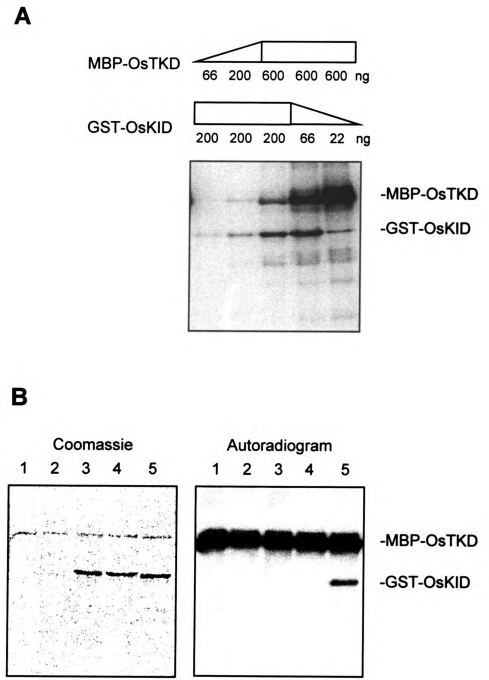

Figure 4.7. Decrease in autophosphorylation of MBP-OsTKD.

C

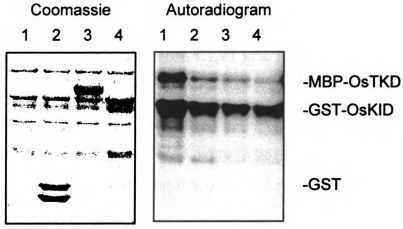

Figure 4.7. Decrease in autophosphorylation of MBP-OsTKD. (**A**) Phosphorylation assay in the presence of different amounts of fusion proteins as indicated above the lanes. The reactions were incubated at room temperature for 20 min. (**B**) MBP-OsTKD, 3.5 μg, was allowed to autophosphorylate at 30°C for 1 h. Free γ-[^{32}P]ATP was removed by Sephadex G-50 gel filtration and phosphorylated MBP-OsTKD was distributed in aliquots over five Eppendorf tubes. Lane 1, MBP-OsTKD was precipitated by TCA directly. MBP-OsTKD present in all other lanes was incubated at 30°C for an additional 20 min in the presence of: lane 2, 20 μM ATP and 10 mM $MnCl_2$; lane 3, 250 ng GST-OsKID and 10 mM $MnCl_2$; lane 4, 250 ng GST-OsKID, 20 μM ATP, and 10 mM $MnCl_2$; lane 5, 250 ng GST-OsKID, 20 μM ATP + 10 μCi γ-[^{32}P]ATP , and 10 mM $MnCl_2$. The amount of MBP-OsTKD per reaction was approximately 150 ng. (**C**) Inhibition of MBP-OsTKD activity. Phosphorylation assay with 500 ng MBP-OsTKD and 500 ng GST-OsKID in the presence of: lane 1, no additions; lane 2, 3 μg GST; lane 3, 2.5 μg BSA; lane 4, additional 750 ng of GST-OsKID. The reactions were incubated at 30°C for 20 min.

KAPP was shown to interact *in vitro* with several RLKs (Braun *et al.*, 1997). Whether KAPP interacts *in vivo* is, in most cases, unclear. An exception may be the interaction between CLV1 and KAPP (Williams *et al.*, 1997). To determine whether OsTMK and OsKAPP may interact *in vivo*, the expression patterns of these genes were investigated by Northern blot analysis. High transcript levels of *OsTMK* were detected in many tissues in rice, in particular in regions containing dividing and elongating cells (see Fig. 4.8). Lower levels of expression were detected in the basal part of the second youngest leaf blade and in the oldest part of the internode; those tissues show reduced or no growth, respectively. The transcript levels for *OsKAPP* mirror those of *OsTMK* almost perfectly. This indicated that *OsTMK* and *OsKAPP* are expressed in the same tissue and, therefore, may interact *in vivo*. While the transcript levels of *OsTMK* clearly increased during GA treatment of stem sections, the increase in transcript levels of *OsKAPP* in response to GA was small, reaching only a 3-fold increase after 24 h (data not shown).

4.5. DISCUSSION

In deepwater rice, a LRR-RLK that was highly expressed in growing regions of the plant was identified. The gene was named *OsTMK* for several reasons. (i) The highest amino acid sequence identity is to TMK1 from *Arabidopsis* (Chang *et al.*, 1992). (ii) The expression of *OsTMK1* is ubiquitous and is high in regions undergoing cell proliferation as is the expression of *TMK1* in *Arabidopsis* (Chang *et al.*, 1992; A.B. Bleecker, personal

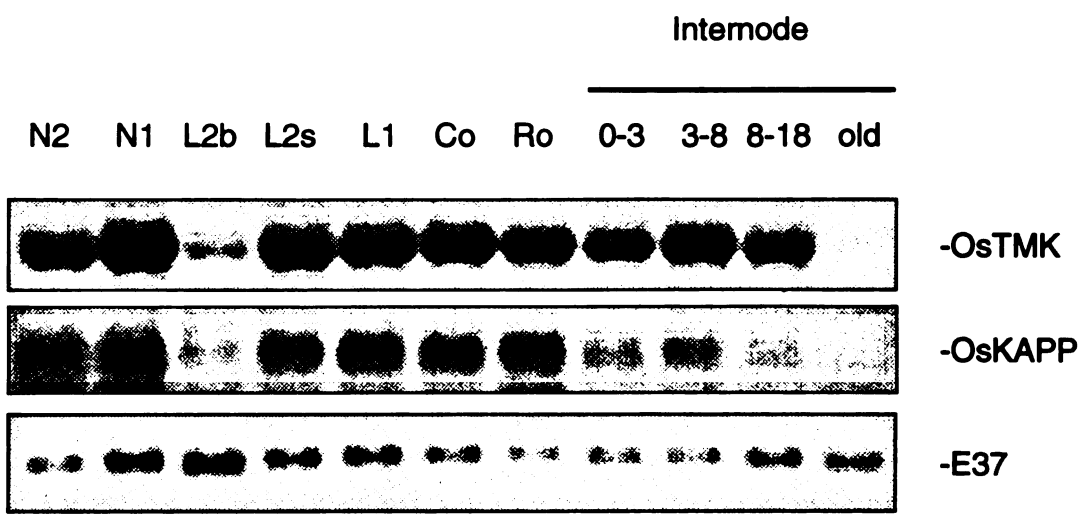

Figure 4.8. Tissue-specific expression of *OsTMK* and *OsKAPP* in rice. N2, second highest node; N1, highest node containing the shoot apex; L2b, basal 2 cm of second youngest leaf blade; L2s, basal 2 cm of second youngest leaf sheath; L1, youngest leaf; Co, coleoptile 3 days after germination; Ro, root 3 days after germination; 0-3, internodal region 0-3 mm above N2 containing the IM; 3-8, internodal region 3-8 mm above N2 containing mostly the EZ; 8-18, internodal region 8-18 mm above N2 containing the upper part of the EZ and the DZ; old, oldest part of the internode. The upper panel shows hybridization signals with *OsTMK* as probe, the middle panel shows hybridization signals with *OsKAPP* as probe, the lower panel shows hybridization signals with *E37* as internal loading control.

communications). Although Southern blot analysis indicated that *TMK1* is a unique gene in *Arabidopsis*, a related gene showing 53.3% amino acid identity to TMK1 was identified by the genome sequencing project. Southern blot analysis with rice genomic DNA and the region corresponding to the OsTMK kinase domain as probe also indicated the presence of only one gene in the rice genome. One rice EST (D39936) was identified, however, with high sequence similarity to a part of the LRR domain of OsTMK. Therefore, it is possible that homologs of *OsTMK* exist in rice as well. *Arabidopsis AC000103* and *TMK1* are likely to be evolutionarily related. The position of a unique intron (84 nucleotides in both *TMK1* and *AC000103*) is conserved between the first and the second nucleotide of the codon corresponding to valine at postion 766 in TMK1, immediately after kinase subdomain VIII (Chang *et al.*, 1992). For *OsTMK* the intron position(s) have not been determined. However, the lane containing *Hind*III-digested genomic DNA was expected to show a band of 1.7 kb, based on the cDNA sequence. Instead, the band detected was 2 kb, suggesting the presence of an intron in this fragment. This fragment spans the region containing the intron in AC000103 and TMK1.

Based on amino acid sequence similarity, TMK1 is more related to OsTMK than to AC000103. Several gaps exist in the sequence alignment of TMK1 and AC000103. In *Arabidopsis*, TMK1 was in the membrane fraction and was glycosylated *in vivo* (Schaller and Bleecker, 1995). Six of the eight potential glycosylation sites in the presumed extracellular domain were conserved between OsTMK and TMK1. Between AC000103 and OsTMK or TMK1, only two of the eight potential glycosylation sites were conserved. Furthermore, phylogenetic analysis by the Clustal method with the PAM250 residue weight table, showed that TMK1 and OsTMK were more related to each other than to AC000103 (data not shown). The high sequence

conservation between two RLKs from a monocot and a dicot species and the similar expression pattern suggests an important role for this gene in the plant and suggests functional relatedness.

The transcript levels of *OsTMK* were induced by GA in deepwater rice internodes. Furthermore, the expression of this gene is particularly high in all regions undergoing cell division and elongation, whereas low transcript levels were detected in the non-growing region of the internode. This suggests a role for this gene in plant growth and possibly in GA signal transduction. Evidence for a role of *OsTMK* in growth is substantiated by the dwarfed phenotype observed in *Arabidopsis* plants overexpressing *TMK1* in the antisense orientation (E. Maher, personal communication). GA is a hydrophobic molecule and may pass through the plasma membrane by simple diffusion. It may then interact with cytosolic receptors. However, evidence in the cereal aleurone pointed to a receptor at the plasma membrane (Hooley *et al.*, 1991) and not in the cytosol (Gilroy and Jones, 1994). Recently, a LRR-RLK, BRI1 (Li and Chory, 1997), has been identified to play a role in brassinosteroid (BR) signaling. Structurally, GA and BR are related, suggesting that an LRR-RLK may be involved in GA signaling as it is in BR signaling.

The transcript levels of some genes encoding RLKs in plants are mediated by hormones and external stimuli. The transcript levels of *SFR*, a *S*-locus-like RLK found in *Brassica oleracea*, increases after wounding and bacterial infection (Pastuglia *et al.*, 1997). Also, the transcript levels of *RPK1*, encoding a LRR-RLK from *Arabidopsis*, increases after abscisic acid treatment and in response to a variety of environmental stresses (Hong *et al.*, 1997). Inducible gene expression has been observed for some receptor kinases in animals as well. Interestingly, epidermal growth factor (EGF) and platelet-

derived growth factor were able to increase the transcript levels of their respective receptors (Clark *et al.*, 1985; Ericksson *et al.*, 1991). Ligand-induced changes in receptor transcript levels have been observed in plants as well. The transcript levels for the ethylene receptor *NR* in tomato (Wilkinson *et al.*, 1995) and *ERS* in pea (Peck and Kende, manuscript in preparation), increase in response to ethylene. The transcript levels corresponding to phytochrome A, one of the red/far-red light receptors, decreases in response to red light (Somers *et al.*, 1991). Therefore, it is not unprecedented that ligands change the transcript levels of their respective receptors. It will be interesting to know whether GA by itself or via an accessory protein can bind to OsTMK and, therefore, is responsible as its ligand for changes in transcript levels. Alternatively, increased transcript levels of *OsTMK* may be a result of growth in general and may not be involved in GA signaling.

The kinase domain of OsTMK is an active kinase autophosphorylating primarily on threonine and to a lesser extent on serine residues, as shown for TMK1 (Chang *et al.*, 1992). The autophosphorylation mechanism of MBP-OsTKD is complex, and suggests that autophosphorylation is accomplished via a higher order reaction mechanism. Complex autophosphorylation was found as well for RLK5. Phosphorylation of the inactive RLK5 kinase domain by active RLK5 kinase showed that RLK5 uses primarily an intermolecular mechanism (Horn and Walker, 1994). In animals, it is known that inactive receptor monomers are in equilibrium with active receptor dimers, and ligand binding stabilizes the active dimeric form (Ullrich and Schlessinger, 1990). Dimerization (or higher order oligomerization) is responsible for activation of the intrinsic protein kinase activity and for autophosphorylation; both processes are mediated by an intermolecular

mechanism (Lemmon and Schlessinger, 1994). For animal tyrosine kinase receptors, phosphorylation of a conserved tyrosine residue within the kinase domain leads to an increase in kinase activity. Phosphorylation of residues outside the kinase domain will create docking sites for downstream signal transduction molecules (Heldin, 1995). Therefore, the complex reaction order observed may reflect changes in activity of the kinase due to a different level of phosphorylation.

One candidate for a signal transduction component downstream of several RLKs is KAPP. Far-western analysis has indicated that KAPP interacts only with active, phosphorylated kinase (Stone *et al.*, 1994) and that the KID of *Arabidopsis* KAPP interacts *in vitro* with TMK1 (Braun *et al.*, 1997). Here, the interaction between the rice homologs was indicated by phosphorylation of GST-OsKID by MBP-OsTKD. No rapid turnover of the phosphates on MBP-OsTKD occurred even in the presence of ATP, and phosphates were not transferred from MBP-OsTKD to GST-OsKID. This was expected because of the low-energy phosphoester bond in phosphoserine and phospothreonine. This is contrary to the high-energy phosphoester bond of phosphohistidine and phosphoaspartate found in bacterial two-component systems, which all signal by phosphorelay (reviewed in Wurgler-Murphy and Saito, 1997).

Increasing amounts of inactive kinases were shown *in vitro* to inhibit autophosphorylation of active kinases (Horn and Walker, 1994; Williams *et al.*, 1997). *In vivo* coexpression of an active and an inactive EGF receptor kinase led to changes in the mitogenic response towards EGF (Honegger *et al.*, 1990), possibly because of the formation of partially inactive heterodimers. Here it is shown that autophosphorylation of MBP-OsTKD can be inhibited also by increasing amounts of another substrate, GST-OsKID. However, the *in vitro* inhibition of autophosphorylation needs to be interpreted with caution.

Kinase activity was not only inhibited by its substrate, but also by BSA and GST. This indicated that *in vitro* inhibition of MBP-OsTKD activity is not specific to its substrate.

KAPP may function in a number of signaling pathways. This is indicated by its interaction with several RLKs *in vivo* and *in vitro*, by the ubiquitous expression of KAPP and by the presence of a single gene in both *Arabidopsis* and maize (this work; Braun *et al.*, 1997; Williams *et al.*, 1997). The expression pattern of *OsKAPP* was very similar to that of *OsTMK*, which indicated that *in vivo* interaction is possible and that OsKAPP may function in the OsTMK signaling pathway. The *in vivo* role of this interaction is unknown. As was the case for another RLK, SRK-A14, it is expected that more proteins are interacting directly with the kinase domain of OsTMK (Braun *et al.*, 1997; Gu *et al.*, 1998) to signal changes in the environment.

4.6 LITERATURE

Altschul, S.F., Warren, G., Gish, W., Myers, E.W. and Lipman, D.J. (1990) Basic local alignment search tool. J Mol Biol **215**:403-410.

Ausubel, F.M., Brent, R., Kingston, R.E., Moore, D.D., Seidman, J.G., Smith, J.A. and Struhl, K. (1987) Current Protocols in Molecular Biology (Wiley, New York).

Bethke, P.C., Schuurink, R. and Jones, R.L. (1997) Hormonal signalling in cereal aleurone. J Exp Bot **48**:1337-1356.

Bleecker, A.B., Schuette, J.L. and Kende, H. (1986) Anatomical analysis of growth and developmental patterns in the internode of deepwater rice. Planta **169**:490-497.

Boyle, W.L., van der Geer, P. and Hunter, T. (1991) Phosphopeptide mapping and phosphoamino acid analysis by two-dimensional separation on thin-layer cellulose plates. Methods Enzymol **201**:110-149.

Braun, D. M. and Walker, J.C. (1996) Plant transmembrane receptors: new pieces in the signaling puzzle. Trends Biochem Sci **21**:70-73.

Braun, D.M., Stone, J.M. and Walker, J.C. (1997) Interactions of the maize and *Arabidopsis* kinase interaction domains with a subset of receptor-like protein kinases: implications for transmembrane signaling in plants. Plant J **12**:83-95.

Catling, H.D. (1992) Rice in Deepwater. The Macmillan Press Ltd, London and Basingstoke, UK.

Chang, C., Schaller, G.E., Patterson, S.E., Kwok, S.F., Meyerowitz, E.M. and Bleecker, A.B. (1992) The TMK1 gene from *Arabidopsis* codes for a protein with structural and biochemical characteristics of a receptor protein kinase. Plant Cell **4**:1263-1271.

Chang, C., Kwok, S.F., Bleecker, A.B. and Meyerowitz, E.M. (1993) *Arabidopsis* ethylene-response gene *ETR1*: similarity of product to two-component regulators. Science **262**:539-544.

Clark, A.J.L., Ishii, S., Richert, N., Merlino, G.T. and Pastan, I. (1985) Epidermal growth factor regulates the expression of its own receptor. Proc Natl Acad Sci USA **82**:8374-8378.

Clark, S.E., Williams, R.W. and Meyerowitz, E.M. (1997) The *CLAVATA1* gene encodes a putative receptor kinase that controls shoot and floral meristem size in *Arabidopsis*. Cell **89**:575-585.

Elich, T.D. and Chory, J. (1997) Phytochrome: if it looks and smells like a histidine kinase, is it a histidine kinase? Cell **91**:713-716.

Erickkson, A., Nistér, M., Leveen, P., Westermark, B., Heldin, C.-H. and Claesson-Welsh, L. (1991) Induction of platelet-derived growth factor α- and β-receptor mRNA and protein by platelet-derived growth factor BB. J Biol Chem **266**:21138-2144.

Gilroy, S. and Jones, R.L. (1994) Perception of gibberellin and abscisic acid at the external face of the plasma membrane of barley (*Hordeum vulgare* L.) aleurone protoplasts. Plant Physiol **104**:1185-1192.

Gu, T., Mazzurco, M., Sulaman, W., Matias, D.D. and Goring, D.R. (1998) Binding of an arm repeat protein to the kinase domain of the *S*-locus receptor kinase. Proc Natl Acad Sci USA **95**:382-387.

Hanks, S.K. and Quinn, A.M. (1991) Protein kinase catalytic domain sequence database: identification of conserved features of primary structure and classification of family members. Methods Enzymol **200**:38-62.

Heldin, C.-H. (1995) Dimerization of cell surface receptors in signal transduction. Cell **80**:213-223.

Hoffmann-Benning, S. and Kende, H. (1992) On the role of abscisic acid and gibberellin in the regulation of growth in rice. Plant Physiol **99**:1156-1161.

Honegger, A.M., Schmidt, A., Ullrich, A. and Schlessinger, J. (1990) Evidence for epidermal growth factor (EGF)-induced intermolecular autophosphorylation of the EGF receptors in living cells. Mol Cell Biol **10**:4035-4044.

Hong, S.W., Jon, J.H., Kwak, J.M. and Nam, H.G. (1997) Identification of a receptor-like protein kinase gene rapidly induced by abscisic acid, dehydration, high salt, and cold treatments in *Arabidopsis thaliana*. Plant Physiol **113**:1203-1212.

Hooley, R., Beale, M.H. and Smith, S.J. (1991) Gibberellin perception at the plasma membrane of *Avena fatua* aleurone protoplasts. Planta **183**:274-280.

Horn, M.A. and Walker, J.C. (1994) Biochemical properties of the autophosphorylation of RLK5, a receptor-like protein kinase from *Arabidopsis thaliana*. Biochim Biophys Acta **1208**:65-74.

Jacobsen, S.E., Binkowski, K.A. and Olszewski, N.E. (1996) SPINDLY, a tetratricopeptide repeat protein involved in gibberellin signal transduction in *Arabidopsis*. Proc Natl Acad Sci USA **93**:9292-9296.

Jones, H.D., Smith, S.J., Desikan, R., Plakidou-Dymock, S., Lovegrove, A. and Hooley, R. (1998) Heterotrimeric G-proteins are implicated in gibberellin induction of α-Amylase gene expression in wild oat aleurone. Plant Cell **10**:245-253.

Kakimoto, T. (1996) CKI1, a histidine kinase homolog implicated in cytokinin signal transduction. Science **274**:982-985.

Kim, J.-K. and Wu, R. (1993) A rice (*Oryza sativa* L.) cDNA encodes a protein sequence homologous to the eukaryotic ribosomal 5S RNA-binding protein. Plant Mol Biol **23**:409-413.

Kobe, B. and Deisenhofer, J. (1994) The leucine-rich repeat: a versatile binding motif. Trends Biochem Sci **19**:415-421.

Lemmon, M.A. and Schlessinger, J. (1994) Regulation of signal transduction and signal diversity by receptor oligomerization. Trends Biochem Sci **19**:459-463.

Li, J. and Chory, J. (1997) A putative leucine-rich repeat receptor kinase involved in brassinosteroid signal transduction. Cell **90**:929-938.

Mu, J.-H., Lee, H.-S. and Kao, T.-h. (1994) Characterization of a pollen-expressed receptor-like kinase gene of *Petunia inflata* and the activity of its encoded kinase. Plant Cell **6**:709-721.

Olszewski, N. (1997) Evidence that dynamic O-linked N-acetylglucosamine modification of proteins plays a role in gibberellin signal transduction. 8th International conference on Arabidopsis research. Madison, Wisconsin.

Pastuglia, M. Roby, D., Dumas, C. and Cock, J.M. (1997) Rapid induction by wounding and bacterial infection of an *S* gene family receptor-like kinase gene in *Brassica oleracea*. Plant Cell **9**:49-60.

Peng, J., Carol, P., Richards, D.E., King, K.E., Cowling, R.J., Murphy, G.P. and Harberd N.P. (1997) The *Arabidopsis GAI* gene defines a signaling pathway that negatively regulates gibberellin responses. Genes Dev **11**:3194-3205.

Puissant, C. and Houdebine, L.M. (1990) An improvement of the single-step method of RNA isolation by acid guanidium thiocyanate-phenol-chloroform extraction. BioTechniques **8**:148-149.

Raskin, I. and Kende, H. (1984a) Role of gibberellin in the growth response of submerged deepwater rice. Plant Physiol **76**:947-950.

Raskin, I. and Kende, H. (1984b) Regulation of growth in stem sections of deepwater rice. Planta **160**:66-72.

Ritchie, S. and Gilroy, S. (1998) Calcium-dependent protein phosphorylation may mediate the gibberellic acid response in barley aleurone. Plant Physiol **116**:765-776.

Sauter, M. and Kende, H. (1992) Gibberellin-induced growth and regulation of the cell division cycle in deepwater rice. Planta **188**:362-368.

Schaller, G.E. and Bleecker, A.B. (1993) Receptor-like kinase activity in membranes of *Arabidopsis thaliana*. FEBS Letters **333**:306-310.

Schaller, G.E. and Bleecker, A.B. (1995) Ethylene-binding sites generated in yeast expressing the *Arabidopsis ETR1* gene. Science **270**:1809-1811.

Schmidt, E.D.L., Guzzo, F., Toonen, M.A.J. and de Vries, S.C. (1997) A leucine-rich repeat containing receptor-like kinase marks somatic plant cells competent to form embryos. Development **124**:2049-2062.

Silverstone, A.L., Ciampaglio, C.N. and Sun, T.-p. (1998) The Arabidopsis *RGA* gene encodes a transcriptional regulator repressing the gibberellin signal transduction pathway. Plant Cell **10**:155-169.

Somers, D.E., Sharrock, R.A., Tepperman, J.M. and Quail, P.H. (1991) The *hy3* long hypocotyl mutant of Arabidopsis is deficient in phytochrome B. Plant Cell **3**:1263-1274.

Song, W.-Y., Wang, G.-L., Chen, L.-l., Kim, H.-S., Pi, L.-Y., Holsten, T., Gardner, J., Wang, B., Zhai, W.-X., Zhu, L.-H., Fauquet, C. and Ronald, P. (1995) A receptor kinase-like protein encoded by the rice disease resistance gene, *Xa21*. Science **270**:1804-1806.

Song, W.-Y., Pi, L.-Y., Ruan, D.-L., Braun, D.M., Walker, J.C. and Ronald, P.C. (1998) The rice disease resitance gene, *Xa21*, encodes an active serine/threonine protein kinase and does not interact with a rice kinase-associated protein phosphatase. *Submitted*

Stone, J.M., Collinge, M.A., Smith, R.D., Horn, M.A. and Walker, J.C. (1994) Interaction of a protein phosphatase with an *Arabidopsis* serine-threonine receptor kinase. Science **266**:793-795.

Stünzi, J.T. and Kende, H. (1989) Gas composition in the internal air spaces of deepwater rice in relation to growth induced by submergence. Plant Cell Physiol **30**:49-56.

Torii, K.U., Mitsukawa, N., Oosumi, T., Matsuura, Y., Yokoyama, R., Whittier, R.F. and Komeda, Y. (1996) The *Arabidopsis ERECTA* gene encodes a putative receptor protein kinase with extracellular leucine-rich repeats. Plant Cell **8**:735-746.

Ullrich, A. and Schlessinger, J. (1990) Signal transduction by receptors with tyrosine kinase activity. Cell **61**:203-212.

Van der Knaap, E. and Kende, H. (1995) Identification of a gibberellin-induced gene in deepwater rice using differential display of mRNA. Plant Mol Biol **28**:589-592.

Walker, J.C. (1993) Receptor-like protein kinase genes of *Arabidopsis thaliana*. Plant J **3**:451-456.

Wilkinson, J.Q., Lanahan, M.B., Yen, H.-C., Giovannoni, J.J. and Klee, H.J. (1995) An ethylene-inducible component of signal transduction encoded by *Never-ripe*. Science **270**:1807-1809.

Williams, R.W., Wilson, J.M. and Meyerowitz E.M. (1997) A possible role for kinase-associated protein phosphatase in the *Arabidopsis* CLAVATA1 signaling pathway. Proc Natl Acad Sci USA **94**:10467-10472.

Wurgler-Murphy, S.M. and Saito, H. (1997) Two-component signal transducers and MAPK cascades. Trends Biochem Sci **22**:172-176.

CHAPTER 5

A gibberellin-induced gene from deepwater rice confers delayed bolting, fasciated stems and gross alterations in flower morphology when overexpressed in *Arabidopsis*

5.1. ABSTRACT

In search for differentially expressed genes, a novel gene, *OsDD4*, was identified whose transcript levels increased in response to gibberellin (GA) in the intercalary meristem (IM) of deepwater rice internodes. Its tissue-specific expression indicated that *OsDD4* is exclusively expressed in regions containing meristems. The encoded protein is novel and is localized to the nucleus. *OsDD4* was overexpressed in *Arabidopsis thaliana* and individual T1 lines were analyzed. Overexpression of *OsDD4* led to delayed bolting and fasciated stems. The severe phenotype showed reduction in inflorescence stem elongation and apical dominance. The severe lines also displayed altered leaf and flower morphology. In particular the development of the gynoecia was impaired. At later stages of plant development, changes in floral organ number, and organ and floral meristem identity were observed.

5.2. INTRODUCTION

Deepwater rice belongs to a group of rice cultivars whose survival during flooding is based on its capacity for rapid increase of internodal elongation when it becomes submerged. Under field conditions growth rates of up to 25 cm/day have been reported resulting in plants that are up to 6 m tall (Catling, 1992). The signal for accelerated growth is an increase in ethylene levels (Métraux and Kende, 1983) which, via a decrease in abscisic levels (Hoffman-Benning and Kende, 1992), enhances the responsiveness of the internode to GA (Raskin and Kende, 1984a). While ethylene signals, in part, the change in the environment, the growth response is, ultimately, elicited by GA. In rice stems, the primary site of action of GA is the IM located at the base of the growing internode (Sauter *et al.*, 1993). GA has been shown to increase cell size and the rate of cell production in the IM. GA also results in a 3- to 4-fold increase in final cell size of cells that emerge from the IM into the elongation zone (EZ) (Bleecker *et al.*, 1986; Sauter and Kende, 1992). Recently, several signal transduction components that mediate responses to GA have been identified. Two putative transcription factors with high sequence similarity to each other, GAI (Peng *et al.*, 1997) and RGA (Silverstone *et al.*, 1998), have been shown to mediate responses to GA. The *gai* mutant is a GA-insensitive dwarf, and *rga* was identified for its ability to partially suppress some of the defects observed in the severe GA biosynthesis mutant, *ga1-3*. Epistasis analyses have indicated that downstream of *GAI* is *SPY* (Wilson and Somerville, 1995; Jacobsen *et al.*, 1996). The *spy* mutant partially suppresses both *gai* (Wilson and Somerville, 1995) and *ga1-3* (Silverstone *et al.*, 1997). *SPY* encodes a protein with O-linked N-acetylglucosamine transferase activity

which may modify post-translationally target proteins in the GA signaling pathway (Jacobsen *et al.*, 1996; Olszewski, 1997).

GAI, RGA, and SPY are negative regulators of the GA signal transduction pathway. So far, no positive regulator in GA signaling has been identified. A search for early GA-induced genes was initiated to identify potential positive regulators. Deepwater rice provides an excellent system to study GA-mediated growth. Changes in the internodal growth rate are observed 40 min after application of GA (Sauter and Kende, 1992), which results in a maximum growth rate of 5 mm/h (Stünzi and Kende, 1989). Using differential display (Liang and Pardee, 1992), we have identified a gene, *OsDD4*, whose transcript level increases rapidly in the IM of deepwater rice internodes in response to GA and submergence. The protein encoded by *OsDD4* is novel and is partially localized in the nucleus. To investigate its role in GA-mediated growth, *OsDD4* was overexpressed in *Arabidopsis thaliana*. This has led to what appeared to be a dominant negative phenotype in which several processes mediated by GA are affected.

5.3. MATERIALS AND METHODS

PLANT MATERIAL

Seeds of deepwater rice (*Oryza sativa* L., cv. Pin Gaew 56) were obtained from the International Rice Research Institute (Los Baños, Philippines). Plants were grown as described in Stünzi and Kende (1989). For submergence experiments, 12-week-old plants were partially submerged under continuous light (Métraux and Kende, 1983). Twenty-cm-long stem sections containing

the growing internode were excised and treated with 50 μM GA_3 (Raskin and Kende, 1984b). Incubation was allowed to proceed for the periods indicated, after which the IM was excised, frozen immediately, and stored at -80°C until use.

IDENTIFICATION OF *OsDD4* AND *D40170*

A differentially displayed 222 bp cDNA band, *dd4*, was identified using the primers T_{12}MG and OPA04 (Van der Knaap and Kende, 1995). The differential displayed product was inserted in pUC19, and the cloned DNA fragment was used to screen a IM-specific cDNA library to obtain a full-length cDNA insert, *OsDD4*. The phage insert was cloned into the *Not*I site of pBluescript SK(-) phagemid (Stratagene), and sequence analysis was performed at the W.M. Keck Facility at Yale University, New Haven, CT. The sequences were aligned using Sequencher, version 3.0 (Gene Codes Corporation).
One rice EST, *D40170*, with deduced amino acid sequence similarity to OsDD4 was obtained from Japan, and sequenced entirely in one orientation. The EST contained a partial cDNA since approximately 500 bp at the 5'end were missing.

NUCLEAR LOCALIZATION OF OsDD4

To facilitate the insertion of OsDD4 in frame to the reporter protein β-glucuronidase (GUS), restriction enzyme sites were introduced by PCR with Pwo polymerase (BMB). The primer sequences were: 5'-TCGGTCTAGAGGCGGTCGGTCGACGCTGAA-3' and 5'-TCATTGTGGATCCGGGAGGTGGTGGTGATC-3'. The PCR product that

contained the full ORF of OsDD4, except for the last 5 amino acids, was digested with *Xba*I and *Bam*HI and inserted in the same sites of p*BS::GUS.3* (Varagona *et al.*, 1992). Sequence analysis over the primer regions in p*BS::DD4::GUS* was performed to verify that the proper fusion construct had been obtained. p*BS::DD4::GUS* was digested with *Sal*I and *Cla*I and inserted into the *Xho*I and *Cla*I sites of p*MF6*, a monocot-specific transient assay transformation vector. The onion epidermal cell transformation was performed as described (Varagona *et al.*, 1992) by Emily Avila in Dr. M. Varagona's laboratory (New Mexico State University, Las Crucas).

NORTHERN BLOT ANALYSIS

Twenty μg of total RNA, isolated according to Puissant and Houdebine (1990), was electrophoretically separated in a 1.2% formaldehyde-agarose gel (Ausubel *et al.*, 1987) and transferred to Hybond-N+ membrane (Amersham). DNA fragments containing the insert derived from the 3' 737 bp of *OsDD4*, or the full-length *D40170*, the *E37*, and the histone H3 insert (Van der Knaap and Kende, 1995) were isolated from agarose gels by digestion with β-agarase (NEB). Fifty ng of template DNA was labeled in the presence of α-[^{32}P]dCTP (3000 Ci/mmol, NEN), using a random prime labeling kit (BMB). Northern blots were prehybridized for 4 h at 42°C in 5x SSC, 10x Denhardt's solution, 0.2% SDS, 0.1 M K-PO_4, pH 6.8, and 100 μg/ml denatured salmon sperm DNA and hybridized overnight at 42°C in 5x SSC, 10x Denhardt's solution, 0.1% SDS, 0.1 M K-PO_4, pH 6.8, 100 μg/ml denatured salmon sperm DNA, 10% dextran sulfate, and 30% formamide (BMB). The blots were washed twice in 2x SSC and 0.5% SDS and twice in 0.1x SSC and 0.3% SDS at 65°C for 30 min each. For *cycOs1*, the RNA probe was prepared in the presence of α-[^{32}P]UTP

(800 Ci/mmol, NEN) and contained the 3'UTR and most of the coding region (Sauter *et al.*, 1995). The RNA probe used for the bottom panel of Figure 5.11 was derived from the 5' UTR region (107 bp) of *OsDD4*. The blots were prehybridized and hybridized in 3x SSPE, 10x Denhardt's solution, 0.5% SDS, 50 μg/ml denatured salmon sperm DNA, and 50% deionized formamide (BMB) at 65°C overnight. Blots were washed twice for 5 min each in 2x SSC and 0.5% SDS followed by two washes in 0.1x SSC and 0.5% SDS for 30 min each at 65°C. The radioactivity on blots was quantified by PhosphorImager analysis (Molecular Dynamics).

SOUTHERN BLOT ANALYSIS

Rice genomic DNA was isolated from a CsCl gradient according to Ausubel *et al.* (1987). *Arabidopsis* genomic DNA was isolated by grinding two lyophilized leaves in liquid nitrogen. The tissue was thawed in hot hexadecyltrimethylammonium bromide (CTAB) buffer (2% CTAB, 1.4 M NaCl, 20 mM EDTA, 100 mM Tris-HCl, pH 8.0, and 0.2% β-mercaptoethanol at 65°C) and incubated at 65°C for 30 min. After addition of an equal volume of chloroform, the organic phase was separated from the aqueous phase by centrifugation. The DNA in the aqueous phase was precipitated with 0.6 volumes of isopropanol. The pellet was dissolved in TE and the RNA was removed by RNase A treatment (10 μg/ml) at 37°C for 30 min. After organic extraction, the DNA was precipitated with 1/3 volume of 7.5 M NH_4-acetate and 2.5 volumes of ethanol and subsequently dissolved in the appropriate amount of TE. Five μg of rice DNA and 500 ng of *Arabidopsis* DNA were digested overnight, and fragments were separated on a 0.8% agarose gel at 30 V for 20 h. The gel was then treated for 15 min in 0.25 N HCl; 30 min in 0.5 N

NaOH and 1.5 M NaCl; and 15 min in 1 M Tris-HCl, pH 8 and 1.5 M NaCl; after which the DNA was transferred to Hybond N+. The blots were prehybridized and hybridized in the same buffer and conditions as described above for Northern blot analysis. For the rice Southern blot, the probe used was derived from the 3' 737 bp of *OsDD4*. For the *Arabidopsis* Southern blot, the probe used was derived from the full-length *OsDD4*.

OVEREXPRESSION OF *OsDD4* IN *A. THALIANA*

OsDD4 was inserted in the sense orientation into the *Xba*I-*Cla*I site of the *Agrobacterium* binary vector p*GA643* (An *et al.*, 1988). This vector contains a neomycin phophotransferase II gene conferring kanamycin resistance. For cloning purposes, the construct thus created, p*GA::DD4*, lacked the 3' 428 bp of *OsDD4*, leaving only 74 bp of the 3' UTR. p*GA::DD4* was transformed into *Agrobacterium* strain GV3101 (C58C1 Rif^R) pMP90 (Gm^R). p*GA::DD4* and p*GA643* were each vacuum infiltrated into 40 *A. thaliana* ecotype Columbia and 40 ecotype Landsberg *erecta* plants as described (Van Hoof and Green, 1996). Seeds obtained were surface sterilized and plated on MS medium containing 1% sucrose, 10 mM MES, 0.8% phytagar, 500 µg/ml vancomycin (Clinical Center, Michigan State University), and 50 µg/ml kanamycin (Sigma). After two weeks, transgenic plants were transferred to soil and grown in the growth chamber at 20°C, 16h light, 8 h dark, 100 µmol m^{-2} s^{-1}.

5.4. RESULTS

IDENTIFICATION OF *OsDD4* AND AMINO ACID SEQUENCE ANALYSIS

We used differential display of mRNA to identify genes whose transcript had changed in the IM in response to GA (Van der Knaap and Kende, 1995). A 222-bp differentially displayed product, *dd4*, appeared 2.5 h after start of GA treatment and was investigated further. After cloning, one insert was used as probe and hybridized to a Northern blot containing polyadenylated RNA isolated from GA-treated stem sections (data not shown, see also Fig. 5.4). The results from this experiment indicated that the *dd4* insert identified was derived from a differentially expressed gene. A rice IM-specific cDNA library was screened with *dd4*, and a full-length clone of 1882 bp was isolated. The sequence showed an ORF from position 193 to 1380, yielding a 43-kD protein (Fig. 5.1). The protein encoded by *OsDD4* contains homopolymeric sequences of proline, threonine, alanine and glutamine. It has a histidine-rich region as well as a region rich in acidic residues. Furthermore, a putative bipartite nuclear localization signal (NLS) was identified (Hicks and Raikhel, 1995). These features are reminiscent of transcription factors (Mitchell and Tjian, 1989). Database searches indicated indeed weak similarities to a range of transcription factors, transcriptional activators and homeo box proteins. With the BLASTP program (Altschul *et al.*, 1997), the highest similarity was found to a domain of unknown function in the yeast SWI2/SNF2 and related genes in human, chicken and *Drosophila*. The alignment of this domain is shown in Figure 5.2A. Because of the conserved spacing of the glutamine and leucine residues as **Q**XXX**L**XX**Q**, we refer to this region as the QLQ domain. Searches through EST

Figure 5.1. Amino acid sequence of OsDD4. The QLQ domain is indicated the dark grey box, the WRC domain in the light grey box (see Fig. 5.2). The histidine-rich region is underlined by dashes; the acidic region is underlined with a solid line. Residues potentially involved in nuclear localization are found in the WRC domain and are indicated by the circles above the amino acid.

and genomic databases indicated that the QLQ domain was also found in other plant genes, namely in the rice EST D40170 and in two putative proteins identified by the *Arabidopsis* genome sequencing project. The adjacent domain in OsDD4 contains a putative NLS, and database searches with this sequence identified high sequence similarity to several plant genes. The alignment of this domain, which we refer to as the WRC domain for its conserved core, is shown in Figure 5.2B. Sofar, this motif has not been found outside the plant kingdom. The position of the QLQ and WRC motifs in the different proteins is variable as shown in Figure 5.2C. In most cases, except for the SWI2/SNF2 orthologs and for AC000106, the proteins containing the QLQ and/or the WRC domain are small, ranging from 269 to 430 amino acids. The *Arabidopsis* AC002387 contains two WRC domains.

NUCLEAR LOCALIZATION OF OsDD4

The features of the protein encoded by *OsDD4* including a putative NLS, are found in transcriptional regulators. To address the cellular localization, a construct containing OsDD4 fused in frame to the reporter protein GUS was made. After biolistic bombardment of onion epidermal cells with this construct, the localization of the fusion proteins was determined by histochemical staining, with the GUS substrate 5-bromo-4-chloro-3-indolyl-β-D-glucuronide (X-gluc). Blue staining was found associated with the nucleus, a result confirmed by coincident staining of the nucleus with the DNA-specific dye 4,6-diamidino-2-phenylindole (DAPI) (data not shown). Some level of staining was also observed in the cytoplasm, however, GUS itself is exclusively localized in the cytoplasm. Of the 44 onion cells counted, 30% showed exclusive nuclear localization, 64% showed nuclear and cytoplasmic

Figure 5.2. Alignment of QLQ and WRC motifs present in OsDD4. (**A**) Amino acid sequence alignment of proteins containing the QLQ domain. The numbers indicate the position of the domain in the protein (**B**) Amino acid sequence alignment of proteins containing the WRC domain. (**C**) Position of QLQ and WRC domains in the different proteins. Numbers indicate the length of the protein in amino acid residues. *O.s.*, *Oryza sativa*; *A.t.*, *Arabidopsis thaliana*; *H.s.*, *Homo sapiens*; *G.g.*, *Gallus gallus*; *D.m.*, *Drosophila melanogaster*; *S.c.*, *Saccharomyces cerevisiae*. The locus for AC002387 is 2583107; for AC002343 is 2262102; for AC000106 is 2342679; for U90439 is 1871180.

A

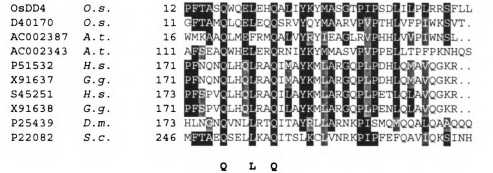

B

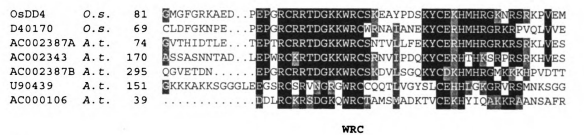

C

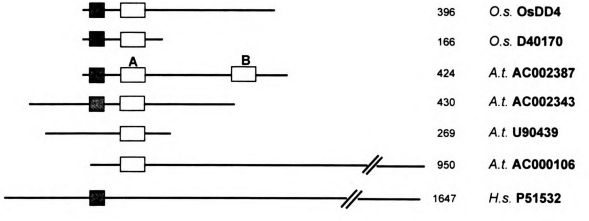

Figure 5.2. Alignment of QLQ and WRC motifs present in OsDD4.

localization and 7% showed cytoplasmic staining (data not shown). This indicated that OsDD4 contains a functional NLS that can redirect GUS to the nucleus.

EXPRESSION OF *OsDD4* IN RICE AND SOUTHERN BLOT ANALYSIS

GA treatment of rice stem sections containing the growing internode led to an increase in transcript abundance of *OsDD4* as shown in Figure 5.3A. The signals were quantified and normalized for equal loading using a cDNA, *E37*, corresponding to a gene whose transcript levels did not change over the course of the experiment. Figure 5.3B shows that the level of *OsDD4* in the IM of GA-treated stem sections had increased more than 3-fold 3 h after start of GA treatment and 8-fold 4 h after start of treatment. Since the rice EST D40170 contained the QLQ and the WCR domains, we were interested in investigating its expression in GA-treated stem sections. The probe was hybridized to the same Northern blot, but the transcript levels of *D40170* were not found to change in response to GA (Fig. 5.3A).

The expression pattern of *OsDD4* was also investigated in submerged plants as shown in Figure 5.4. The transcript levels had increased after 4 h, reaching a maximum 8 h after start of treatment. The increase in transcript levels for *OsDD4* was compared to the increase in transcript level for histone H3 and *cycOs1*. Histone H3 is a marker for the S-phase of the cell cycle (Van der Knaap and Kende, 1995) and *cycOs1* for the transition from the G2 to M phase (Sauter *et al.*, 1995; Sauter, 1997). The signals for histone H3 and *cycOs1* were quantified by PhosphorImager and normalized for equal loading with *E37*. A greater than 3-fold increase in histone H3 transcript level was detected 8 h after start of treatment, while that of *cycOs1* was detected after 16 h.

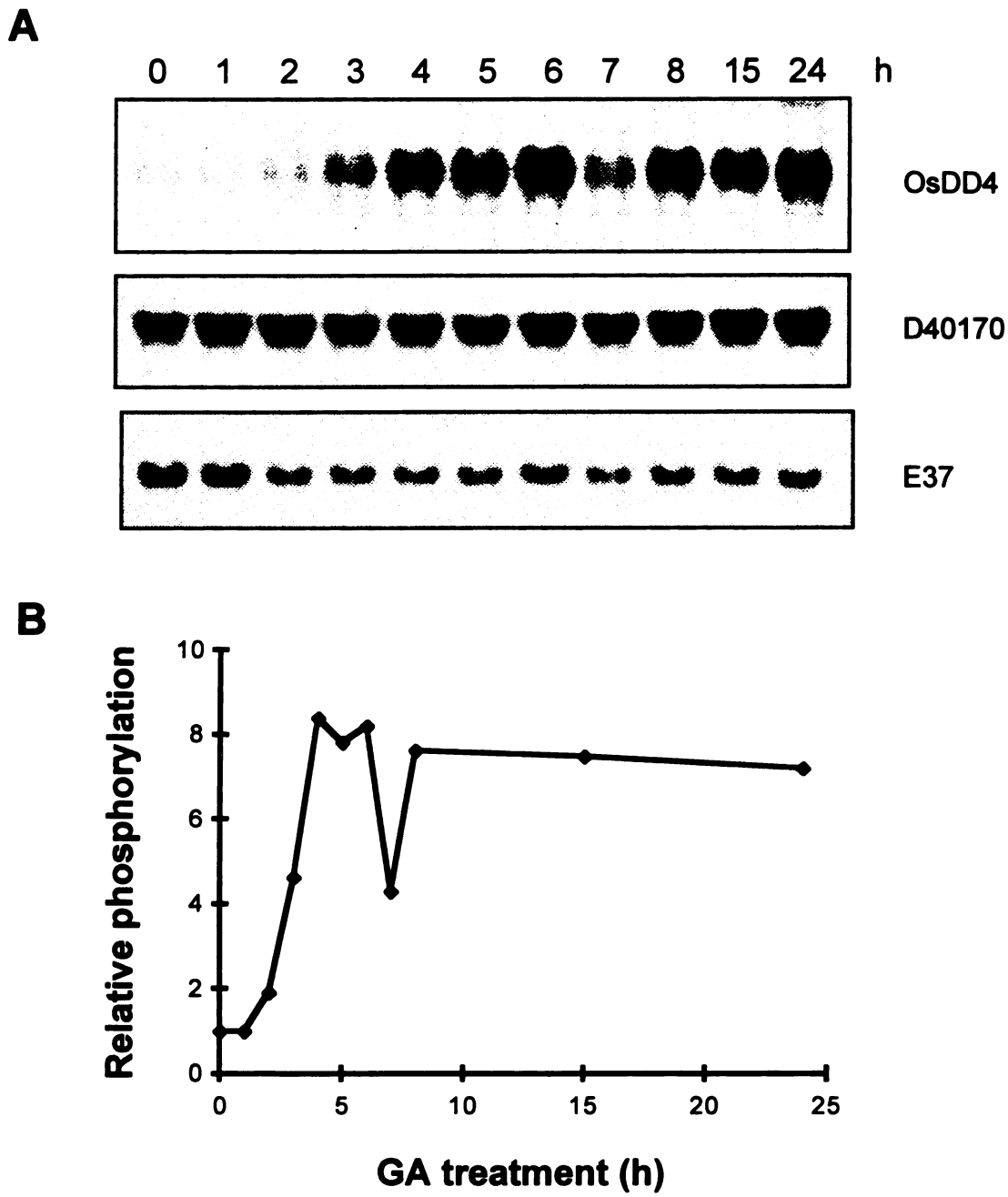

Figure 5.3. Expression of *OsDD4* and *D40170* in GA-treated rice stem sections. Stem sections were incubated in 50 µM GA_3 for the times indicated above the lanes, after which RNA was isolated from the IM. (**A**) Northern blot containing 20 µg of RNA was hybridized to *OsDD4*, *D40170*, and *E37*. (**B**) Quantitative analysis of the induction of *OsDD4* transcript levels using a PhosphorImager. The values were normalized to the *E37* loading control.

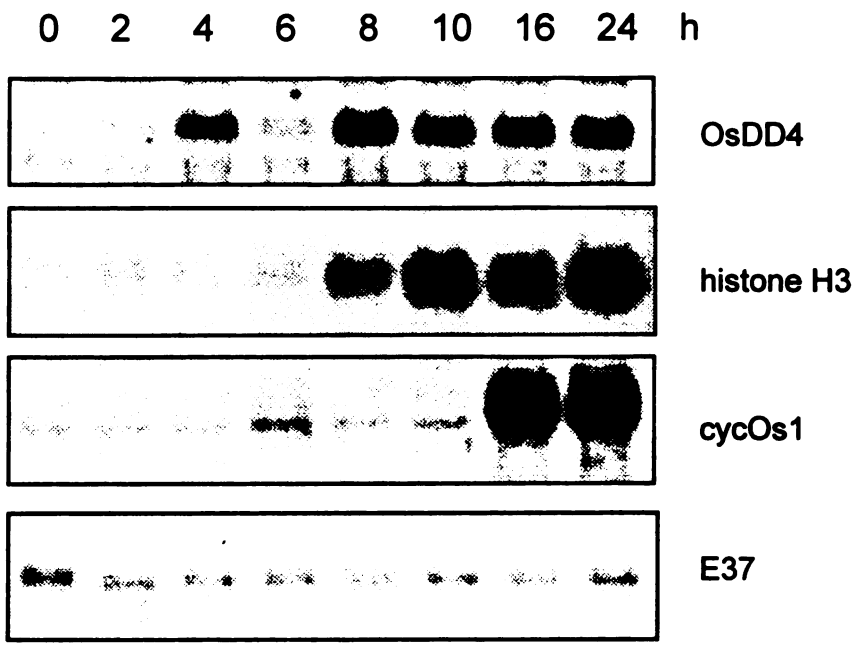

Figure 5.4. Expression of *OsDD4* in submerged rice plants. Plants were submerged for the times indicated above the lanes, after which RNA was isolated from the IM. Northern blots containing RNA isolated from the same submergence experiment were hybridized to *OsDD4*, histone H3, and *cycOs1*. Equal loading was verified by hybridization of the same blots to *E37*.

Because the signal for *OsDD4* could not be detected at the 0 h timepoint by PhosphorImager analysis, the signals were not quantified. It is clear however, that the increase in expression of *OsDD4* preceded that of histone H3 and of *cycOs1*. Interestingly, a transient decrease in OsDD4 transcript levels was observed in both stem sections and in submerged plants. The significance of this is unknown but it has been observed reproducibly in different experiments.

The tissue-specific expression of *OsDD4* is shown in Figure 5.5. The highest transcript levels were found in the N1, which contained the shoot apex, and in the IM. Slightly lower expression was detected in the coleoptile and in the youngest leaf. Weak expression was detected in the N2, in the basal part of the second youngest leaf sheath, and in the root. Along the internode, *OsDD4* was expressed in the IM, while no transcript was detected in the EZ, in the differentiation zone (DZ), and in the oldest part of the internode. This indicated that *OsDD4* is expressed exclusively in the IM, which is the primary site of GA action in the internode (Sauter *et al.*, 1993).

Southern blot analysis was employed to address the question whether genes related to *OsDD4* exist in rice. The probe was derived from the 3' region of *OsDD4* that does not overlap with the regions corresponding to the QLQ and WRC domains. As can be seen in Figure 5.6, three digests produced one predominant band. The lane containing *Bam*HI-digested DNA showed two additional faint bands, while the lanes containing *Eco*RI- and *Hind*III-digested DNA showed one additional faint band. Four bands were observed in the lane containing *Pst*I-digested DNA. The probe used contained a *Pst*I restriction enzyme site, which explains the presence of more bands. This indicates that *OsDD4* is not a member of a large gene family. However, the rice genome contains at least one and maybe two additional homologs of

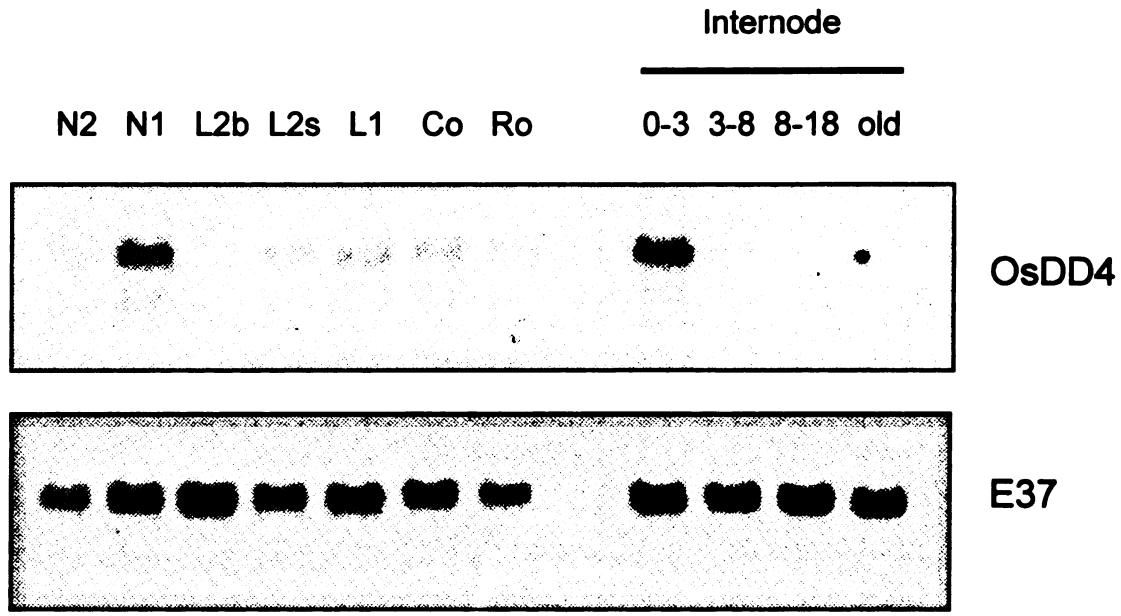

Figure 5.5. Tissue-specific expression of *OsDD4* in rice. N2, second highest node; N1, highest node containing the shoot apex; L2s, basal 2 cm of second youngest leaf blade; L2s, basal 2 cm of second youngest leaf sheath; L1, youngest leaf; Co, coleoptile 3 days after germination; Ro, root 3 days after germination; 0-3; internodal region 0-3 mm above N2 containing the IM; 3-8, internodal region 3-8 mm above N2 containing mostly the EZ; 8-18, internodal region 8-18 mm above N2 containing the upper part of the EZ and the DZ; old, oldest part of the internode. The upper panel shows hybridization signals with *OsDD4* as probe, the lower panel shows hybridization signals with *E37* as internal loading control.

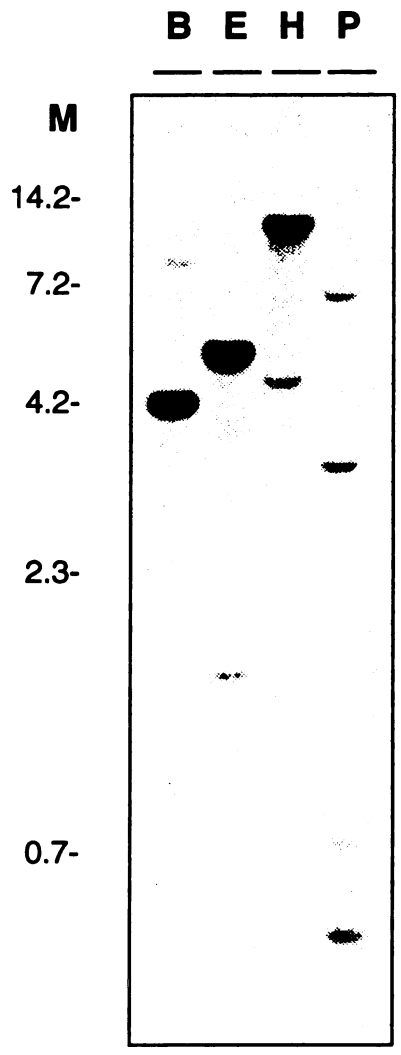

Figure 5.6. Southern blot analysis of *OsDD4* in rice. Southern blot containing rice genomic DNA, digested with either *Bam*HI (B), *Eco*RI (E), *Hind*III (H), or *Pst*I (P). The blot was probed with random prime labeled insert derived from the 3' 737 bp region of *OsDD4*.

OsDD4. The same Southern blot was also hybridized to *D40170* (data not shown). The pattern obtained was, however, different from the pattern obtained with *OsDD4* as probe. None of the faint bands on the Southern blot shown in Figure 5.6, hybridized to *D40170*.

OVEREXPRESSION OF *OsDD4* IN *A. THALIANA*

The rapid increase in transcript levels of *OsDD4* in response to GA and to submergence indicated that *OsDD4* is involved in early GA-regulated growth. The expression pattern in the internode showed that *OsDD4* is expressed exclusively in the IM, which is the region of primary responsiveness to GA. Moreover, the protein encoded by *OsDD4* is nuclear localized suggesting a regulatory role in GA-mediated growth. To test this hypothesis further, *OsDD4* was introduced into *Arabidopsis*, and transgenic seedlings were selected by plating the seeds on MS medium containing kanamycin. To ensure that the lines obtained were independent, one seedling per transformed plant was transplanted to soil. In cases where two seedlings were transplanted, subsequent Southern blot analysis was performed to prove that the lines were indeed independent (data not shown; see Fig. 5.10). In *A. thaliana* ecotype Columbia, 23 independent kanamycin-resistant T1 lines were obtained. The overexpression of *OsDD4* resulted in a range of phenotypes from wild type to severe. The phenotype became apparent in the early vegetative adult phase when *Arabidopsis* grows as a rosette. Six independent lines exhibiting a severe phenotype are described in detail in the section below. The less severe phenotypes displayed delayed flowering and bolting (see Fig 5.7A) and, in some cases, a fused and flattened stem (fasciation).

Figure 5.7A shows the range of phenotypes observed when *OsDD4* is overexpressed in *A. thaliana* ecotype Columbia. Control transformed plants had started bolting five weeks after germination, whereas, the lines overexpressing *OsDD4* were delayed in bolting. Six severe lines developed flowers around the same time as did control transformed plants, but the inflorescence stem did not elongate. However, the pedicel elongation was normal in these lines, as shown in Figure 5.7B. An additional phenotype observed in the lines displaying a severe phenotype, was curly rosette leaves. The nature of this phenotype has not been investigated, but the presence of curly leaves predicted the severity of the phenotype.

Eventually, some stem elongation was observed in all six severe lines, as shown in Figure 5.7C. As a result of reduced apical dominance, many secondary inflorescence stems had elongated. The bushy appearance was further enhanced by the severely fasciated and bifurcated inflorescence stems as shown in Figure 5.7E. In Figure 5.7D, the inflorescence stem of an ten-week-old overexpressing severe line was compared to the inflorescence stem of a four-week-old wild type plant. In the overexpressing lines, stem elongation between siliques was variable, but mostly reduced. In wild type *Arabidopsis*, leaves and flowers are initiated in a spiral phyllotaxis, with successive organs being offset by approximately 140° (see Fig. 5.7D; Furner and Pumfrey, 1992). Figure 5.7E shows the altered phyllotaxy in the overexpressing lines, indicating that the initiation of the flowers is highly irregular compared to wild type. The apparent alteration in phyllotaxy may be due to the fasciated stems. It is possible that the fused stems each display correct phyllotaxy. Irregular phyllotaxy may then occur as a result of the fusion of individual stems into one flattened stem. Changes in phyllotaxy of the rosette leaves were not recorded.

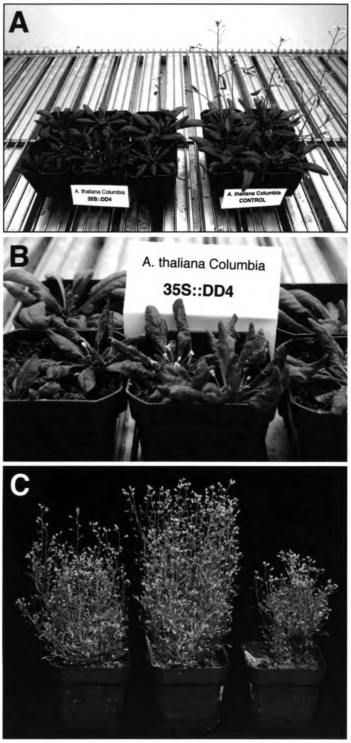

Figure 5.7. Overexpression of *OsDD4* in T1 lines of *A. thaliana* Columbia.

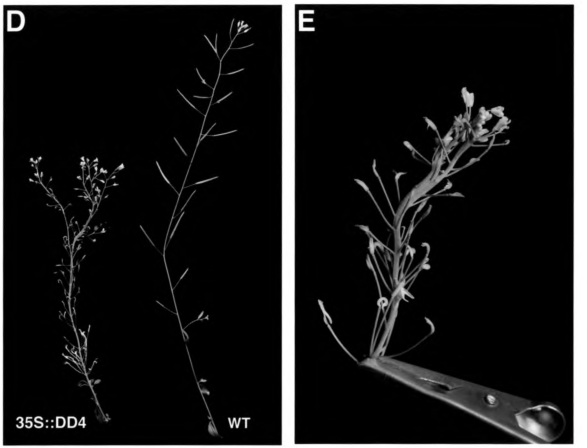

Figure 5.7. Overexpression of *OsDD4* in T1 lines of *A. thaliana* Columbia. (**A**) Five-week-old *Arabidopsis* plants transformed with *OsDD4* (left six pots) or transformed with vector without insert (right four pots). (**B**) Five-week-old plants comprising the severe class. Note the curly leaves and the flowering prior to bolting. (**C**) Plants displaying the severe phenotype, 10 weeks after germination. (**D**) A ten-week-old stem from a severe line (left) and a four-week-old stem from a wild type plant (right). (**E**) Close-up of a stem from a severe line. Note the fasciation of the stem and the altered phyllotaxy compared to wild type in (D).

As can be seen in Figure 5.7D and E, the formation of siliques was impaired in the severe lines overexpressing *OsDD4*. These lines showed complete female sterility and impaired male fertility, although later in development a few seed-bearing siliques were obtained from two lines. The flower organs in *Arabidopsis* are formed in four concentric rings or whorls. The innermost whorl contains the gynoecium which is composed of two fused carpels, a short style and stigmatic tissue on top of the style (Clark and Meyerowitz, 1994). In Figures 5.8A to C, the development of wild type flowers and siliques is shown. That of the overexpressing lines is shown in Figures 5.8D to H. The most noticeable phenotype was the partially unfused carpels, visible at flower stage 12 as shown in Figure 5.8D (Smyth *et al.*, 1990). The ovules, which develop at the edge of each carpel, became exposed at later stages of flower development. In some cases instead of an ovule a filamentous structure was formed, as indicated most clearly in Figure 5.8G. At the time when wild type stigmas were pollinated and the developing siliques were elongating, the siliques of the mutant flowers were not elongating, as shown in Figures 5.8G and H. The unfused carpels were observed in all flowers in all six lines displaying the severe phenotype.

During development of the plant, the carpel defect worsened. Early in development, the gynoecium showed a relatively normal stigma which, however, was not as symmetrical shaped as wild type (see Fig. 5.8E). These gynoecia developed into siliques as shown in Figure 5.8G, and displayed various growth alterations. Flowers formed later in development showed changes in identity of the inner whorl. The stigmatic tissue was replaced by a leaf-like outgrowth as shown in Figure 5.8F, and the top of the gynoecium was completely open. Siliques developing from these gynoecia are shown in

Figure 5.8. Overexpression of *OsDD4* in T1 lines of *A. thaliana* Columbia flowers. Development of wild type flowers and siliques (A to C) and the development of flowers and siliques in the severe lines (D to K). (**A**) and (**D**) stage 12 flower. (**B**), (**E**) and (**F**) flower at time of pollination. (**C**), (**G**) and (**H**) maturing siliques. The arrow in (G) indicates the replacement of an ovule with a filamentous structure. (**I**) and (**J**) Inflorescence stem of an 14-week-old severe line. (**K**) Inflorescence stem of an 18-week-old severe line. The size of the images in Figures (A) to (H) are on the same scale, as are the images in Figures (I) to (K).

Figure 5.8.
Overexpression of *OsDD4* in *A. thaliana* Columbia flowers

Figure 5.8H. The leaf-like structure continued elongating somewhat as if the carpel were reverting to a leaf. Even later in development, the leaf-like carpel phenotype had extended to the other flower organs. In Figure 5.8I, a transition from relatively normal flowers to flowers containing only leaf-like carpels is shown. The oldest flower showed all organs and appeared normal, except for the unfused carpels. The second oldest flower showed two petals which were reduced in size, while the other two appeared normal. The third oldest flower showed a decrease in floral organ number and a change in organ identity, while in the youngest flower all organs displayed a leaf-like carpel structure. A partial reversion of this progression is shown in Figure 5.8J. Also shown in Figure 5.8J is the absence of the pedicel in the leaf-like carpel flowers. Instead, the organs in this altered flower were emerging in a spiral phyllotaxy, and elongation between the organs was observed (see also the oldest flower in Fig. 5.8K). This is a pattern reminiscent of the inflorescence stem. As shown in Figure 5.8K, many flowers eventually displayed a complete change to leaf-like carpel flowers in which stem elongation between the successive flowers was severly reduced. This suggested that overexpression of *OsDD4* may lead to a change in the identity from a floral meristem to an inflorescence or even a vegetative meristem.

OsDD4 was also overexpressed in *A. thaliana* ecotype Landsberg *erecta*, and 16 independent T1 lines were obtained. The phenotypes ranged from wild type to severe. Two Landsberg *erecta* lines showed an extreme severe phenotype, similar to the phenotypes observed in the Columbia background described above. However, flowering was severely delayed, and the inflorescence stem never elongated. In one line, the only flowers observed were reminiscent of the leaf-like carpel flowers shown in Figure 5.8K. In the other line, the flowers contained partially unfused carpels (data not shown).

Figure 5.9. Overexpression of *OsDD4* in T1 lines of *A. thaliana* Landsberg *erecta*. (**A**) Four-week-old *Arabidopsis* plants transformed with *OsDD4* (left four pots) or transformed with vector without insert (right two pots). (**B**) Four-week-old plants comprising the less-severe class. Note the curly leaves and the enhanced compact inflorescence. (**C**) Inflorescence stem of an eight-week-old plant in the less-severe class. Note the fasciated stem.

Figure 5.9. Overexpression of *OsDD4* in T1 lines of *A. thaliana* Landsberg *erecta*.

As for the Columbia lines overexpressing *OsDD4*, the less severe Landsberg *erecta* T1 lines showed delayed bolting compared to control transformed plants (see Fig. 5.9A), and showed fasciated stems (see Fig. 5.9C). The difference between the phenotypes observed in the Columbia *versus* Landsberg *erecta* background was that the phenotype in Landsberg *erecta* was more severe at an earlier age (in the early vegetative adult phase) than in Columbia. In contrast to Columbia, the Landsberg *erecta* lines (except for the two described above) overcame the dwarf phenotype and bore fertile flowers, as shown in Figures 5.9B and C. In Figure 5.9B the curly leaves and very compact inflorescence are shown, although the plants have started bolting. Shown in Figure 5.9C is the stem fasciation and the presence of siliques developed from later flowers.

SOUTHERN AND NORTHERN BLOT ANALYSES OF *A. THALIANA* OVEREXPRESSING *OsDD4*

Southern and Northern blot analyses were performed with 12 T1 lines overexpressing *OsDD4* in the Columbia background. This included the six severe lines. In Figure 5.10, Southern blot analysis indicated that these lines were independent, and carried one to several copies of the transgene. The genomic DNA was digested with *Bam*HI, which cuts once within the T-DNA inserted into the *Arabidopsis* genome. The presence of more than one band unequivocally determines the presence of more than one insert in the genome. Interestingly, Southern blot analysis indicated that a single band was present in the six severe lines 11, 12, 13, 16, 22.2, and 23, suggesting the presence of one copy of the transgene. The remaining lines contained at least two inserts and showed the less severe phenotype. A band of 9.4 kb on the

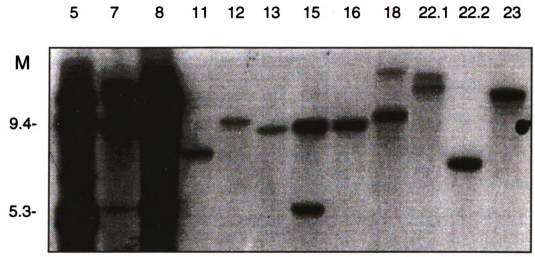

Figure 5.10. *OsDD4* copy number in T1 lines of *A. thaliana* Columbia. The Southern blot contains *Bam*HI-digested DNA. The blot was hybridized with random prime labeled probe derived from the full length *OsDD4* cDNA. Numbers above the lanes indicate the individual lines.

Southern blot indicates the presence of two T-DNA copies inserted head-to-head in the same location. This band was observed in the severe lines 13 and 16. Therefore, the presence of one or two T-DNA inserts in these lines cannot be determined from the data presented in Figure 5.10. Northern blot analysis of the same lines was performed to correlate the severity of the observed phenotype with the *OsDD4* transcript levels. In Figure 5.11, the upper panel is a Northern blot hybridized with a probe derived from the 3' 737-bp region of *OsDD4*, while the bottom panel is hybridized with a probe derived from the 5' 107-bp region of *OsDD4*. Equal RNA loading was confirmed by ethidium bromide staining of the ribosomal RNA (data not shown). Based on intensity of the bands in Figure 5.10, lines containing many copies of the transgene (lines 5, 7, and 8) showed high levels of transcript, ranging from full-length to partial-size transcripts. The lines containing one or few copies showed less RNA. The level of full-length *OsDD4* could, however, not be correlated to the phenotype. Only the presence of an RNA species, approximately 100 bp shorter than full-length shown in lines 5, 7, 8, 15, 18, and 22.1, correlated with the less severe phenotype.

5.5. DISCUSSION

We have identified a novel gene, *OsDD4*, whose expression is rapidly induced in the IM of rice internodes by GA and submergence. Southern blot analysis indicated that *OsDD4* is part of a small gene family, and database searches suggest that OsDD4 may belong to a larger class of regulatory proteins containing QLQ and WRC domains. The overexpression of *OsDD4* in

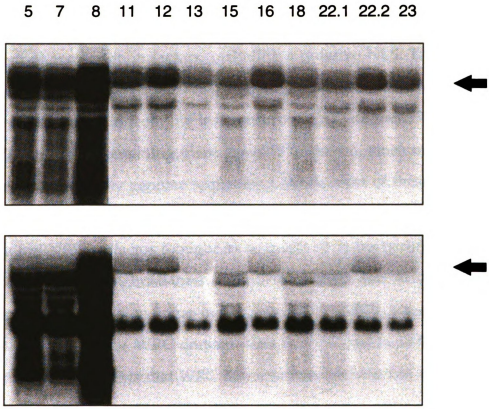

Figure 5.11. *OsDD4* transcript levels in T1 lines of *A. thaliana* Columbia. Northern blot containing RNA isolated from mature leaves of *A. thaliana* ecotype Columbia T1 lines. The top panel is hybridized with random prime labeled probe derived from the 3' 737 bp region of *OsDD4*. The bottom panel is hybridized with an RNA probe derived from the 5' 107 bp region of *OsDD4*. The arrow indicates the full length RNA (~1.8 kb). The numbers above the lanes indicate the individual lines.

Arabidopsis led to a pleiotropic phenotype, suggesting that overexpression resulted in changes in several developmental pathways.

The amino acid sequence of OsDD4 indicated several features reminiscent of transcription factors, including a putative NLS. The most conserved region comprises the WRC domain, which is found in several plant genes downstream from the less conserved QLQ domain. The function of the WRC domain-containing plant genes is unknown, since most of those genes were identified by genome sequencing. While most of these genes show no similarity to known proteins, AC000106 does exhibit high sequence similarity to ENBP1, a factor thought to be involved in transcriptional regulation of *ENOD12* (Christiansen *et al.*, 1996). ENBP1 and AC000106 contain two conserved zinc-finger motifs, which, in ENBP1, were shown to bind DNA. Although the WRC domain itself is not found in ENBP1 but only in AC000106, this suggests that WRC domains may be found in nuclear proteins.

The less conserved QLQ domain is present in proteins related to SWI2/SNF2 from yeast. SWI2/SNF2 is a subunit of a large 2 MDa complex that uses the energy of ATP hydrolysis to drive transcription factors onto nucleosomal transcription-factor-binding sites (Peterson and Tamkun, 1995). While the orthologs are highly related in the C-terminal region, the homology at the N-terminus between the yeast, *Drosophila*, human and chicken is restricted to two short regions. These regions were called domain I and II in brahma, the *Drosophila* ortholog (Tamkun *et al.*, 1992) and are present in the N-terminally located proline-rich and highly charged domain, respectively, of the SWI2/SNF2 orthologs (Peterson and Tamkun, 1995). The QLQ domain shows similarity to domain I, and this domain appears to be

conserved from yeast to plants to mammals. Genetically, the yeast SWI-SNF complex was shown to be essential for nuclear receptor-activated transcription in yeast (Yoshinaga *et al.*, 1992). Using the yeast two-hybrid system, the region of the human orthologs of SWI2/SNF2 important for ligand-dependent interaction with the estrogen receptor was found to span the two conserved domains, including QLQ (Ichinose *et al.*, 1997). This suggests that QLQ itself may be involved in the interaction. Gibberellins are lipophilic molecules that may traverse membranes by diffusion. Although evidence from other GA-regulated processes suggests that GA is perceived at the plasma membrane (Hooley *et al.*, 1991), it is also possible that GA is perceived by cytoplasmic receptors. In analogy to the animal nuclear receptors that, after ligand binding, activate transcription of target genes, OsDD4 may provide the coactivator of transcription of genes that are regulated by GA-receptor transcription factors.

OsDD4 contains a functional NLS and this motif is most likely located in the conserved WRC domain. The distribution of the OsDD4-GUS fusion protein in both the cytoplasm and the nucleus indicates that the NLS is not very efficient and that other factors may be involved in regulating the cellular localization of OsDD4. It will be interesting to know whether the cellular localization of OsDD4 is regulated by GA. Usually, the amino acid sequence surrounding NLSs is not highly conserved. The amino acids surrounding the putative NLS in OsDD4 comprise the most conserved motif found in this protein. For transcription factors in the basic-domain leucine-zipper class (bZIP), a functional NLS is present in the conserved DNA binding domain (Varagona and Raikhel, 1994). In several other classes of transcription factors, NLSs were found overlapping with or adjacent to DNA-binding domains as

well (Hicks and Raikhel, 1995). This suggests that one of the functions of the WRC domain may be in DNA binding.

Overexpression of *OsDD4* in *Arabidopsis* leads to delayed bolting, to fasciated stems and altered phyllotaxy. In addition, in severe lines it also leads to reduced apical dominance, flowering before bolting, impaired inflorescence stem elongation, altered leaves and flowers, impaired male fertility, and complete female sterility. Later in development, changes in flower organ identity and number, and changes in floral meristem identity were observed. GA positively regulates flowering, stem elongation (bolting), apical dominance, male fertility, and vegetative phase change. Although flowering time was not affected in the severe Columbia lines, the other processes were negatively regulated in the lines overexpressing *OsDD4*. This would suggest that OsDD4 is a negative regulator of GA-regulated processes, much like GAI and SPY. However, the rapid increase in transcript levels of *OsDD4* in the IM of rice internodes in response to GA and submergence suggest a positive role of this gene in GA-regulated processes. The alternative explanation then for the observed phenotype is that overexpression leads to a dominant negative phenotype. The overexpression of the rice DD4 in *Arabidopsis* may inactivate the larger protein complex in which the endogenous DD4 is an essential component. Alternatively, overexpression of OsDD4 may titrate out all components important for endogenous DD4 to function properly. Reduced stem elongation, reduced apical dominance, reduced male fertility, and delayed bolting are observed as well in the *ga1-3/rga* double mutant (Silverstone *et al.*, 1997) and in *gai* (except male fertility; Koornneef *et al.*, 1985). The *ga1-3* mutant is a severe GA biosynthesis mutant whose phenotype is partially restored by a mutation in the *RGA* gene. Application of

GA leads to full reversion of the mutant phenotype to wild type (Silverstone *et al.*, 1997). The *gai* mutant confers GA insensitivity and GA application will not restore the phenotype (Koornneef *et al.*, 1985). The phenotype observed in the severe lines overexpressing *OsDD4* was not restored by GA application either.

Not all GA-regulated processes were affected. For example the rate of germination and the length of the pedicel were similar to control transformed plants. On the other hand, some processes not known to be regulated by GA were affected. For example, extreme fasciation was observed in the severe Columbia lines and, to a lesser extent, in the weaker Columbia and Landsberg *erecta* lines. The few fasciated mutants described in *Arabidopsis* display altered phyllotaxy, reduced stem elongation, a change in floral organ number (Leyser and Furner, 1992), and delayed bolting (Medford *et al.*, 1992). The fasciation in those mutants was associated with an enlarged apical meristem, and it is, therefore, likely that overexpression of OsDD4 leads to an enlarged meristem. Fasciation can be the result of a disease caused by *Corynebacterium fascians* and has been linked to increased cytokinin levels (Agrios, 1978). It is, therefore, possible that overexpression of *OsDD4* interferes with cytokinin signaling. Another process not known to be regulated by GA is gynoecium development. Partially unfused carpels and replacement of ovules for filamentous structures were observed in all flowers of the six severe Columbia lines and one severe Landsberg *erecta* line. A null mutation at the *TOUSLED* (Roe *et al.*, 1993; 1997) locus leads to impaired carpel fusion, delayed flowering, and a loss of floral organs. Mutations at the *LEUNIG* locus (Liu and Meyerowitz, 1995) also affect carpel fusion, and mutations at the *AINTEGUMENTA* locus lead to similar gynoecium and ovule development defects as observed for severe lines overexpressing *OsDD4* (Elliot *et al.*, 1996).

This suggests that *OsDD4* overexpression interferes with pathways in which TOUSLED, LEUNIG, and/or AINTEGUMENTA play an important role.

The pleiotropic phenotypes observed suggest that OsDD4 plays a role in some GA-regulated processes as well as in other processes in plant development. On the other hand, overexpression of *OsDD4* under a general and highly active promoter could potentially affect several developmental pathways due to the inappropriate expression of the transgene. It is possible, for example, that overexpression of *OsDD4* interferes with the function of other proteins containing the QLQ and WRC domains. Ectopic expression of a gene can help reveal its *in vivo* role as shown for the maize homeo box gene, *KNOTTED* (Sinha *et al.*, 1993). In the case of *OsDD4*, for example, the putative change in floral meristem identity due to overexpression may not indicate a role for this gene in floral meristems but in vegetative meristems, where it may play a role in delaying vegetative phase change. During submergence of deepwater rice, the IM becomes more sensitive to GA and this leads to increased growth (Raskin and Kende, 1984a). Flowering in deepwater rice is under strict photoperiod control. However, in *Arabidopsis*, which is a facultative long day plant, flowering time under short days can be reduced by application of GA. Flowering time in deepwater rice is correlated with the receding water levels at the end of the growing season. This is a very important trait since plants that flower prematurely will drown, because of the change from an indeterminate to a determinate shoot meristem. Therefore, increased sensitivity of the rice tissue to GA should not lead to flowering but only to enhanced internodal elongation. Maintenance of the apical meristem in the vegetative phase will accomplish this.

The transgene copy number correlated with the phenotype, suggesting that, in the case of two or more inserted T-DNAs, partial or complete

cosuppression of the transgenes was observed. Cosuppression is manifested at the transcriptional or the post-transcriptional level, resulting in reduced RNA levels (Matzke *et al.*, 1996). However, in the lines examined, the transcript levels did not correlate to the phenotype. Therefore, it is unclear how the observed phenotypes are attained. However, the identification of six independent T1 lines in Columbia and two in Landsberg *erecta* displaying similar severe phenotypes suggests that the phenotype observed is not due to position effects of the transgene in the *Arabidopsis* genome.

In conclusion, overexpression of *OsDD4* in *Arabidopsis* leads to negative regulation of several growth-related processes. To understand whether this is achieved via a dominant negative interference or via the overexpression of a negative regulator of growth will require the analysis of transgenic plants which down-regulate the endogenous *DD4*. The phenotypes observed can be classified in three groups: (i) Fasciation, which, in severe cases, resulted in reduced height, altered phyllotaxy and altered organ numbers. (ii) Altered organ morphology, which resulted in altered leaves and partially unfused carpels. (iii) Changes in organ and meristem identity, which resulted in altered flower organs, a floral meristem identity switch, and delayed vegetative phase change. All these phenotypes combined suggest that overexpression leads to a change in apical meristem structure and function. However, our current knowledge about *OsDD4* is too limited to distinguish between an enhancement of its *in vivo* role or an interference in an unrelated signaling pathway. To understand the role of OsDD4 in the meristem and to understand its role in GA signaling, it will be important to know more about *OsDD4* in rice and about its ortholog in *Arabidopsis*.

5.6. LITERATURE

Altschul, S.F., Madden, T.L., Schaffer, A.A., Zhang, J., Zhang, Z., Miller, W. and Lipman, D.J. (1997) Gapped BLAST and PSI-BLAST: a new generation of protein database search programs. Nucleic Acids Res **25**:3389-3402.

Agrios, G.N. (1978) Plant Pathology. Academic Press, New York, New York, USA.

An, G., Ebert, P.R., Mitra, A. and Ha, S.B. (1988) Binary vectors. *In* Plant Molecular Biology Manual A3. Kluwer Acad Publishers, Dordrecht, the Netherlands, pp 1-19.

Ausubel, F.M., Brent, R., Kingston, R.E., Moore, D.D., Seidman, J.G., Smith, J.A. and Struhl, K. (1987) Current Protocols in Molecular Biology (Wiley, New York).

Bleecker, A.B., Schuette, J.L. and Kende, H. (1986) Anatomical analysis of growth and developmental patterns in the internode of deepwater rice. Planta **169**:490-497.

Catling, H.D. (1992) Rice in Deepwater. The Macmillan Press Ltd, London and Basingstoke, UK.

Christiansen, H., Hansen, A.C., Vijn, I., Pallisgaard, N., Larsen, K., Yang, W.-C., Bisseling, T., Marcker, K.A. and Jensen, E.Ø. (1996) A novel type of DNA-binding protein interacts with a conserved sequence in an early nodulin *ENOD12* promoter. Plant Mol Biol **32**:809-821.

Clark, S.E. and Meyerowitz, E.M. (1994) Flower development. *In Arabidopsis*. E.M. Meyerowitz and C.R. Somerville, eds. Cold Spring Harbor, New York: Cold Spring Harbor Laboratory, pp 435-466.

Elliot, R.C., Betzner, A.S., Huttner, E., Oakes, M.P., Tucker, W.Q.J., Gerentes, D., Perez, P. and Smyth, D.R. (1996) *AINTEGUMENTA*, an *APETALA2*-like gene of Arabidopsis with pleiotropic roles in ovule development and floral organ growth. Plant Cell **8**:155-168.

Furner, I.J. and Pumfrey, J.E. (1992) Cell fate in the shoot apical meristem of *Arabidopsis thaliana*. Development **115**:755-764.

Hicks, G.R. and Raikhel, N.V. (1995) Protein import into the nucleus: an integrated view. Annu Rev Cell Dev Biol **11**:155-188.

Hoffmann-Benning, S. and Kende, H. (1992) On the role of abscisic acid and gibberellin in the regulation of growth in rice. Plant Physiol **99**:1156-1161.

Hooley, R., Beale, M.H. and Smith, S.J. (1991) Gibberellin perception at the plasma membrane of *Avena fatua* aleurone protoplasts. Planta **183**:274-280.

Ichinose, H., Garnier, J.-M., Chambon, P. and Losson, R. (1997) Ligand-dependent interaction between the estrogen receptor and the human homologues of SWI2/SNF2. Gene **188**:95-100.

Jacobsen, S.E., Binkowski, K.A. and Olszewski, N.E. (1996) SPINDLY, a tetratricopeptide repeat protein involved in gibberellin signal transduction in *Arabidopsis*. Proc Natl Acad Sci USA **93**:9292-9296.

Koornneef, M., Elgersma, A., Hanhart, C.J., van Loenen-Martinet, E.P., van Rijn, L. and Zeevaart, J.A.D. (1985) A gibberellin insensitive mutant of *Arabidopsis thaliana*. Plant Physiol **65**:33-39.

Leyser, H.M.O. and Furner, I.J. (1992) Characterization of three shoot apical meristem mutants of *Arabidopsis thaliana*. Development **116**:397-403.

Liang, P. and Pardee, A.B. (1992) Differential display of eukaryotic messenger RNA by means of the polymerase chain reaction. Science **257**:967-971.

Liu, Z. and Meyerowitz, E.M. (1995) *LEUNIG* regulates *AGAMOUS* expression in *Arabidopsis* flowers. Development **121**:975-991.

Matzke, M.A., Matzke, A.J.M. and Eggleston, W.B. (1996) Paramutation and transgene silencing: a common response to invasive DNA. Trends Plant Sci **1**:382-388.

Medford, J.I., Behringer, F.J., Callos, J.D. and Feldmann, K.A. (1992) Normal and abnormal development in the Arabidopsis vegetative shoot apex. Plant Cell **4**:631-643.

Métraux, J.-P. and Kende, H. (1983) The role of ethylene in the growth response of submerged deepwater rice. Plant Physiol **72**:441-446.

Mitchell, P.J. and Tjian, R. (1989) Transcriptional regulation in mammalian cells by sequence-specific DNA binding proteins. Science **245**:371-378.

Olszewski, N. (1997) Evidence that dynamic O-linked N-acetylglucosamine modification of proteins plays a role in gibberellin signal transduction. 8th International conference on Arabidopsis research. Madison, Wisconsin.

Peng, J., Carol, P., Richards, D.E., King, K.E., Cowling, R.J., Murphy, G.P. and Harberd N.P. (1997) The *Arabidopsis GAI* gene defines a signaling pathway that negatively regulates gibberellin responses. Genes Dev **11**:3194-3205.

Peterson, C.L. and Tamkun, J.W. (1995) The SWI-SNF complex: a chromatin remodeling machine? Trends Biochem Sci **20**:143-146.

Puissant, C. and Houdebine, L.M. (1990) An improvement of the single-step method of RNA isolation by acid guanidium thiocyanate-phenol-chloroform extraction. BioTechniques **8**:148-149.

Raskin, I. and Kende, H. (1984a) Role of gibberellin in the growth response of submerged deepwater rice. Plant Physiol **76**:947-950.

Raskin, I. and Kende, H. (1984b) Regulation of growth in stem sections of deepwater rice. Planta **160**:66-72.

Roe, J.L., Rivin, C.J., Sessions, R.A., Feldmann, K.A. and Zambryski, P.C. (1993) The *Tousled* gene in A. thaliana encodes a protein kinase homolog that is required for leaf and flower development. Cell **75**:939-950.

Roe, J.L., Nemhauser, J.L. and Zambryski, P.C. (1997) *TOUSLED* participates in apical tissue formation during gynoecium development in Arabidopsis. Plant Cell **9**:335-353.

Sauter, M. and Kende, H. (1992) Gibberellin-induced growth and regulation of the cell division cycle in deepwater rice. Planta **188**:362-368.

Sauter, M., Seagull, R.W. and Kende, H. (1993) Internodal elongation and orientation of cellulose microfibrils and microtubules in deepwater rice. Planta **190**:354-362.

Sauter, M., Mekhedov, S.L. and Kende, H. (1995) Gibberellin promotes histone H1 kinase activity and the expression of *cdc2* and cyclin genes during the induction of rapid growth in deepwater rice internodes. Plant J **7**:623-632.

Sauter, M. (1997) Differential expression of a CAK (cdc2-activating kinase)-like protein kinase, cyclins and *cdc2* genes from rice during the cell cycle and in response to gibberellin. Plant J **11**:181-190.

Silverstone, A.L., Mak, P.Y.A., Martinez, E.C. and Sun, T.-p. (1997) The new *RGA* locus encodes a negative regulator of gibberellin response in *Arabidopsis thaliana*. Genetics **146**:1087-1099.

Silverstone, A.L., Ciampaglio, C.N. and Sun, T.-p. (1998) The Arabidopsis *RGA* gene encodes a transcriptional regulator repressing the gibberellin signal transduction pathway. Plant Cell **10**:155-169.

Sinha, N.R., Williams, R.E. and Hake, S. (1993) Overexpression of the maize homeo box gene, *KNOTTED-1*, causes a switch from determinate to indeterminate cell fates. Genes Dev **7**:787-795.

Smyth, D.R., Bowman, J.L. and Meyerowitz, E.M. (1990) Early flower development in Arabidopsis. Plant Cell **2**:755-767.

Stünzi, J.T. and Kende, H. (1989) Gas composition in the internal air spaces of deepwater rice in relation to growth induced by submergence. Plant Cell Physiol **30**:49-56.

Tamkun, J.W., Deuring, R., Scott, M.P., Kissinger, M., Pattatucci, A.M., Kaufman, T.C. and Kennison, J.A. (1992) brahma: A regulator of Drosophila homeotic genes structurally related to the yeast transcriptional activator SNF2/SWI2. Cell **68**:561-572.

Van der Knaap, E. and Kende, H. (1995) Identification of a gibberellin-induced gene in deepwater rice using differential display of mRNA. Plant Mol Biol **28**:589-592.

Van Hoof, A. and Green, P.J. (1996) Premature nonsense codons decrease the stability of phytohemagglutinin mRNA in a position-dependent manner. Plant J **10**:415-424.

Varagona, M.J., Schmidt, R.J. and Raikhel, N.V. (1992) Nuclear localization signal(s) required for nuclear targeting of the maize regualtory protein Opaque-2. Plant Cell **4**:1213-1227.

Varagona, M.J. and Raikhel, N.V. (1994) The basic domain in the bZIP regulatory protein Opaque2 serves two independent functions: DNA binding and nuclear localization. Plant J **5**:207-214.

Wilson, R.N. and Somerville, C.R. (1995) Phenotypic suppression of the gibberellin-insensitive mutant (*gai*) of *Arabidopsis*. Plant Physiol 108:495-502.

Yoshinaga, S.K., Peterson, C.L., Herskowitz, I. and Yamamoto, K.R. (1992) Roles of SWI1, SWI2, and SWI3 proteins for transciptional enhancement by steroid receptors. Science **258**:1598-1604.

CHAPTER 6

A putative type 1a plasma membrane receptor is induced by gibberellin in deepwater rice

6.1. ABSTRACT

In search for differentially expressed genes, a novel gene was identified whose transcript levels had increased in response to gibberellin (GA) in the internodes of deepwater rice. The expression was high in regions undergoing cell division and lower in the elongation and differentiation zones. The gene may encode a type 1a receptor with an extracellular domain, a single transmembrane domain and a short cytoplasmic domain.

6.2. INTRODUCTION

Survival of deepwater rice during flooding is based on its capacity for rapid internodal elongation when it becomes submerged. The signal for accelerated growth is an increase in ethylene levels, which enhances the responsiveness of the internode to GA (Raskin and Kende, 1984a). Enhanced growth is initiated in the intercalary meristem (IM) at the base of the growing internode and is based on increased production of cells and increased elongation of these cells after they emerge from the meristem into the elongation zone (EZ) (Bleecker *et al.*, 1986; Sauter and Kende, 1992). To understand the molecular events taking place during growth, a search was initiated to identify genes that are differentially regulated by GA in the IM of rice internodes. By means of differential display (Liang and Pardee, 1992), several genes have been identified whose transcript levels increase in response to GA (Van der Knaap and Kende, 1995; Van der Knaap *et al.*, 1997). Here, we report on the identification of *OsDD3*, a gene whose transcript levels increase in response to GA and to submergence in the IM of deepwater rice internodes. The gene product may encode a novel type 1a receptor located at the plasma membrane.

6.3. MATERIALS AND METHODS

PLANT MATERIAL

Seeds of deepwater rice (*Oryza sativa* L., cv. Pin Gaew 56) were obtained from the International Rice Research Institute (Los Baños, Philippines). Plants were

grown as described in Stünzi and Kende (1989). For submergence experiments, 12-week-old plants were partially immersed under continuous light (Métraux and Kende, 1983). Twenty-cm-long stem sections containing the growing internode were excised and treated with 50 μM GA_3 (Raskin and Kende, 1984b). Incubation was allowed to proceed for the periods indicated, after which the IM was excised, frozen immediately, and stored at -80°C until use.

IDENTIFICATION OF *OsDD3*

A differentially displayed 228 bp cDNA band, *dd3*, was identified using primers T_{12}MG and OPA04 (Van der Knaap and Kende, 1995). The differential displayed product was inserted in pUC19, and the cloned cDNA was used to screen a IM-specific cDNA library to obtain a full-length cDNA insert, *OsDD3*. The phage insert was cloned into the *Eco*RI site of pBluescript SK(-) phagemid (Stratagene) and sequence analysis was performed at the Biochemistry Facility of the Plant Research Laboratory at Michigan State University. The sequences were aligned using Sequencher, version 3.0 (Gene Codes Corporation).

NORTHERN BLOT ANALYSIS

Twenty μg of total RNA, isolated according to Puissant and Houdebine (1990), was electrophoretically separated in a 1.2% formaldehyde-agarose gel (Ausubel *et al.*, 1987) and transferred to Hybond-N+ membrane (Amersham). For *OsDD3*, the RNA probe was made from the *Bst*XI - *Eco*RI fragment containing the 3' UTR (see Fig. 6.5) in the presence of α-[^{32}P]UTP (NEN). For *cycOs1*, the RNA probe contained the 3' UTR and most of the coding region

(Sauter *et al.*, 1995). Blots were prehybridized and hybridized in 3x SSPE, 10x Denhardt's solution (Sambrook *et al.*, 1989), 0.5% SDS, 50 µg/ml denatured salmon sperm DNA, and 50% deionized formamide (BMB) at 65°C overnight. Blots were washed twice for 5 min each in 2x SSC and 0.5% SDS at 65°C followed by two washes in 0.1x SSC and 0.5% SDS for 30 min each. Probes for histone H3 and *E37* were prepared by random prime labeling and hybridized to the blots as described in Van der Knaap *et al.* (1997). The radioactivity on blots was quantified by PhosphorImager analysis (Molecular Dynamics).

SOUTHERN BLOT ANALYSIS

Rice genomic DNA was isolated from a CsCl gradient according to Ausubel *et al.* (1987). Five µg of DNA was digested overnight, and fragments were separated on a 0.8% agarose gel for 20 h at 30 V. The gel was then treated for 15 min in 0.25 N HCl, 30 min in 0.5 N NaOH and 1.5 M NaCl and 15 min in 1 M Tris-HCl, pH 8 and 1.5 M NaCl after which the DNA was transferred to Hybond N+ (Amersham). Blots were prehybridized in 5x SSC, 10x Denhardt's solution, 0.2% SDS, 0.1 M K-phosphate, pH 6.8 and 100 µg/ml denatured salmon sperm for 4 h and hybridized in 5x SSC, 10x Denhardt's solution, 0.1% SDS, 0.1 M K-phosphate, pH 6.8, 10% dextran sulphate, 30% deionized formamide, and 100 µg/ml denatured salmon sperm overnight at 42°C. A probe derived from the *Bst*XI - *Eco*RI fragment (see Fig. 6.5) was prepared in the presence of α-[^{32}P]dCTP (NEN) with a random prime labeling kit (BMB). Blots were washed twice for 30 min each in 2x SSC and 0.5% SDS at 65°C followed by two washes in 0.1x SSC and 0.5% SDS for 30 min each.

IN-VITRO TRANSLATION REACTION

A plasmid containing a full-length *OsDD3* λ 10.1, was linearized, and sense RNA was prepared in an in-vitro transcription reaction with T3 RNA polymerase (BMB). RNA was purified by organic extractions and precipitated with ethanol. Approximately 100 ng of RNA was translated in a rabbit reticulocyte lysate (Promega) in the presence of [^{35}S]methionine (1,200 Ci/mmol; NEN) or [^{3}H]leucine (100-200 Ci/mmol; NEN) in a total volume of 25 µl. The translation reaction was allowed to proceed at 30°C for 1 h, either in the presence or absence of 1.8 µl canine pancreatic microsomal membranes (Promega). Three µl of translation products were separated on 15% SDS-PAGE. Prior to drying, the gel was fixed in 30% methanol and 10% acetic acid and subsequently incubated in 1M Na-salicylate, pH 6, to enhance the signal for autoradiography.

6.4. RESULTS

GA treatment of rice stem sections, containing the growing internode, led to an increase in transcript abundance of *OsDD3* as shown in Figure 6.1A. The signals were quantified and normalized for equal loading using a cDNA, *E37*, corresponding to a gene whose transcript levels did not change over the course of the experiment. Figure 6.1B shows that the level of *OsDD3* in the IM of GA-treated stem sections had increased over 3-fold 4 h after start of GA treatment. The expression pattern of *OsDD3* was also investigated in submerged plants as shown in Figure 6.2A. The transcript levels had increased after 8 h, reaching a 6-fold increase 24 h after start of treatment (Fig.

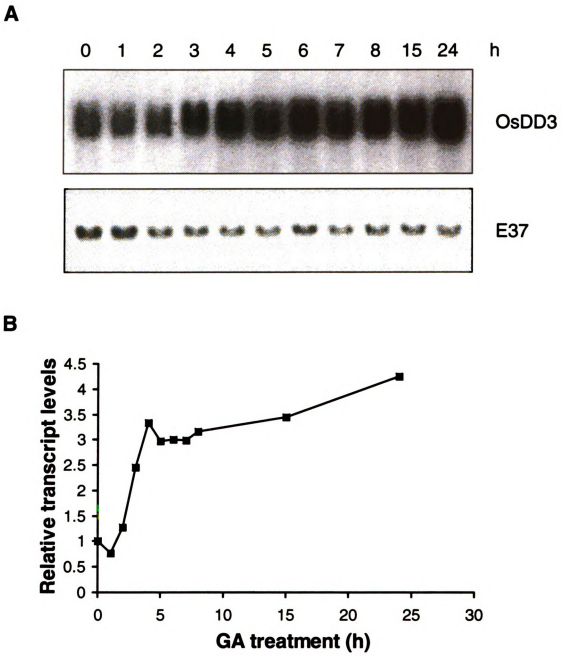

Figure 6.1. GA-induced expression of *OsDD3* in the IM of rice stem sections. Rice stem sections were incubated in 50 μM GA_3 for the times indicated above the lanes, after which RNA was isolated from the IM. (**A**) Northern blot, containing 20 μg of RNA, was hybridized to *OsDD3* and *E37*. (**B**) Quantitative analysis of the Northern blot shown in (A) using a PhosphorImager. All values were normalized to the *E37* loading control.

Figure 6.2. Submergence-induced expression of the *OsDD3*, histone H3 and *cycOs1* genes. Plants were submerged for the times indicated above the lanes, after which RNA was isolated from the IM. (**A**) The Northern blots were hybridized to *OsDD3*, histone H3, *cycOs1* and *E37*. (**B**) Quantitative analysis of the Northern blots by Phosphor-Imager. All values were normalized to the *E37* loading control obtained from the same blot.

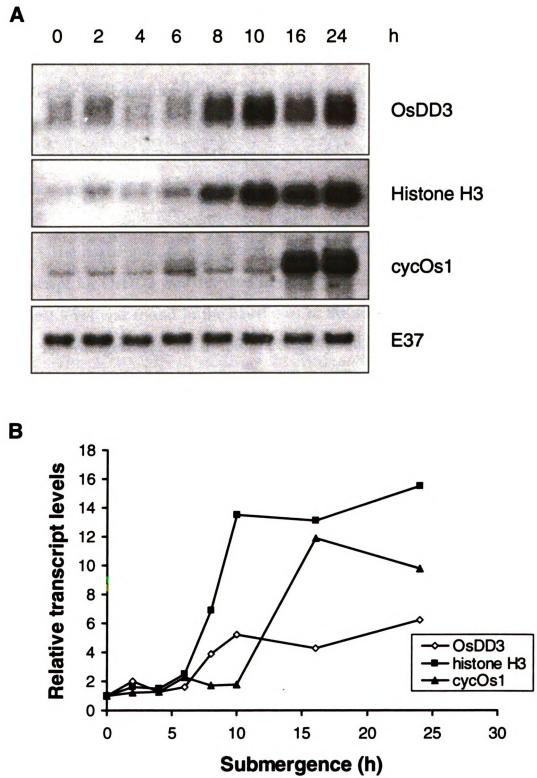

Figure 6.2. Submergence-induced expression of the *OsDD3*, histone H3 and *cycOs1* genes.

6.2B). The increase in transcript level for *OsDD3* was compared to the increase in transcript level for histone H3 and *cycOs1*. Histone H3 is a marker for the S-phase of the cell cycle (Van der Knaap and Kende, 1995) and *cycOs1* is a marker for the transition of the G2 to M phase (Sauter et al., 1995; Sauter, 1997). As shown in Figure 6.2B, the increase in expression of *OsDD3* coincided with an increase in histone H3 transcript levels. This was followed by an increase in *cycOs1* transcript levels.

The tissue-specific expression of *OsDD3* is shown in Figure 6.3. The transcript for *OsDD3* was detected in many tissues of rice. However, the highest level was found in the basal part of the sheath of the second youngest leaf, the youngest leaf and in the IM. Slightly lower expression was detected in the coleoptile containing the youngest leaf and in the root tip. Along the internode, *OsDD3* was expressed at much lower levels in the EZ and in the differentiation zone, than in the IM, while no transcript was detected in the oldest part of the internode.

Southern blot analysis was employed to address the question whether the probe used in this study is gene specific and whether close homologs of *OsDD3* exist in rice. As can be seen in Figure 6.4, all digests produced one band, indicating that the probe used is gene specific.

A full-length clone encoding *OsDD3* was obtained from an IM-specific cDNA library, of which the largest clone (λ 5.1, see Fig. 6.5B) was sequenced. The cDNA was 1188 nucleotides long and showed an ORF of 196 amino acids yielding a predicted protein of 20 kD (Fig. 6.5A). Searches to find homologous sequences in the non-redundant or EST database using the BLAST program

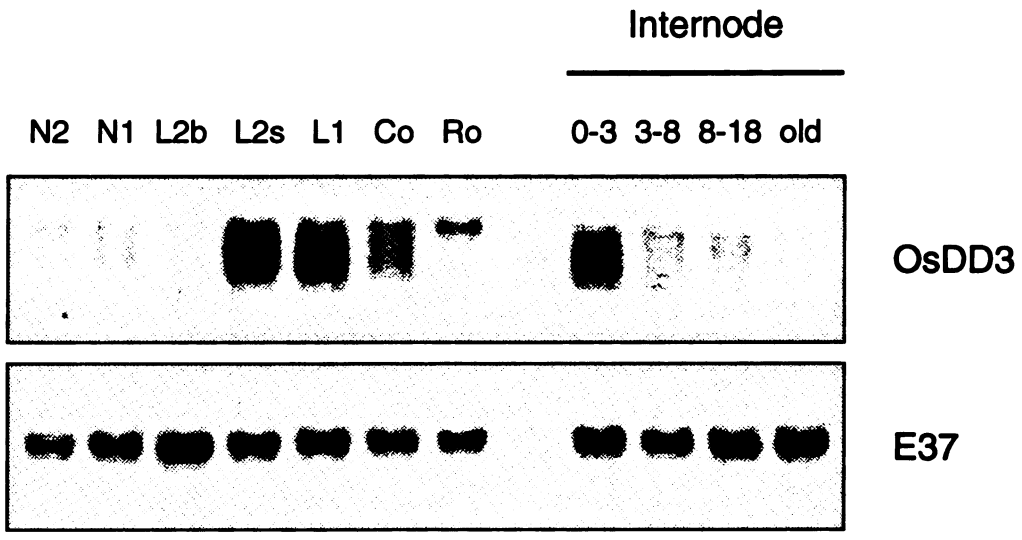

Figure 6.3. Tissue-specific expression of *OsDD3* in rice. N2, second highest node; N1, highest node containing the apical meristem; L2b, basal 2 cm of second youngest leaf blade; L2s, basal 2 cm of second youngest leaf sheath; L1, youngest leaf; Co, coleoptile 3 days after germination; Ro, root 3 days after germination; 0-3, internodal region 0-3 mm above N2 containing the IM; 3-8, internodal region 3-8 mm above N2 containing mostly the EZ; 8-18, internodal region 8-18 mm above N2 containing the upper part of the EZ and the DZ; old, oldest part of the internode. The upper panel shows hybridization signals with *OsDD3* as probe, the lower panel shows hybridization signals with *E37* as internal loading control.

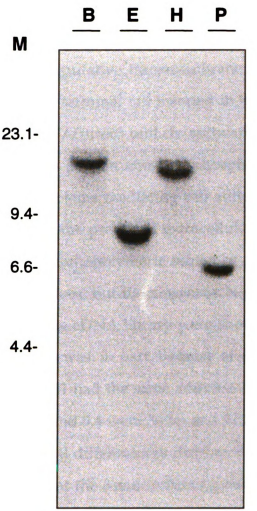

Figure 6.4. Southern blot analysis of *OsDD3* in rice. Southern blot containing rice genomic DNA, digested with either *Bam*HI (B), *Eco*RI (E), *Hind*III (H) or *Pst*I (P). The blot was probed with random prime labeled insert derived from the 3' UTR of *OsDD3*.

(Altschul *et al.*, 1990) did not identify related genes. As is indicated in Figure 6.5A, the protein contains a putative signal sequence, with a potential cleavage site between residue 33 and 34 (von Heijne, 1986). PSORT (http://psort.nibb.ac.jp/) predicted a type 1a membrane protein, located at the plasma membrane. The putative transmembrane region is between residue 167 and 183, with the C-terminal tail inserted in the cytoplasm. Motif searches using PrositeScan (http://ulrec3.unil.ch/software/PSTSCAN_form. html) indicated two consensus protein kinase C phosphorylation sites as well as a RGD motif found in proteins mediating cell adhesion (D'Souza *et al.*, 1991). Besides the RGD motif, the predicted extracellular domain contains a cysteine-rich region, a homopolymeric sequence of alanines, as well as several proline and serine residues, but no consensus N-glycosylation site. Other inserts obtained from the cDNA library were shorter than λ 5.1. As can be seen in Figure 6.5B, this was, in part, because of different additions of the poly(A) tail. While λ 10.1 had the same addition of the poly(A) tail as λ 5.1, the poly(A) tail of 10.4 and 5.4 were 36 bp and 91 bp respectively upstream of that in λ 5.1. The original differentially displayed product, *dd3*, was amplified by the oligo dT primer at the 3'end indicating that this product was derived from an mRNA species containing the poly(A) tail 143 bp upstream of the one in λ 5.1. All four inserts identified from the cDNA library contained the same putative ORF.

In-vitro translation reactions were performed to determine whether *OsDD3* encodes a protein of approximately 20 kD. Also, the presence of the signal sequence was tested by allowing the reactions to take place in the presence or absence of dog pancreatic microsomes. A functional signal sequence will direct the translating ribosomes to the microsomes. After

A

```
MRTAATPPLAAAAAAVAAVFLSALLLASASASASRLPPPRRLLPLVGGEV      50

AVAVVAGEEEKVRLGSSPPSCYSKCYGCSPCVAVQVPTLSAPSVPAAAAA     100

AARRRAARGDVHQLQAARVEVPVPRPPVRPLTLRRARPVARRGVAWRVHG     150

GARARALAVNYGVCGRVACPAAHGAALLLMLVVVESLSSRRAERDC         196
```

B

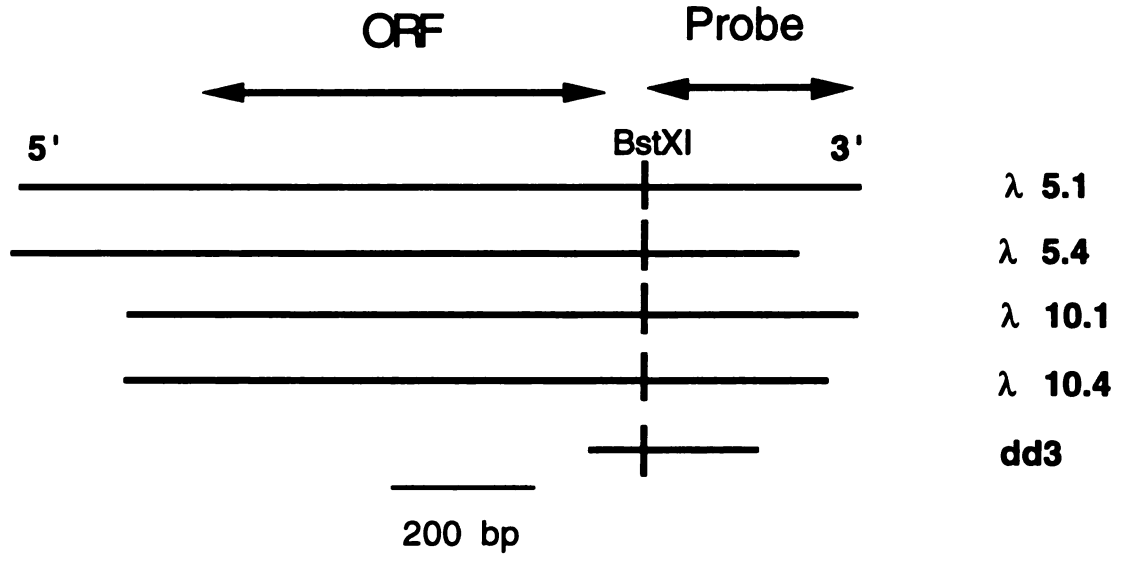

Figure 6.5. Amino acid sequence of *OsDD3*. (**A**) Putative ORF of *OsDD3*. The signal sequence is double underlined and the potential transmembrane region is boxed. Motifs found in OsDD3 are two potential protein kinase C phosphorylation sites (single underlined) and one RGD motif (dark boxed). Cysteine residues that may participate tertiary structure, in ligand binding, or in dimerization via disulfide bridges are shown as outline letters. (**B**) Independent clones isolated from an IM-specific cDNA library showing differences in 5' ends and addition of the polyadenylated tail at the 3' end. The location of the ORF and the region used as probe are indicated.

transfer into the microsomes, the signal sequence will be cleaved off. As shown in Figure 6.6, the in-vitro translated control mRNA, encoding β-lactamase, was processed from 31.5 kD to 29 kD. The in-vitro translated *OsDD3* mRNA showed a product of expected size, which, in the presence of microsomes, was processed from 20 kD to 17 kD. This indicated that a functional signal sequence is present in OsDD3 and that OsDD3 enters the secretory pathway.

6.5. DISCUSSION

A gene, *OsDD3*, whose transcript levels increased during GA treatment of stem sections and during submergence of whole plants, was identified by differential display. The difference in timing of the increase in transcript levels between the two treatments was expected since the lag phase of GA-induce growth is 40 min (Sauter and Kende, 1992), and that of submergence-induced growth is 3 h 20 min (Rose-John and Kende, 1985). Although the increase in transcript levels was only 3- to 4-fold and 6-fold in stem sections and in submerged plants, respectively, this response was reproducible. The early events leading to growth are more clearly separated time-wise in submerged plants than in GA-treated stem sections (Lorbiecke and Sauter, 1998). Therefore, submerged plants were used to compare the increase in transcript levels of *OsDD3* to markers of the cell cycle. Changes in expression of histone H3 and *cycOs1* were shown before to correlate well with the S-phase and the G2 to M-phase transition, respectively (Sauter *et al.*, 1995; Van der Knaap and Kende, 1995; Lorbieke and Sauter, 1998). The increase in *OsDD3* transcript level coincided with the first noticeable change in cell cycle

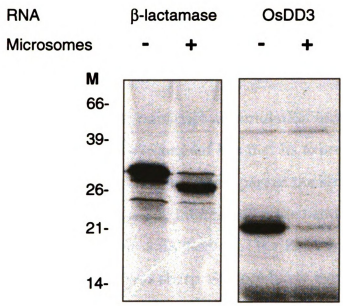

Figure 6.6. In-vitro translation of *OsDD3*. Control RNA, encoding β-lactamase, and *OsDD3* were in-vitro translated in the absence or presence of canine pancreatic microsomal membranes as indicated above the lanes. β-lactamase RNA was in-vitro translated in the presence of [^{35}S]methionine and *OsDD3* was in-vitro translated in the presence of [^{3}H]leucine.

activity, as was indicated by histone H3 expression. This indicates that the transcript levels of *OsDD3* increase early during submergence-induced growth. However, this was not as early as that of *Os-RPA1* and *OsDD4*, whose transcript levels increased 4 h after start of submergence (Van der Knaap *et al.*, 1997; Chapter 5).

The tissue-specific transcript accumulation indicated that *OsDD3* is expressed in most tissues examined but that its expression is highest in actively growing regions, *i.e.*, the basal part of the second youngest leaf sheath, the youngest leaf, and the IM. Interestingly, the band pattern was smeary in most tissues examined. It is unlikely that the RNA was partially degraded since the signal for *E37* was sharp. A more likely explanation is the size difference in mRNA due to the difference in addition of the poly(A) tail, as was indicated by the different clones isolated from the cDNA library. The addition of the poly(A) tail may be under tissue-specific control since the lane containing RNA isolated from the root tip showed a sharp band in contrast to RNA isolated from other tissues. Whether the 5' end of *OsDD3* is heterogeneous as well cannot be concluded from the clones isolated from the cDNA library, and this question has not been further investigated.

Southern blot analysis showed one band in all lanes. The size of the smallest band on the Southern blot was 6.2 kb and was found in the lane containing *Pst*I-digested DNA. If the genomic region spanning *OsDD3* contained no intron, it is possible that the fragments on the Southern blot contained two linked copies of *OsDD3*. The presence of genes related to the protein encoded by *OsDD3* can not be determined since the probe used was entirely derived from the 3' UTR.

No significant similarity was detected between the nucleotide sequence of *OsDD3* and the protein it encodes to entries in the DNA and protein databases. One rice EST, D23940, has 25.8% amino acid identity and 37.4% similarity to OsDD3. The significance of this similarity is unclear since the available sequence was only 264 nucleotides long, and the amino acid sequence alignment showed gaps between OsDD3 and amino acid sequence derived from the rice EST. BLASTP searches in the non-redundant databases identified potential homologs of low probability. They ranged from membrane proteins to antifreeze proteins and transcriptional activators. One protein with limited homology to OsDD3 is an allergen from Japanese cedar pollen (Namba *et al.*, 1994). The significance of that finding can be debated as well since the sequence similarity is over a short region, and this region is not present in the mature allergen protein.

Analysis by PSORT predicts that the OsDD3 protein is a type 1a membrane protein that spans the plasma membrane and contains a short C-terminal tail in the cytoplasm. The presence of a functional signal sequence provides support for the plasma membrane localization of OsDD3. It may function there as a receptor and signal transmitter between the cell wall matrix and the cytoplasm. During plant growth, communication between the cell wall and in the cytoplasm is likely to be essential. Interestingly, database searches indicated some sequence similarity to CD8 α chain. CD8 α and β are glycoproteins expressed on T cells and contain an immunoglobulin-like extracellular domain, a membrane spanning segment, and a short cytoplasmic tail (Leahy, 1995). The extracellular domain recognizes the appropriate major histocompatibility complex molecules while the cytoplasmic tail interacts with a src-like tyrosine kinase, $p56^{lck}$. The

significance of this similarity is mostly structural since OsDD3 has no similarity to the immunoglobulin-like extracellular domain, but only to the region preceding and spanning the plasma membrane, as well as the C-terminal region. Overall amino acid identity between CD8 α and OsDD3 is 22.6% while the similarity is 44.4%. Like CD8, OsDD3 may signal through cytoplasmic kinases which interact with its C-terminal tail. The serines located in the C-terminal domain of OsDD3 (see Fig. 6.5A) may be targets for phophorylation.

The proposed extracellular domain of OsDD3 bears no sequence similarity to any known or suspected receptors in either animals or plants. It contains several cysteine residues, which may be involved in the tertiary structure, in ligand binding, or in dimerization via disulfide bridges. Another motif found in the presumed extracellular domain is the RGD motif found in proteins mediating cell adhesion in animals (D'Souza *et al.*, 1991). Fibronectin is an extracellular glycoprotein and is the prototype cell adhesion molecule. The minimum functional unit for cell adhesion is RGD, which is recognized by receptors belonging to the integrin family of cell adhesion molecules. The role of integrins is to integrate the extracellular matrix outside the cell with the actin-containing cytoskeleton inside the cell. In plants, effects of peptides containing the RGD motif have been observed (Schindler *et al.*, 1989). In soybean suspension cells, addition of these peptides led to enhanced growth rates and aberrant cell wall - plasma membrane interactions. The relevance of this is unknown. In plants, several proteins have been identified to contain an RGD domain. However, the function of this domain in any of the plant proteins is unknown.

Many extracellular plant proteins are glycosylated, and proline residues may be hydroxylated (Carpita and Gibeaut, 1993). While no consensus N-

linked glycosylation site is present in OsDD3, the serine and potentially hydroxylated proline residues may be glycosylated via O-linkage to their hydroxyl group.

The in-vitro translation experiment in the presence or absence of microsomes confirmed the existence of a functional signal sequence in OsDD3. This indicated that OsDD3 enters the secretory pathway. Motifs known to be transport or retrieval signals between compartments along the vesicular transport pathway (Rothman and Wieland, 1996) were not found in OsDD3. This strengthens the possibility that OsDD3 is plasma membrane localized. However, before the role of OsDD3 in GA-regulated growth can be elucidated, the precise location of OsDD3 in the cell needs to be addressed.

6.6. LITERATURE

Altschul, S.F., Warren, G., Gish, W., Myers, E.W. and Lipman, D.J. (1990) Basic local alignment search tool. J Mol Biol **215**:403-410.

Ausubel, F.M., Brent, R., Kingston, R.E., Moore, D.D., Seidman, J.G., Smith, J.A. and Struhl, K. (1987) Current Protocols in Molecular Biology (Wiley, New York).

Bleecker, A.B., Schuette, J.L. and Kende, H. (1986) Anatomical analysis of growth and developmental patterns in the internode of deepwater rice. Planta **169**:490-497.

D'Souza, S.E., Ginsberg, M.H. and Plow, E.F. (1991) Arginyl-glycyl-aspartic acid (RGD): a cell adhesion motif. Trends Biochem Sci **16**:246-250.

Carpita, N.C. and Gibeaut, D.M. (1993) Structural models of primary cell walls in flowering plants: consistency of molecular structure with the physical properties of the walls during growth. Plant J **3**:1-30.

Leahy, D.J. (1995) A structural view of CD4 and CD8. FASEB J **9**:17-25.

Liang, P. and Pardee, A.B. (1992) Differential display of eukaryotic messenger RNA by means of the polymerase chain reaction. Science **257**:967-971.

Lorbiecke, R. and Sauter, M. (1998) Induction of cell growth and cell division in the intercalary meristem of submerged deepwater rice (*Oryza sativa* L.). Planta **204**:140-145.

Métraux, J.-P. and Kende, H. (1983) The role of ethylene in the growth response of submerged deepwater rice. Plant Physiol **72**:441-446.

Namba, M., Kurose, M., Torigoe, K., Hino, K., Taniguchi, Y., Fukuda, S., Usui, M. and Kurimoto, M. (1994) Molecular cloning of the second major allergen, *Cry* II, from Japanese cedar pollen. FEBS Letters **353**:124-128.

Puissant, C. and Houdebine, L.M. (1990) An improvement of the single-step method of RNA isolation by acid guanidium thiocyanate-phenol-chloroform extraction. BioTechniques **8**:148-149.

Raskin, I. and Kende, H. (1984a) Role of gibberellin in the growth response of submerged deepwater rice. Plant Physiol **76**:947-950.

Raskin, I. and Kende, H. (1984b) Regulation of growth in stem sections of deepwater rice. Planta **160**:66-72.

Rose-John, S. and Kende, H. (1985) Short-term growth response of deepwater rice to submergence and ethylene. Plant Sci **38**:129-134.

Rothman, J.E. and Wieland, F.T. (1996) Protein sorting by transport vesicles. Science **272**:227-234.

Sambrook, J., Fritsch, E.F. and Maniatis, T. (1989) Molecular Cloning: A Laboratory Manual (Cold Spring Harbor Laboratory Press, Plainview, NY), 2nd ed.

Sauter, M. and Kende, H. (1992) Gibberellin-induced growth and regulation of the cell division cycle in deepwater rice. Planta **188**:362-368.

Sauter, M., Mekhedov, S.L. and Kende, H. (1995) Gibberellin promotes histone H1 kinase activity and the expression of *cdc2* and cyclin genes during the induction of rapid growth in deepwater rice internodes. Plant J **7**:623-632.

Sauter, M. (1997) Differential expression of a CAK (cdc2-activating kinase)-like protein kinase, cyclins and *cdc2* genes from rice during the cell cycle and in response to gibberellin. Plant J **11**:181-190.

Schindler, M., Meiners, S. and Cheresh, D.A. (1989) RGD-dependent linkage between plant cell wall and plasma membrane: consequences for growth. J Cell Biol **108**:1955-1965.

Stünzi, J.T. and Kende, H. (1989) Gas composition in the internal air spaces of deepwater rice in relation to growth induced by submergence. Plant Cell Physiol **30**:49-56.

Van der Knaap, E. and Kende, H. (1995) Identification of a gibberellin-induced gene in deepwater rice using differential display of mRNA. Plant Mol Biol **28**:589-592.

Van der Knaap, E., Jagoueix, S. and Kende, H. (1997) Expression of an ortholog of replication protein A1 (RPA1) is induced by gibberellin in deepwater rice. Proc Natl Acad Sci USA **94**:9979-9983.

Von Heijne, G. (1986) A new method for predicting signal sequence cleavage sites. Nucleic Acids Res **14**:4683-4690.

CONCLUSION

This thesis reports on the identification of five genes encoding histone H3, *Os-RPA1*, *OsTMK*, *OsDD3*, and *OsDD4*, whose transcript levels increase in response to gibberellin (GA) and to submergence in deepwater rice internodes. In addition, several other GA-regulated genes in deepwater rice have been identified in our laboratory. Broadly, the genes can be grouped in three categories:

(i) Genes involved in the cell cycle. GA increases the rate at which new cells are produced in the intercalary meristem. Therefore, an increase in transcript levels for cell cycle-specific genes is expected. Histone H3 and *Os-RPA1* were identified by differential display, while two cyclin genes, *cycOs1* and *cycOs2*, were identified by other means. Changes in the cell cycle, as measured by flow cytometry and [^{3}H]thymidine labeling, correlate well with the changes in expression of histone H3, *Os-RPA1* and the two cyclin genes. Throughout this thesis, we have used the change in transcript levels for histone H3 and *cycOs1* as markers for the different phases of the cell cycle and compared their increase with that of the other genes identified.

(ii) Genes involved in cell wall property changes. *Os-EXP2* and *Os-EXP4* encode two expansin proteins, and their transcript levels are increased by GA. Expansins were identified originally because of their cell wall loosening property. During growth, the cell wall has to yield or loosen, and expansins are thought to play a critical role in this process by disrupting the hydrogen bonds between cellulose microfibrils and hemicelluloses.

(iii) Genes whose role in plant growth and development is unknown. This thesis reports on the identification of three genes in this class: *OsTMK*, encoding a leucine-rich receptor-like kinase; *OsDD3*, encoding a putative type 1a plasma membrane receptor; and *OsDD4*, encoding a putative transcription factor. *OsTMK* transcript levels increase during GA treatment, and the expression is high in growing regions, suggesting a role for this gene in plant growth. A potential downstream component of OsTMK is a kinase-associated protein phosphatase. The expression of *OsDD4* is restricted to regions containing meristems. Overexpression of *OsDD4* in *Arabidopsis* leads to a pleiotropic phenotype in which several growth related processes are affected.

Data shown in this thesis indicate that the transcript levels for *Os-RPA1* and *OsDD4* increase before changes in cell cycle activity are observed. This suggests that *Os-RPA1* and *OsDD4* may be primary response genes. It will be interesting to understand how GA regulates the increase in transcript levels. If is this accomplished through an increase in transcription, the promoters of these genes may help elucidate important components of the GA signal transduction pathway. The transcription of *Os-RPA1* and *OsDD4* may be regulated by GAI and/or RGA, two putative transcription factors in the GA signaling pathway.

Studies to learn more about the function of the proteins encoded by *OsDD3* and *OsDD4* will be important. These two genes are interesting since no homologs have been identified and they may encode plant-specific genes. Before the role for OsDD3 can be elucidated, the precise localization of this protein in the cell needs to be addressed. For the partially nuclear-localized

OsDD4, it will be interesting to know whether it can bind DNA, activate transcription, and which domains are responsible for those two activities. It will be intriging to find out whether GA plays a role in the cell-specific location of OsDD4 and whether GA can modulate DNA binding or transcriptional regulation. If OsDD4 plays a role in GA signal transduction, it is possible that it is a substrate for SPY, a protein containing a domain of N-acetylglucosamine transferase activity. It has been hypothesized, for example, that GAI and RGA are likely substrates of SPY.

The role of *OsTMK*, *OsDD3*, and *OsDD4* in GA-regulated growth in the whole plant should be addressed, at least in part, via experiments designed to increase or decrease the transcript levels of the respective genes. For *OsDD4*, the expression is relatively high in the intercalary meristem of growing internodes and may be limiting in modern rice varieties that do not display early internodal elongation. Overexpression of *OsDD4* in modern rice varieties may indicate whether the protein encoded by this gene plays a critical role in internodal elongation. Alternatively, the function of these genes can be addressed in a genetically more amenable system such as *Arabidopsis*. The identification of the *Arabidopsis* orthologs and subsequent antisense and overexpression experiments may allow a faster indication for the role of these genes in plant growth and development.